

Copyright
by
Ulan Onbergenov
2012

**The Thesis Committee for Ulan Onbergenov
Certifies that this is the approved version of the following thesis:**

**Simulation of Thermally Active and pH-Sensitive Polymers for
Conformance Control**

**APPROVED BY
SUPERVISING COMMITTEE:**

Supervisor:

Kamy Sepehrnoori, Supervisor

Mojdeh Delshad

**Simulation of Thermally Active and pH-Sensitive Polymers for
Conformance Control**

by

Ulan Onbergenov, B.S.

Thesis

Presented to the Faculty of the Graduate School of
The University of Texas at Austin
in Partial Fulfillment
of the Requirements
for the Degree of

MASTER OF SCIENCE IN ENGINEERING

The University of Texas at Austin

May 2012

Dedication

To my family

Acknowledgements

I would like to express my sincere gratitude to my supervisor, Professor Kamy Sepehrnoori, for providing support and leadership in writing this thesis. His knowledge and experience were invaluable, and his guidance and instruction throughout his research are greatly appreciated.

I would also like to extend my appreciation to Professor Mojdeh Delshad for her valuable advice and for reviewing this thesis. Professor Chun Huh deserves special recognition for his help and constructive ideas. Additionally, special thanks go to Dr. AbdolJalil Varavei for his continuous assistance during this research and availability for extensive valuable discussions.

Thanks to my parents for their continued love, support and encouragement throughout my stay at the University of Texas at Austin. I am also grateful to my wife, Zhazira Sultanova. Her patience and moral support have helped me to successfully complete my studies.

I also want to thank the Kazakhstan government for awarding me a scholarship for my Master's degree, and providing continuous financial and logistical support. Last but not least, much gratitude is extended to the people I did not mention individually. Their help in completing this thesis in a timely manner is greatly appreciated.

Abstract

Simulation of Thermally Active and pH-Sensitive Polymers for Conformance Control

Ulan Onbergenov, M.S.E.

The University of Texas at Austin, 2012

Supervisor: Kamy Sepehrnoori

A waterflood has been used as a secondary recovery process to maintain the reservoir pressure and displace the oil towards the producer. However, the existence of high-permeability zones (thief zones) can cause early water breakthrough and excessive water production, thus, leaving a significant amount of oil bypassed in heterogeneous reservoirs. In this work, thermally active (Bright Water®) and pH-sensitive polymers have been proposed as an in-depth conformance tool with detailed simulation studies.

Thermally active polymers are triggered by temperature change, whereas pH-sensitive polymers are triggered by pH change. Upon activation, polymers provide high resistance to subsequent fluid flow and divert the flow into adjacent unswept zones. As a result, this leads to improved sweep efficiency, low oil-water-ratio, and incremental oil recovery.

The modeling of a pH-sensitive polymer was based on the principles of the microgel modeling procedure developed by Huh *et al.* (2005). In addition, a modified

model was developed to calculate equilibrium swelling ratio explicitly in terms of pH and ionic strength of solution instead of using a root-finding algorithm. Thermal active polymers were modeled in terms of gelation reaction, gel viscosity, gel adsorption, and permeability reduction factor. Thermally active and pH-sensitive polymers were coupled with UTGEL reservoir simulator in an attempt to assess applicability of these gels as a conformance tool.

Sensitivity analysis studies were conducted through 3D synthetic models to investigate technical feasibility of thermally active and pH-sensitive polymers as an in-depth conformance tool. Results indicated that incremental oil recovery and conformance control depend on the polymer concentration, slug size, permeability contrast between matrix and thief zone, vertical to horizontal permeability ratio (k_v/k_h), treatment location, oil-to-water viscosity ratio, and adsorption level, among others.

It is concluded in this study that the permeability contrast between matrix and thief zones appears to be one of the most important parameters that impacts treatment performance. Therefore, a high permeability contrast is a prerequisite to achieve technically and economically successful treatment.

Table of Contents

List of Tables	x
List of Figures	xi
Chapter 1: Introduction	1
Chapter 2: Literature Review	3
2.1 Preformed Particle Gel (PPG).....	6
2.2 Colloidal Dispersion Gel (CDG)	9
2.3 pH-Sensitive Polymer	10
2.4 Thermally Active Polymer.....	12
Chapter 3: Thermally Active and pH-Sensitive Polymer Modeling in UTGEL ...	18
3.1 Thermally Active Polymer.....	19
3.1.1 Introduction.....	19
3.1.2 Gelation Reaction.....	21
3.1.3 Gel Viscosity.....	21
3.1.4 Gel Adsorption.....	24
3.1.5 Permeability Reduction Factor	25
3.2 pH-Sensitive Polymer	26
3.2.1 Equilibrium Swelling Ratio	27
3.2.1.1 Equilibrium Swelling Ratio	27
3.2.1.2 Modified Equilibrium Swelling Ratio	30
3.2.2 Intrinsic Viscosity using Modified Mark-Houwink Equation	32
3.2.3 Martin Equation	33
3.2.4 Carreau Equation	33
Chapter 4: Sensitivity Analysis of Thermally Active and pH-Sensitive Polymers	39
4.1 Sensitivity Analysis of Thermally Active Polymers.....	39
4.1.1 Base Case Model.....	39
4.1.2 Treatment Fluid Concentration	40
4.1.3 Treatment Slug Size	41

4.1.4 Vertical-to Horizontal Permeability Ratio	41
4.1.5 Permeability Contrast.....	42
4.1.6 Oil-to-Water Viscosity Ratio	42
4.2 Sensitivity Analysis of pH-Sensitive Polymers	43
4.2.1 Base Case Model.....	43
4.2.2 Treatment Fluid Concentration	44
4.2.3 Treatment Slug Size	44
4.2.4 Vertical-to-Horizontal Permeability Ratio.....	45
4.2.5 Permeability Contrast.....	45
4.2.6 Oil-to-Water Viscosity Ratio	46
4.3 Summary and Conclusions	46
Chapter 5: Field Case Simulation of Thermally Active Polymers	58
5.1 Introduction.....	58
5.2 Simulation Strategy.....	59
5.2.1 Initial Water Saturation.....	59
5.2.2 Thermally Active Polymer Treatments.....	60
5.3 Simulation Results	60
5.4 Summary and Conclusions	61
Chapter 6: Summary, Conclusions, and Recommendations	69
6.1 Summary	69
6.2 Conclusions.....	69
6.3 Recommendations.....	70
Appendix A	71
Appendix B	81
Appendix C	90
Nomenclature.....	110
REFERENCES	113

List of Tables

Table 3.1 Summary of the Best-Fit Model Parameters (Huh <i>et al.</i> , 2005)	35
Table 4.1 Simulation Data for Base Case Bright Water® Treatment	47
Table 4.2 Simulation Data for Base Case pH-Sensitive Polymer Treatment.....	47
Table 5.1 Simulation Data for Field Case	63

List of Figures

Figure 3.1 Equilibrium Swelling Ratio Versus pH	36
Figure 3.2 Empirical Constant (E) Versus Ionic Strength of Solution	36
Figure 3.3 Empirical Constant (B) Versus Ionic Strength of Solution	37
Figure 3.4 Empirical Constant (C) Versus Ionic Strength of Solution	37
Figure 3.5 Empirical Constant (D) Versus Ionic Strength of Solution	38
Figure 3.6 Comparison of Newton-Raphson and Modified Model	38
Figure 4.1 The Conceptual 3D Model with Three Layers. Permeability of the Thief Zone is 1500 mD and Other Layers are 50 mD.	48
Figure 4.2 Temperature Profile after 540 Days (1 PV) of Water Injection	48
Figure 4.3 Permeability Reduction Factor in Thief Zone	49
Figure 4.4 Cumulative Oil Recovery after Bright Water® Treatment	49
Figure 4.5 Incremental Oil Production Rate after Bright Water® Treatment	50
Figure 4.6 Comparison of Incremental Oil Recovery for Different Treatment Concentrations	50
Figure 4.7 Comparison of Incremental Oil Recovery for Different Treatment Slug Sizes	51
Figure 4.8 Permeability Reduction Profile for $k_v / k_h = 0.1$	51
Figure 4.9 Permeability Reduction Profile for $k_v / k_h = 0.001$	52
Figure 4.10 Impact of K_v/K_h on Incremental Oil Recovery	52
Figure 4.11 Impact of Permeability Contrast on Incremental Oil Recovery	53
Figure 4.12 Impact of Oil-To-Water Viscosity Ratio on Incremental Oil Recovery	53
Figure 4.13 The Conceptual 3D Model with Three Layers. Permeability of the Thief Zone is 1500 mD and Other Layers are 50 mD.	54

Figure 4.14 Cumulative Oil Recovery after pH-sensitive Polymer Treatment.....	54
Figure 4.15 Incremental Oil Production Rate after pH-sensitive Polymer Treatment	55
Figure 4.16 Comparison of Incremental Oil Recovery for Different Treatment Concentrations	55
Figure 4.17 Comparison of Incremental Oil Recovery for Different Treatment Slug Sizes	56
Figure 4.18 Impact of k_v / k_h on Incremental Oil Recovery	56
Figure 4.19 Impact of Permeability Contrast on Incremental Oil Recovery	57
Figure 4.20 Impact of Oil-To-Water Viscosity Ratio on Incremental Oil Recovery	57
Figure 5.1 Temperature Profile before Bright Water® Treatment	63
Figure 5.2 Permeability Distribution in the Field	64
Figure 5.3 Water Saturation Profile after 367 days (5 PV).....	64
Figure 5.4 Comparison of Bottomhole Pressure for Waterflood and Bright Water® Treatment	65
Figure 5.5 Permeability Reduction Profile	65
Figure 5.6 Comparison of Oil Cut for Waterflood and Bright Water® Treatment at Producer 1.	66
Figure 5.7 Comparison of Oil Cut for Waterflood and Bright Water® Treatment at Producer 3	66
Figure 5.8 Comparison of Cumulative Oil Recovery for Waterflood and Bright Water Treatment	67
Figure 5.9 Comparison of Water-Oil-Ratio for Waterflood and Bright Water® Treatment at Producer 1	67

Figure 5.10 Comparison of Water-Oil-Ratio for Waterflood and Bright Water®

Treatment at Producer 3	68
-------------------------------	----

Chapter 1: Introduction

Traditionally, a waterflood has been used as a secondary recovery process to maintain the reservoir pressure and displace the oil towards the producer. However, the existence of high-permeability zones (thief zones) can cause early water breakthrough and excessive water production, thus, leaving a significant amount of oil bypassed in heterogeneous reservoirs. Excessive water production causes many problems such as water treatment and disposal costs, scaling, and corrosion (Pritchett *et al.*, 2003). Lee *et al.* (2002) reported that the oil industry in the United States produces an average of more than 7 bbl of water for every barrel of oil, which is equal to an average of 88% water cut (Sydansk *et al.*, 2011).

Various types of fluid diversion methods have been proposed to reduce water channeling and high water cuts. These methods have been noted in the literature as conformance control, gel treatments, or profile control. The purpose of this study is to investigate the use of thermally active and pH-sensitive polymers as an in-depth conformance control agent with numerical simulations using the UTGEL simulator (Delshad *et al.*, 2011).

This thesis consists of six chapters: Chapter 1 provides information about the purpose of this study and gives general information about each chapter. Chapter 2 presents a literature review about the applications of polymer and polymer gel systems for conformance control, types of polymer gels, gel characteristics, laboratory observations, and field applications.

Chapter 3 describes the modeling procedure of thermally active and pH-sensitive polymers in UTGEL. This chapter also presents the modified model to calculate the equilibrium swelling ratio in terms of pH and ionic strength of solution.

In Chapter 4, sensitivity analysis is performed for thermally active and pH-sensitive polymer to understand the impact of the most important design parameters such as polymer concentration, vertical-to-horizontal permeability ratio, slug size, oil-to-water viscosity ratio, and permeability contrast on treatment performance. The sensitivity analysis is based on a 3D synthetic model with three vertical simulation layers.

Chapter 5 describes the simulation study of thermally active polymer in synthetic oil field with seven production and ten injection wells. The purpose of this study was to evaluate the effectiveness of thermally active polymer treatments. The final chapter describes the summary and main conclusions, and provides recommendations for future work.

Chapter 2: Literature Review

The purpose of this literature survey is to review technical documents regarding different types of polymer gels applied for conformance control. This survey includes Preformed Particle Gels (PPG), pH-Sensitive Gels, and Thermally Active Polymers (Bright Water®).

Waterflooding is a secondary recovery process to displace oil that has not been recovered by the primary recovery method. However, the waterflooding is often associated with a problem of unwanted water production resulting from unfavorable displacement caused by channeling through high-permeable layers. Excess water production leads to many problems such as additional water treatment and disposal costs, corrosion, scaling, increased environmental issues, etc. (Pritchett *et al.*, 2003). Therefore, it is important to improve the sweep efficiency of the waterflooding

Since the 1960's, polymers have been used as an Improved Oil Recovery (IOR) process to improve sweep efficiency in waterfloods, especially in heterogeneous reservoirs. Polymer flooding can be used to deal with unfavorable mobility ratio waterflood and excessive reservoir heterogeneity. A small concentration of polymer is added to increase the viscosity of the injected water and decrease its mobility. This improves the linear displacement efficiency and areal sweep efficiency by suppressing viscous fingers (Sorbie, 1991).

Seright *et al.* (1994) classified polymer techniques into two groups: traditional polymer flooding and gel treatments for conformance control. It should be noted that traditional polymer floods and gel treatments are used for different purposes even though their ultimate objective is to improve reservoir sweep efficiency. In a traditional polymer flood, the injected polymer solution is designed to penetrate as far as possible into the poorly swept zones. In a gel treatment, the injected gel solution is designed to maximize its penetration into the high permeable channels while minimizing its penetration into less permeable zones saturated with oil (Seright *et al.*, 1994).

Traditional polymers have been used for long time to control mobility and improve sweep efficiency in poorly swept reservoirs. However, there are some technical issues associated with this process. Polymer solutions have high viscosity and require a high pressure drop in order to inject them at a desired rate. This causes injectivity problems and may result in artificially induced fractures near the wellbore region. Most polymers exhibit shear-thinning behavior. As polymer solution enters the formation, its shear rate rapidly falls. As a result, its viscosity starts to increase and a viscous bank can be formed in the vicinity of the wellbore. They also require large volumes of polymers to compensate for adsorption and retention (Sorbie, 1991; Pritchett *et al.*, 2003).

Gel treatment is one of the most cost-effective methods to reduce water or gas flow through high-permeable zones or fractures without damaging highly oil saturated unswept zones. Gel treatments are designed by adding a small concentration of crosslinker to the polymer solution in order to link polymer molecules, forming relatively large diameter gels.

Gel treatments can be classified into two groups: in-situ gels and preformed particle gels. In-situ gel technology involves injecting a mixture of polymer and crosslinker (called gelant) together or separately by slugs. Then a crosslinking reaction occurs by a specific trigger to generate gels in-situ. However, this technology has some drawbacks such as a lack of reaction kinetics control, gelling uncertainty due to shear degradation, chromatographic separation between polymer and crosslinker, and dilution by formation water and minerals that restrict its applications for conventional reservoirs (Bai *et al.*, 2007; Zhang *et al.*, 2011). In contrast, preformed gels are formed at the surface and no gelation takes place in the reservoir. Since gels usually have a single component when they are injected, they are less sensitive to physical and chemical properties of the reservoir (Bai *et al.* 2007). Particle gels may include micrometer to millimeter-sized preformed particle gels (Coste *et al.*, 2000; Bai *et al.*, 2007), pH-sensitive crosslinked polymers (Al-Anazi and Sharma 2002; Huh *et al.*, 2005), microgels (Chauveteau *et al.*, 1999; Rousseau *et al.* 2005;), and sub-micrometer-sized polymers (Pritchett *et al.*, 2003; Frampton *et al.*, 2004).

Traditionally, gels were placed near the wellbore of injection or production wells to correct sweep profile. However, near-wellbore treatments are not effective if there is a cross-flow between adjacent layers. It can be explained by the fact that injected fluids can circumvent plugs placed in the high permeability layers (Root *et al.*, 1965).

In recent years, newer gel systems have been developed for in-depth conformance control (Pritchett *et al.*, 2003; Chang, 2004; Sydansk *et al.*, 2005; Bai *et al.*, 2007). These gels are able to propagate deep into the reservoir and create high flow resistance in high-

permeability zones; thus, diverting the chase water into previously unswept zones (Bai *et al.*, 2007).

Gel treatments can be applied for matrix and high-permeable channels, or fractures depending on gel size. If gel treatments are applied for the matrix, the gel size should be small enough to penetrate into the pore throat of the matrix. Traditionally, in-situ gels have been used for matrix treatments because gelants have small viscosity to propagate through a matrix (Seright *et al.*, 2003; Zhang *et al.*, 2010). Currently, application of commercially available submicron-sized particle gels (Bright Water®) is becoming a new trend for matrix treatments because of their smaller size compared to reservoir rock pore size (Pritchett *et al.*, 2003; Cheung 2007).

If gel treatments are applied for fractures or high-permeable channels, gels should be designed to be able to propagate through highly permeable channels while minimizing penetration into oil saturated unswept zones. Published research shows that gels have effectively mitigated channeling through fractures, voids in waterfloods (O'Brien *et al.*, 1999; Sydansk and Seright 2007) and gasfloods (Woods *et al.*, 1986; Lane *et al.*, 2000).

2.1 PREFORMED PARTICLE GEL (PPG)

PPG is a mm-sized preformed particle gel widely used for conformance control purposes. It is formed at surface, then dried and crushed into small particles to be injected into a reservoir.

PPGs have some advantages over in-situ and other preformed gels. In the porous medium, in-situ gels propagate as a polymer solution before gelation. Since polymers

have higher viscosity than water, in-situ gels will enter low permeability zones and damage the potential oil-bearing zones. In contrast, PPGs can preferentially penetrate into high permeability channels and should not enter low permeable oil containing zones. PPG can be prepared with produced water, while traditional and sub-micron gels are very sensitive to salinity, hydrogen sulfide, and multivalent cations in the produced water. Moreover, they have an adjustable size so that real-time monitoring data can be used to design proper sizes and enhance gel treatment results (Bai *et al.*, 2012).

Bai suggested criteria of well selection for PPG based on experience from field applications:

- Reservoir temperature below 120°C
- Reservoir with high permeability channels or fractures
- High injectivity and low pressure index
- Well group with low oil recovery and high water cut
- Salinity not limited

A number of published papers show that PPG has been successfully implemented in reservoirs with high salinity, high temperature, carbon dioxide flooding, reservoirs with severe sand production, thick heterogeneous zones, and reservoirs with previous polymer flooding (Bai *et al.*, 2012).

The first successful PPG field trial was performed in Zhongyuan oilfield in 1999. This reservoir had severe conditions, such as high temperature (107°C) and high salinity (150,000 ppm). Two injection wells were treated using PPG suspension. This PPG trial

results indicated that water cut decreased from approximately 80% to approximately 70%, and 3,239 tons (23,742 barrels) of incremental oil was recovered (Bai *et al.*, 2012).

The first PPG treatment in Daqing oilfield was performed in a sandstone reservoir with thick oil layers. Profile tests showed that about 85% of injected water directly passed through high permeability zones and inter-well potential measurements showed that the well group had severe areal heterogeneity. About 20,000 barrels of PPG suspension was injected in multiple stages by changing particle size from 1.5 mm (0.059 inches) to 5 mm (0.2 inches). Test results showed that about 2,400 tons (17,592 barrels) of incremental oil was recovered and water cut decreased by 8%. Since large particles were successfully injected without any injectivity problems, these field trial results demonstrate that fracture or high permeability channels may exist in mature waterflooded reservoirs (Seright *et al.*, 1999; Bai *et al.*, 2007).

Larkin *et al.* (2008) described a case study of conformance problems caused by direct communication channels between injector and offset producers in certain patterns of the SACROC Unit CO_2 EOR Project in Scurry County, Texas. The SACROC Unit was characterized as highly-heterogeneous reservoir with limited vertical injection fluid distribution, which resulted in poor sweep and excessive production of CO_2 . Based on extensive studies, crystallized copolymer super absorbent system (CP) was selected to modify inter-well communication problems and reduce CO_2 production. Multiple wells were treated with CP size of 2mm (0.08 inches) to 4mm (0.16 inches). As a result of these treatments, gas production was decreased and injection profiles were improved.

This case study shows that the particle treatment can be applied in CO_2 flooding projects as a profile modification tool (Larkin *et al.*, 2008).

Overall, the PPG system is widely used for conformance control purposes with more than 2000 treated wells in China. Successful treatments include high-temperature and high-salinity reservoirs, as well as fractured and unfractured mature reservoirs.

2.2 COLLOIDAL DISPERSION GEL (CDG)

CDG are used for the in-depth profile modification of high permeability layers in heterogeneous reservoirs. They have been extensively used in the field by using low concentrations of polymer and aluminum citrate as the crosslinker (Mack and Smith, 1994). Because of the small concentrations of polymer and crosslinker, the gel formation rate is slow and can be injected deep into a formation. Gel strength and stability of the CDG depends strongly on the type and quality of polymer used (Smith, 1995).

The CDG performance can be measured by transition pressure. The transition pressure is a laboratory measurement of the highest pressure at which the CDG will plug a core (Fielding *et al.*, 1994). At high pressures above the transition pressure, CDG flows as a crosslinked polymer and behaves as a shear-thinning liquid. At pressures below the transition pressure, CDG gellifies and increase flow resistance (Mack and Smith, 1994).

Shi *et al.* (2011) divided CDGs into two groups: CDG formed in-situ and preformed CDG. Preformed CDG is predominantly intramolecularly crosslinked CDG, whereas CDG formed in-situ is predominantly intermolecularly crosslinked CDG. They then implemented the novel CDG viscosity and transport model into 3D chemical-

process simulator to model the CDG processes for conformance control purposes (Shi *et al.*, 2011).

Many experiments and pilot tests employing CDG have been conducted at different cores and oil fields to see if CDG can propagate through porous medium. Some laboratory experiments showed that CDG can propagate through the core with little formation damage (Spildo *et al.*, 2009). Other coreflood results showed significant CDG retention in the first parts of the cores (Ranganathan *et al.*, 1998).

Mack and Smith (1994) reported successful field applications of CDG in the Rocky Mountain Region. Nineteen of the projects were considered highly successful, three of them marginally successful, and seven of them unsuccessful. Based on field-wide water oil ratio, an estimate of 300,000 STB of incremental oil was produced at a chemical cost of \$2.53 per incremental barrel of oil.

CDG pilot tests were performed in Daqing oilfield. Chang *et al.* (2004) reported a decrease in water cut by up to 19.8%, and an incremental oil recovery of 10.5% of the original oil in place (OOIP) relative to waterflooding, while chemical costs were reported as \$2.72/bbl of incremental oil.

2.3 PH-SENSITIVE POLYMER

pH-sensitive polymer gels have been proposed as a novel deep-penetrating gels injected into a heterogeneous reservoir (Al Anazi *et al.*, 2002). Crosslinked poly(acrylic) polymer is dispersed in water to form a microgel. The properties of these polymer gels are very sensitive to pH, salinity, and shear rate. In acidic conditions, they shrink to have

low viscosity. Upon an increase in pH, they start to swell and adsorb water. As a result, their viscosity can increase up to 1000 times of its initial volume. By changing the solution pH, they can swell and reversibly shrink back to their initial volume. These polymers are attractive due to their affordable cost and environment-friendly nature.

The main purpose of this technology is to use its rheological feature for conformance control to improve sweep efficiency and divert subsequently injected fluids into unswept zones. Because of their small size and low viscosity, they can be easily injected into high-permeability zones without injectivity problems. As microgel solution propagates through the reservoir, it reacts with carbonate and alumino-silicate particles of reservoir rock. As a result, it experiences an increase in pH, and will swell to block the high-permeability zones. Due to blockage of these zones, sweep efficiency of the waterflood will improve and excess water production can be reduced. As we mentioned above, this process is reversible so most of the injected polymers can be recovered by acid injection.

Huh *et al.* (2005) developed a new rheological model that can be used in reservoir simulations for the accurate performance prediction of polymer-related EOR applications. This model consists of the Brannon-Peppas ionic hydrogel swelling theory, modified Mark-Houwink equation, Martin equation, and Carreau equation to describe the apparent viscosity for a wide range of pH, salinity, polymer concentration, and shear rates. Comparisons between laboratory measurements and the model predictions demonstrated the predictive capability of the viscosity model for different types of polymers.

Additionally, pH-sensitive gels have been studied in fractured rocks to divert the injected fluid from fractures into the matrix. Lalehrokh *et al.* (2009, 2010) conducted experiments on both artificially fractured sandstone and carbonate core samples. Their results showed that gel penetration depth is higher for sandstone reservoirs compared to carbonate reservoir rocks. Also, polymer treatment reduced the overall core permeability in all cases in both sandstone and carbonate fractured cores. They concluded that pH-sensitive gels can be applied in sandstone and carbonate formations for in-depth conformance control.

However, this technology has inherent drawbacks related to uncertainties of rock composition in most of the reservoirs. Additionally, acid preflush may dissolve some minerals which complicates the treatment design. Unfortunately, not many papers were published regarding the field application of pH-sensitive polymer gels. Currently, our research group is working on this topic and as part of this thesis, some synthetic cases were run using UTGEL and presented in Chapter 4.

2.4 THERMALLY ACTIVE POLYMER

In the late 1990's, BP, Chevron, and Nalco conducted a joint research project and developed a new thermally activated particle (TAP) known as "Bright Water®". The main objective of this technology was to inject inactive polymer particles so they could easily propagate and swell in the high permeability watered-out zones upon reaching the temperature front. Once they swell, they could divert subsequently injected chase water into less permeable unswept zones (J. Pritchett *et al.*, 2003; H. Frampton *et al.*, 2004).

The particle consists of highly crosslinked sulfonate-containing polyacrilamide microparticles (0.1-3 microns) constrained by both permanent and reversible crosslinks. As it heats up, the reversible crosslinker breaks by hydrolysis and particles begin to expand in size and volume. Permanent crosslinkers provide conformational integrity to particles, especially after they activate. Inactive particles are supplied in a constrained state – called “kernel” particle. After reaching the temperature front, the kernels are able to absorb surrounding water and expand up to 10 times their original size – subsequently being called “popcorn” for convenience (H. Frampton *et al.*, 2004; J. Pritchett *et al.*, 2003).

The Bright Water® kernels are manufactured as a 30% active dispersion of polymer in light mineral oil. They are dispersed into brine by adding the required amount of surfactant under high shear rates to ensure that they are dispersed as single particles. Different grades of sub-micron particles are available for different activation temperature and time profiles (J. Pritchett *et al.*, 2003; H. Frampton *et al.*, 2004).

Propagation and trigger time of the particles depend on rock thermal properties, water injection, and reservoir temperatures. Numerical simulators capable of handling energy equation can be used to optimize the treatment placement. Inactive particles should have proper size in order to propagate through the reservoir before popping (J. Pritchett *et al.*, 2003).

Preliminary laboratory studies are pre-requisite to successfully model the propagation of the sub-micron particles through the porous medium. They might include bottle tests, injectivity tests, propagation tests, and popping tests. Usually particles are

screened using bottle tests and slim tube sand packs (J. Pritchett *et al.*, 2003; H. Frampton *et al.*, 2004; D. Ohms *et al.*, 2009).

Many authors suggested a list of screening criteria for Bright Water® selection compiled below (Yanez *et al.*, 2007; J.L.Mustoni *et al.*, 2010; H. Frampton *et al.*, 2004):

- Available movable oil reserves in low-permeability zones
- Poor sweep efficiency and oil recovery
- High permeability contrast between adjacent layers
- Injection water salinity lower than 70,000 ppm
- Temperature from 50°C (122°F) to 150°C (302°F)
- Minimal reservoir fractures
- Available surface facilities.

Garmeh *et al.* (2011) reported that almost 60 treatments have been tested in Argentina (J.L.Mustoni *et al.*, 2010; Yanez *et al.*, 2007), Alaska (Ohms *et al.*, 2009), North Sea (Frampton *et al.*, 2009), Tunisia (Ghaddab *et al.*, 2010), and Brazil (Roussennac *et al.*, 2010).

The first trial was tested in the Minas field (Indonesia) in 2001. The goal of this field trial was to demonstrate that large volumes of the sub-micron particles can be injected deep into the reservoir at low viscosity without injectivity problems, and then expand after pre-designed time to improve overall sweep efficiency of the reservoir. Forty two thousand barrels water containing 4500 ppm of highly expandable material and 1500 ppm of a surfactant was injected for nine days to divert injected water from high permeable zones into low permeable zones containing high oil saturation. Even though

some of the objectives were met, the amount of incremental oil production resulted from the Bright Water® treatment was uncertain. The authors attribute it to a number of factors, such as pump changes prior to the treatment and injection rate changes during the test pattern (Pritchett *et al.*, 2003). The first offshore project was implemented in the North Sea, but no extra oil was recovered. Another North Sea offshore field application was reported, where 130,000 barrel of incremental oil equivalent and water injection rate reduction was achieved. Total incremental oil volume was estimated to be 317,300 barrels of oil equivalent (N. Lugo *et al.*, 2010).

Ohms *et al.* (2009) have reported a successful Bright Water® treatment results that were performed in the BP Milne Point field located on the North Slope of Alaska. A pattern of one injector and two producers was chosen because of high volumes of bypassed oil. Over 21 days, 15,587 gallons (60.8 tonnes) of thermally active particles using 8,060 gallons (30.4 tonnes) of dispersing surfactant was dispersed into 38,000 barrels of injected water. No injectivity problems were observed during this time. Pressure-fall-off tests were run to check if any changes were observed after the Bright Water® injection to block the high-permeability thief zone. Test results showed both permeability and permeability-thickness values were decreased by more than 50%, while no adverse skin effects were observed. After the first 4 years of application of thermally active particles, over 60,000 barrels of incremental oil were recovered. Also, a combined water-oil ratio pattern associated with the treatment was reduced to confirm that a blocking of high-permeability thief zones was achieved. Finally, the treatment cost is

resulted in at less than \$5 per incremental barrel of oil, and two additional treatments at Milne Point were performed in 2007 (Ohms *et al.*, 2009).

Even though a number of laboratory and field case studies have been reported in the literature, only a few papers have focused on the reservoir simulation aspects of thermally active polymers for in-depth conformance control. Akanni (2010) examined a synthetic two-layered reservoir with a range of permeability contrasts from 2:1 to 20:1 and with oil/water viscosity ratios ranging from 1 to 10,000 cP in an attempt to investigate the effect of popping-agent bank positioning on recovery. His simulation results revealed that in-depth profile modification would have its greatest opportunity to compete with polymer flooding if the permeability contrast between layers was high. He also concluded that higher recovery values favor placing the popping- agent bank in the middle of the high-permeability layer or closer to the producer. Also he concluded that larger popping-agent banks would enhance oil recovery, while economics would favor small popping-agent banks in the high-permeability layers.

Seright *et al.* (2011) investigated when the in-depth profile modification process is a superior choice over conventional polymer flooding. Their results showed that in-depth profile modification can compete with polymer flooding when there is a high-permeability contrast between layers. They concluded that short-term economics might favor in-depth treatments, but ultimate recovery was significantly less than for polymer flooding (Seright *et al.*, 2011).

Garmeh *et al.* (2011) used a single component approach to model characteristics of the thermally active polymer technology with detailed simulation studies. They

performed a sensitivity analysis on several reservoir and design parameters. Their results showed that thermal active polymers can increase oil recovery by viscosification and chemical adsorption/retention by diverting flow into unswept zones.

Chapter 3: Thermally Active and pH-Sensitive Polymer Modeling in UTGEL

The UTGEL simulator equipped with a thermally active and pH-sensitive polymer models was used for this research project. This chapter is divided into two sections. The first section describes the modeling of thermally active polymers. The second section describes the modeling of pH-sensitive polymers. The equations used in UTGEL, pertinent to the modeling of the two gels are also included.

UTGEL Simulator

UTGEL is a three-dimensional, multicomponent, two-phase compositional finite-difference simulator developed at The University of Texas at Austin (Delshad *et al.*, 2011). The simulator can model capillary pressures, two-phase relative permeabilities (water/oil), dispersion, diffusion, adsorption, chemical reactions, non-equilibrium mass transfer between phases, and other related phenomena.

UTGEL can be used to simulate a wide range of displacement processes at both field and laboratory scales. The balance equations are the mass conservation equations, an overall balance equation that determines the pressures for up to two fluid phases, and an energy balance equation to determine the temperature. The number of components is variable depending on the application. The model includes options for multiple wells; horizontal wells, vertical wells, or deviated wells. Aquifer boundaries are modeled as constant-potential surfaces or as closed surfaces.

The resulting flow equations are solved using a block-centered finite-difference scheme. The solution method is implicit in pressure and explicit in concentration (IMPES- type). One-point upstream and third-order spatial discretizations are available as options in the code. To increase the stability and robustness of the third-order method, a flux limiter that is total-variation-diminishing (TVD) has been implemented in the code (Liu, 1993). The third-order method gives the most accurate solution.

3.1 THERMALLY ACTIVE POLYMER

3.1.1 Introduction

Thermally active sub-micron polymer (Bright Water®) is an expandable material that can create resistance to flow in high-permeable zones. Bright Water® treatments have been widely used as an in-depth conformance control tool to improve sweep efficiency of waterfloods. The conformance control is achieved by plugging the high permeability layers and diverting the subsequently injected fluids into unswept zones at a pre-determined temperature. An accurate estimation of treatment design parameters is, therefore, necessary for a successful reservoir treatment.

Garmeh et al. (2011) proposed two approaches to describe modeling of the thermally active diverting agent's characteristics:

- Single-component approach: Bright Water® is injected as a single chemical component and remains as a single component throughout the course of action. However, its physical characteristics such as viscosity and adsorption change with

heat and time. Upon reaching the activation temperature, the resistance against flow takes place in the thief zone away from the injector.

- Chemical reaction approach: Bright Water® is a product of a reaction between polymer and crosslinker and modeled using three water soluble components (polymer, crosslinker, and Bright Water®). In this approach, a chemical reaction is triggered by activation temperature; thus, upon reaching the activation temperature, the reaction between polymer and crosslinker begins and the Bright Water® component is generated. As a result, the Bright Water® component has higher viscosity and adsorption than individual polymer and crosslinker components. The reaction rate (product generation) can be controlled by a reaction rate coefficient.

In this section, the modeling of the chemical reaction approach is described. In this model, the gel is formed by the reaction between the polymer and crosslinker after reaching their respective threshold temperature and threshold concentrations. Thermally active polymer gel properties modeled in UTGEL include:

1. Gelation reaction
2. Gel viscosity
3. Gel adsorption
4. Permeability reduction factor.

The following sections discuss the gel properties in detail. The equations used in the UTGEL, pertinent to the simulations performed, are also included.

3.1.2 Gelation Reaction

The reaction between polymer and crosslinker to form Bright Water Gel (BWG) is modeled by adding the reaction term in concentration equations of corresponding components (polymer, crosslinker, and BWG). The reaction term equations to form the gel are described as

$$r_p = -r_{BW_o} C_{p_o} C_p C_{CL} \exp\left(\beta_k \left(\frac{1}{T} - \frac{1}{T_{ref}}\right)\right), \quad (3.1)$$

$$r_{CL} = -r_{BW_o} C_{CL_o} C_p C_{CL} \exp\left(\beta_k \left(\frac{1}{T} - \frac{1}{T_{ref}}\right)\right), \quad (3.2)$$

$$r_{BWG} = -(r_p + r_{CL}), \quad (3.3)$$

where r_p , r_{CL} , r_{BWG} are the reaction rates of polymer, crosslinker, and BWG; and where r_{BW_o} is the reaction rate coefficient; β_k is the temperature coefficient; C_{p_o} and C_{CL_o} are the polymer and crosslinker reaction rate multipliers, respectively; T_{ref} is the reference temperature and C_p and C_{CL} are the polymer and crosslinker concentrations, respectively. The reactions are occurred when the temperature and concentrations of the polymer and crosslinker are greater than the threshold values (user defined parameters).

3.1.3 Gel Viscosity

The pure water and oil viscosity are the input parameters at reference temperature. The following relationship is used to calculate viscosity as a function of temperature (T):

$$\mu_k = \mu_{k,ref} \exp \left[b_k \left(\frac{1}{T} - \frac{1}{T_{ref}} \right) \right] \text{ for } k=\text{water, oil}, \quad (3.4)$$

where $\mu_{k,ref}$ is the viscosity at a reference temperature T_{ref} and b_k is an input parameter.

The gel solution viscosity model is a function of gel concentration, shear rate, and temperature. The Flory-Huggins equation (Flory, 1953) was modified to account for variation in salinity as

$$\begin{aligned} \mu^\circ = \mu_w [1 + (A_{p1} C_p + A_{p2} C_p^2 + A_{p3} C_p^3) C_{SEP}^S E_p + \\ (A_{G1} C_G + A_{G2} C_G^2 + A_{G3} (C_G - C_{TG})^3) E_G], \end{aligned} \quad (3.5)$$

where C_p and C_G are the polymer and gel concentrations, respectively; μ_w is the water viscosity; A_p and A_G are the coefficients for polymer and gel viscosity equation; C_{TG} is the gel threshold concentration for cubic term which is ignored if $C_{TG} > C_G$. The factor C_{SEP}^S allows for the dependence of polymer viscosity on salinity and hardness. The effective salinity for polymer (C_{SEP}) is calculated by

$$C_{SEP} = \frac{C_{51} + (\beta_p - 1) C_{61}}{C_{11}}, \quad (3.6)$$

where C_{51} , C_{61} , and C_{11} are the anion, calcium, and water concentrations in the aqueous phase and β_p is measured in the laboratory as an input parameter to the model. S_p is the slope of $\left(\frac{\mu_p^0 - \mu_w}{\mu_w} \right)$ versus C_{SEP} on a log-log plot. E_p and E_G are the temperature dependent parameters of polymer and gel, respectively, which are defined as

$$E_p = \exp\left(\beta_p\left(\frac{1}{T} - \frac{1}{T_{ref}}\right)\right), \quad (3.7)$$

$$E_G = \exp\left(\beta_G\left(\frac{1}{T} - \frac{1}{T_{ref}}\right)\right). \quad (3.8)$$

The reduction in polymer viscosity as a function of shear rate ($\dot{\gamma}$) is modeled by Meter's equation (Meter and Bird, 1964)

$$\mu = \mu_w + \frac{\mu^0 - \mu_w}{1 + \left(\frac{\dot{\gamma}}{\dot{\gamma}_{1/2}}\right)^{P_\alpha - 1}}, \quad (3.9)$$

where $\dot{\gamma}_{1/2}$ is the shear rate at which viscosity is the average of μ^0 and μ_w and P_α is an empirical coefficient. When the above equation is applied to flow in permeable media, μ is usually called apparent viscosity and the shear rate is an equivalent shear rate $\dot{\gamma}_{eq}$. The in-situ shear rate for phase l is modeled by the modified Blake-Kozeny capillary bundle equation for multiphase flow (Lin, 1981; Sorbie, 1991) such as

$$\dot{\gamma}_{eq} = \frac{\dot{\gamma}_c |u_l|}{\sqrt{k_{rl} \bar{k} \phi S_l}}, \quad (3.10)$$

where u_l is Darcy flux of phase l , k_{rl} is relative permeability of phase l , ϕ is porosity, S_l is saturation of phase l , $\dot{\gamma}_c$ is equal to $3.97C \text{ sec}^{-1}$ and C is the shear rate coefficient used to account for non-ideal effects such as slip at the pore walls (Wreath *et al.*, 1990; Sorbie, 1991). The appropriate average permeability \bar{k} is given by

$$\bar{k} = \left[\frac{1}{k_x} \left(\frac{u_{xl}}{u_l} \right)^2 + \frac{1}{k_y} \left(\frac{u_{yl}}{u_l} \right)^2 + \frac{1}{k_z} \left(\frac{u_{zl}}{u_l} \right)^2 \right]^{-1}, \quad (3.11)$$

where k_x , k_y , and k_z are absolute permeability in the x, y, and z directions respectively; u_{xl} , u_{yl} , and u_{zl} are Darcy flux in the x, y, and z directions respectively.

3.1.4 Gel Adsorption

The propagation rate of many water soluble components in porous media is strongly affected by its interaction with the rock matrix. The Langmuir isotherm is used to describe the adsorption level of a component as a function of the concentration of component in the aqueous phase.

$$\hat{C}_G = \frac{a_G C_{G,1}^*}{1 + b_G C_{G,1}^*}, \quad (3.12)$$

where

$$C_{G,1}^* = \frac{(C_{G,1} - \hat{C}_G)}{C_w}, \quad (3.13)$$

is the concentration of component in water after adsorption. The maximum adsorption level depends on salinity, permeability, and temperature, using the following correlation:

$$a_G = \left[a_{G,ref} + a_{Gs} (C_s - C_{s,ref}) + a_{GT} (T - T_{ref}) \right] (\bar{k})^{-S_k}, \quad (3.14)$$

where $a_{G,ref}$, a_{Gs} , and a_{GT} , b_G and S_k are the input parameters.

3.1.5 Permeability Reduction Factor

The adsorption, retention, and filtration cause the resistance to flow or permeability reduction at the pore-scale level. There are two options for the permeability reduction factor in UTGEL. In the first option, the effect of gel on aqueous-phase permeability reduction is taken into account through a residual resistance factor commonly used in polymer flooding:

$$R_{RF} = 1 + \frac{(R_{RF, \max} - 1) b_{rk} C_{4l}}{1 + b_{rk} C_{4l}}, \quad (3.15)$$

where the maximum residual resistance factor is calculated by

$$R_{RF, \max} = \left[1 - \frac{c_{rk} \left(A_{p1} C_{SEP}^{S_p} \right)^{1/3}}{\left(\frac{\sqrt{k_x k_y}}{\phi} \right)^{1/2}} \right]^{-4}, \quad (3.16)$$

where l refers to the phase with the highest polymer concentration, b_{rk} and C_{rk} are the input parameters which depends on the gel type. The effect of permeability reduction is assumed to be irreversible *i.e.*, it does not decrease as polymer concentration decreases, thus, $R_{RF} = R_k$. The viscosity of the phase that contains the polymer is multiplied by the value of the R_k to account for the mobility reduction in the simulator.

In another option, the permeability reduction factor due to the adsorption, retention, and filtration effects is considered as a linear function of adsorption as follows

$$R_K = 1 + (R_{K,max} - 1) \frac{\hat{C}}{\hat{C}_{max}} \quad (3.17)$$

where $R_{K,max}$ is the maximum resistance factor at the maximum adsorption \hat{C}_{max} .

If we want to have the permeability reduction factor for both polymer and gel, the permeability reduction is calculated by

$$R_K = 1 + (R_{K,Pmax} - 1) \frac{\hat{C}_P}{\hat{C}_{P,max}} + (R_{K,BWGmax} - 1) \frac{\hat{C}_G}{\hat{C}_{G,max}} \quad (3.18)$$

where $R_{K,Pmax}$ and $R_{K,BWGmax}$ are the polymer and gel maximum resistance factors at the maximum polymer \hat{C}_{max} and gel \hat{C}_{max} adsorption, respectively.

3.2 pH-SENSITIVE POLYMER

pH-sensitive polymers are very sensitive to the pH and salinity and can swell up to 1,000 times of its own volume (Huh *et al.*, 2005). In this study, pH-sensitive polymer gels have been proposed as an in-depth conformance control tool to improve the sweep efficiency of waterfloods. The gel propagation and swelling deep in the reservoir is controlled by the geochemical reactions between the acid (injected with gel) and the mineral components of the rock (Huh *et al.*, 2005). The conformance control is achieved by gel viscosification deep in the reservoir and diverting the subsequently injected fluids into unswept zones at a critical pH. An accurate estimation of treatment design parameters is necessary for a successful reservoir treatment.

The modeling procedure in UTGEL consists of the following steps to compute the viscosity of the pH-sensitive microgels:

- Compute the equilibrium swelling ratio (Q) from the Brannon-Peppas model (1988, 1990, 1991) in terms of salinity and pH
- Compute the intrinsic viscosity ($[\eta]$) by employing the modified Mark-Houwink equation
- Compute the polymer solution viscosity in the low shear limit (η_0) by employing the Martin equation.
- Compute the polymer solution viscosity (η) at a specific shear rate by employing the Carreau equation. The polymer specific constants (λ and n) are correlated by the Lange and Huh equation (1994).

The following sections discuss the gel properties in detail. The equations used in the UTGEL pertinent to the pH-sensitive gel model are also included.

3.2.1 Equilibrium Swelling Ratio

3.2.1.1 Equilibrium Swelling Ratio

The Brannon-Peppas and Peppas model can be used to characterize the equilibrium swelling of hydrogels in terms of the degree of crosslinking, salinity, and pH.

At swelling equilibrium, the chemical potential of the swelling agent, μ_1 , is equal to the chemical potential of the swelling agent in the solution surrounding the polymer,

μ_1^* :

$$\left(\Delta\mu_1^*\right)_{ion} - \left(\Delta\mu_1\right)_{ion} = \left(\Delta\mu_1\right)_{mix} + \left(\Delta\mu_1\right)_{el} . \quad (3.19)$$

The mixing contribution to the chemical potential of the system is obtained from the Flory's lattice theory (Flory, 1953):

$$(\Delta\mu_1)_{mix} = RT \left[\ln(1 - \nu_{2,s}) + \nu_{2,s} + \chi_1 \nu_{2,s}^2 \right]. \quad (3.20)$$

The elastic contribution derived from the statistical theory of rubber elasticity (Bray and Merrill, 1973) is given by:

$$(\Delta\mu_1)_{el} = RT \left(\frac{V_1}{\nu \overline{M}_c} \right) \left(1 - \frac{2\overline{M}_c}{M_n} \right) \nu_{2,r} \left[\left(\frac{\nu_{2,s}}{\nu_{2,r}} \right)^{1/3} - \frac{1}{2} \left(\frac{\nu_{2,s}}{\nu_{2,r}} \right) \right]. \quad (3.21)$$

The ionic contribution is derived from the summation of the activities of the ions in the solution:

$$(\Delta\mu_1^*)_{ion} - (\Delta\mu_1)_{ion} = V_1 RT \sum_j (c_j - c_j^*), \quad (3.22)$$

where c_j and c_j^* are the concentration of j -ion in solution inside and outside of the polymer network, respectively. With the ionic balance requirements, and assuming that the concentration difference of the mobile electrolyte between the inside and outside of the gel, $(c_s^* - c_s)$ is comparable in magnitude to the concentration of counter-ions, the ionic contribution becomes:

$$(\Delta\mu_1^*)_{ion} - (\Delta\mu_1)_{ion} = V_1 RT \left(\frac{i^2 \nu_{2,s}^2}{4I \nu^2} \right), \quad (3.23)$$

where I is the ionic strength defined as $I = \frac{z_+ z_- \nu c_s^*}{2}$.

For anionic ionomer gels, such as the poly(acrylic acid) hydrogel, an equilibrium is obtained as

$$K_a = \frac{[RCOO^-][H^+]}{[RCOOH]}, \quad (3.24)$$

where $[RCOO^-]$ is the concentration of dissociated polymer chains, $[RCOOH]$ is the concentration of undissociated polymer chains, and $[H^+]$ is the concentration of the hydrogen ion.

The ionization of the polymer chains, i , is defined as

$$i = \frac{[RCOO^-]/[RCOOH]}{1 + [RCOO^-]/[RCOOH]}. \quad (3.25)$$

By using Equation (3.24), Equation (3.25) can be rearranged as

$$i = \frac{K_a/[H^+]}{1 + [K_a]/[H^+]} = \frac{K_a}{10^{-pH} + K_a}. \quad (3.26)$$

The ionic contribution, Equation (3.22), then becomes

$$(\Delta\mu_1^*)_{ion} - (\Delta\mu_1)_{ion} = \frac{V_1 RT}{4I} \left(\frac{\nu_{2,s}}{\bar{\nu}} \right)^2 \left(\frac{K_a}{10^{-pH} + K_a} \right)^2. \quad (3.27)$$

By replacing Equations (3.20), (3.21), and (3.27) into (3.19), we obtain the final expression for the equilibrium swelling of a gel by solvent, Equation (3.10):

$$\begin{aligned} \frac{V_1}{4I} \left(\frac{\nu_{2,s}}{\bar{\nu}} \right)^2 \left(\frac{K_a}{10^{-pH} + K_a} \right)^2 &= \ln(1 - \nu_{2,s}) + \nu_{2,s} + \chi_1 \nu_{2,s}^2 \\ &+ \left(\frac{V_1}{\bar{\nu} M_n} \right) \left(1 - \frac{2\bar{M}_c}{M_n} \right) \nu_{2,r} \left[\left(\frac{\nu_{2,s}}{\nu_{2,r}} \right)^{1/3} - \frac{1}{2} \left(\frac{\nu_{2,s}}{\nu_{2,r}} \right) \right], \end{aligned} \quad (3.28)$$

where V_1 is the molar volume of solvent; I is the ionic strength of solvent; $\nu_{2,s}$ is the polymer volume fraction in the swollen network; $\bar{\nu}$ is the specific molar volume of dry

polymer; K_a is the dissociation constant of ionizable groups on polymer; χ_1 is the polymer-solvent interaction parameter; $\overline{M_c}$ is the average polymer molecular weight between crosslinks; $\overline{M_n}$ is the average molecular weight of polymer before crosslinking; and $\nu_{2,r}$ is the polymer volume fraction in the relaxed state. The polymer volume fraction ($\nu_{2,s}$) can be calculated from Equation (3.28) by a root-finding algorithm since it is hard to obtain an analytical solution for this equation.

Finally, equilibrium swelling ratio can be calculated by the following equation:

$$Q = \frac{1}{\nu_{2,s}} . \quad (3.29)$$

3.2.1.2 Modified Equilibrium Swelling Ratio

Detailed knowledge of a microgel solution viscosity is considered to be one of the most important elements of a successful treatment design. Choi (2005) developed a modeling procedure to calculate an apparent viscosity of polymer microgel and programmed it with FORTRAN. The Newton-Raphson method is used to solve the non-linear form of the modified Brannon-Peppas model to obtain the equilibrium swelling ratio. The biggest disadvantage of this modeling procedure is that it requires the solution of a non-linear equation at each time-step using the Newton-Raphson or other root-finding algorithms; thus, it causes an increase in computational time required. Therefore, a new modeling procedure was necessary to achieve significant savings in computation times.

The new modeling procedure is based on the principles of the modified Brannon-Peppas Equation (3.28), to adjust certain empirical constants to compute the equilibrium swelling ratio (Q) in terms of pH and ionic strength of solution (I).

As a starting point, the pH versus Q curve is analyzed to capture the critical features of this curve. Polymer gel properties from **Table 2.1** are used to construct the “pH vs. Q ” curves as shown in **Figure 2.1**. This curve clearly indicates that the “pH vs. Q ” curve has the “S” shape trend, which is known as an error function or sigmoid function. Different mathematical equations can be applied to obtain a good fit for this trend line. In this study, the “Boltzmann Sigmoid” equation is selected to accurately fit the “S” shape trend. The resulting equation has the form

$$Q = B - \frac{E}{1 + \exp\left(\frac{pH - C}{D}\right)}, \quad (3.30)$$

$$E = B - A, \quad (3.31)$$

where A , B , C , D , and E are empirical constants to fit the “pH vs. Q ” curve.

In the next step, the empirical constants (A , B , C , D) were studied to see if they can be related to microgel properties. Based on extensive studies, the ionic strength (I) was found to accurately match with empirical constants (A , B , C , D). **Figures 2.2** through **2.5** illustrate a set of established correlations where empirical constants are expressed in terms of ionic strength. Next, empirical constants are replaced with corresponding ionic strength expressions into Equation (3.29) to calculate Q . The result is given as a simple equation where only pH and ionic strength are needed to predict the equilibrium swelling ratio of the microgel.

The matching results with the Newton-Raphson iteration algorithm are also included to show the accuracy of the modified model. **Figure 2.6** shows the comparison of Newton-Raphson and modified model to calculate Q in terms of pH and there is a good agreement between the two methods.

The modified viscosity model is well suited for numerical simulators and may be updated as data for new types of microgels become available. Recently, it was coupled with the UTGEL reservoir simulator in an attempt to assess the applicability of the pH-sensitive microgels.

3.2.2 Intrinsic Viscosity using Modified Mark-Houwink Equation

Intrinsic viscosity is a widely used quantity to characterize polymer solution rheology in terms of the size and extension of the polymer molecule. It is defined as the limit of the reduced viscosity or inherent viscosity as the solution concentration approaches zero:

$$[\eta] = \lim_{c \rightarrow 0} \frac{\eta_0 - \eta_s}{\eta_s C}, \quad (3.32)$$

where η_0 is the limiting Newtonian viscosity at the zero shear limit; η_s is the solvent viscosity; and C is the polymer concentration. The intrinsic viscosity provides a link between the average size of polymer molecules and solution rheology.

For a homologous series of narrow molecular weight distribution polymer samples, a simple power-law form, known as the Mark-Houwink equation (Bird *et al.*, 1977) can be used:

$$|\eta| = aM_w^b, \quad (3.33)$$

where a and b are polymer specific empirical constants. Huh *et al.* (2005) modified this correlation by replacing molecular weight with the equilibrium swelling ratio:

$$|\eta| = aQ^b, \quad (3.34)$$

where values of a and b are empirically determined from the laboratory viscosity data.

3.2.3 Martin Equation

The polymer solution viscosity in the low shear limit, η_o , can be determined by the Martin equation (Bird *et al.*, 1977) because the low shear limit viscosity, η_o , has the dominant effect on the solution viscosity:

$$\eta_o = \eta_s + \eta_s C|\eta| \exp(k'' C|\eta|), \quad (3.35)$$

where k'' is empirical constant. The high shear limit viscosity, η_∞ , is close to the solvent viscosity.

3.2.4 Carreau Equation

Swollen hydrogel suspensions show purely viscous, shear-thinning rheological behavior (Budtova *et al.*, 1994). The Carreau model is a widely used rheological model for such solutions (Canella *et al.*, 1988):

$$\eta = \eta_\infty + [\eta_o - \eta_\infty] \left[1 + (\lambda\dot{\gamma})^\alpha \right]^{(n-1)/\alpha}, \quad (3.36)$$

where η_o and η_∞ are the limiting Newtonian viscosities at the low and high shear limits, respectively; $\dot{\gamma}$ is shear rate; λ and n are polymer specific constants; and α is generally taken to be 2. The Carreau equation shows a power-law relation at intermediate shear rates.

Lange and Huh (1994) successfully correlated the following empirical relations to define the empirical constants in the Carreau equation:

$$(n-1) = e_1 + e_2 C |\dot{\gamma}|, \quad (3.37)$$

$$\lambda = e_3 + e_4 (C |\dot{\gamma}|)^{e_5}, \quad (3.38)$$

where e_1 , e_2 , e_3 , e_4 are the empirical constants to each specific polymer. With the above equations, the bulk viscosity (viscometer viscosity), η , is obtained in terms of the swollen hydrogel suspension concentration, pH, salinity, and shear rate.

Table 3.1 Summary of the Best-Fit Model Parameters (Huh *et al.*, 2005)

Polymer Name	EZ-2	974 PNF	981	EZ-2	EZ-2	EZ-2	EZ-2
Polymer Concentration, wt%	3	3	3	2	1	3	3
Salt Name	NaCl	NaCl	NaCl	NaCl	NaCl	NaCl	CaCl2
Salt Concentration, wt%	3	3	3	3	3	1	1
I. Equilibrium Swelling Model							
\bar{V}_1 , ccm/g	0.71	0.71	0.71	0.71	0.71	0.71	0.71
pKa	4.35	4.5	4	4.35	4.35	3.8	5.2
Mn ave., gm/mol	1,500,000	1,500,000	1,500,000	1,500,000	1,500,000	1,500,000	1,500,000
Mc ave., gm/mol	80,000	90,000	100,000	80,000	80,000	80,000	80,000
v _{2,r}	0.2	0.2	0.2	0.2	0.2	0.2	0.2
χ_1	0.2	0.9	0.9	0.2	0.2	0.2	0.2
V1, ccm/mol	18	18	18	18	18	18	18
I	0.54	0.54	0.54	0.534	0.529	0.177	0.281
Qmin (low pH)	121.2	1.6	1.6	121.2	121.2	121.2	121.2
Qmax (High pH)	1,379.00	1,455.90	1,565.70	1,387.80	1,396.30	2,676.40	2,035.30
II. Mark-Houwink Equation							
a	0.15	80.66	121.77	0.14	0.13	1.09	0.07
b	1.17	0.28	0.21	1.16	1.11	0.83	1.19
$ \eta $ min (low pH), cP	39.3	92.5	134.8	37.3	26.9	58	22.8
$ \eta $ max (high pH), cP	669.6	641.3	572.7	630	404.4	752.4	662.3
III. Martin Equation							
η_s , cP	1	1	1	1	1	1	1
C, g/ccm	0.03	0.03	0.03	0.02	0.01	0.03	0.03
k''	0.4	0.4	0.4	0.4	0.4	0.4	0.4
η_0 min (low pH), cP	2.9	9.4	21.4	2	1.3	4.5	1.9
η_0 max (high pH), cP	61,995	42,296	16,588	1,947	21.4	188,323	56,199
IV. Carreau Equation							
η^∞ , cP	0	0	0	0	0	0	0
α	2	2	2	2	2	2	2
e1	-0.038	0.056	0.095	-0.03	-0.009	-0.054	-0.022
e2	0.032	0.026	0.022	0.04	0.033	0.031	0.032
nmin (low pH), cP	1	0.872	0.816	1	1	1	1
nmax (high pH), cP	0.393	0.446	0.529	0.521	0.874	0.348	0.389
e3	0	1.96	2.2	0	0	0	0
e4	1.00E-07	1.00E-07	1.00E-07	1.00E-07	1.00E-07	1.00E-07	1.00E-07
e5	5.842	5.62	5.576	6.688	12.013	5.536	5.741
λ_{min} (low pH)	0	1.96	2.202	0	0	0	0
λ_{max} (high pH)	4.093	3.607	2.971	2.285	1.95	3.114	2.835

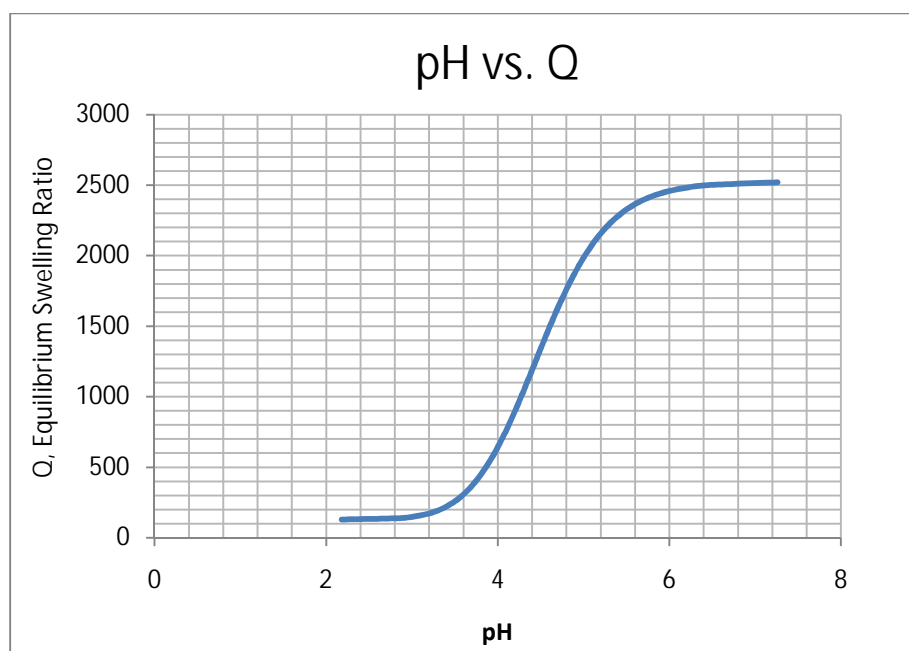


Figure 3.1 Equilibrium Swelling Ratio Versus pH

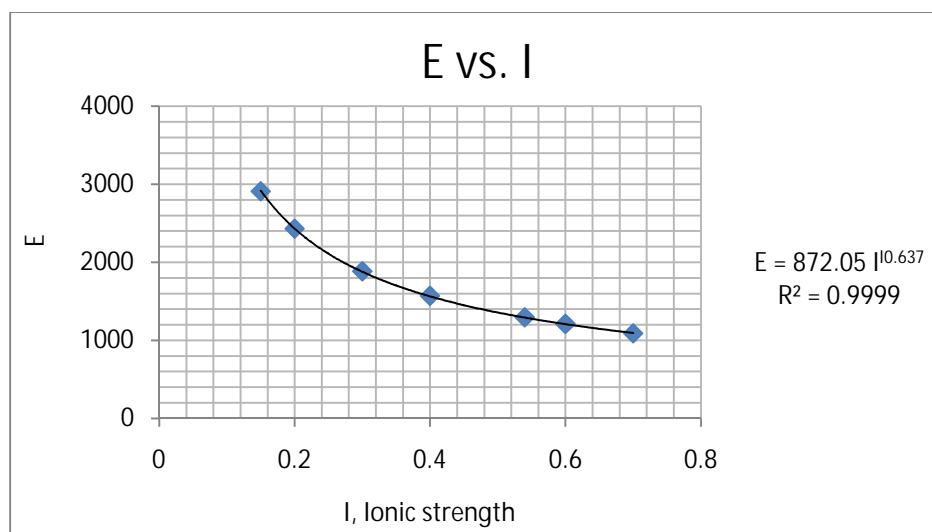


Figure 3.2 Empirical Constant (E) Versus Ionic Strength of Solution

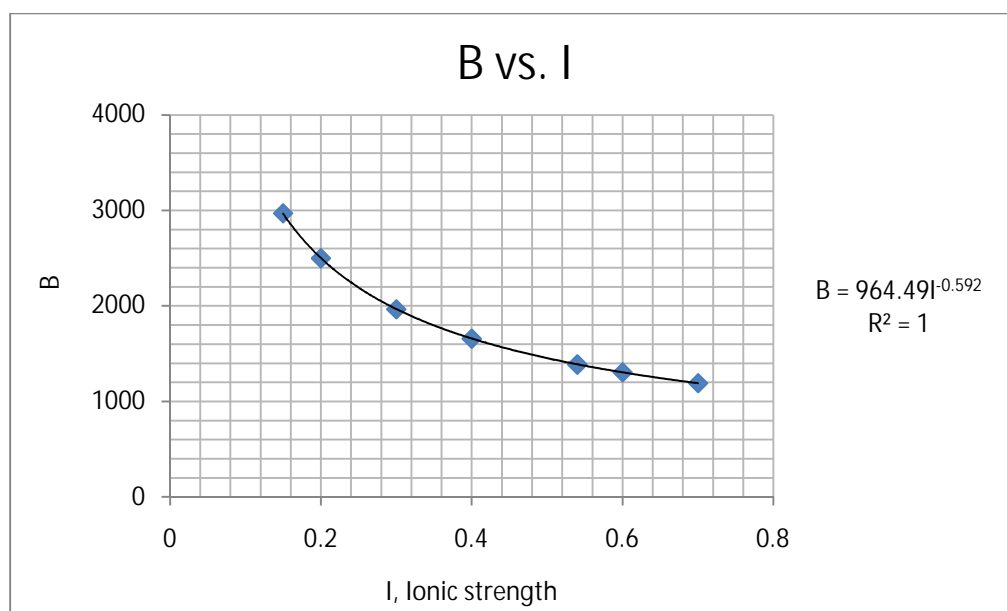


Figure 3.3 Empirical Constant (B) Versus Ionic Strength of Solution

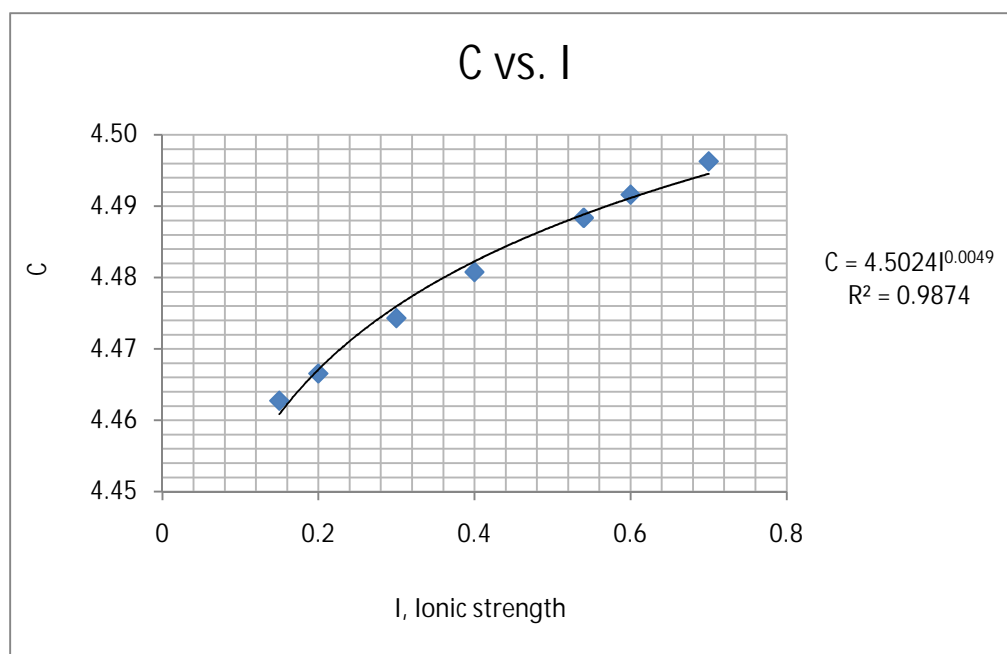


Figure 3.4 Empirical Constant (C) Versus Ionic Strength of Solution

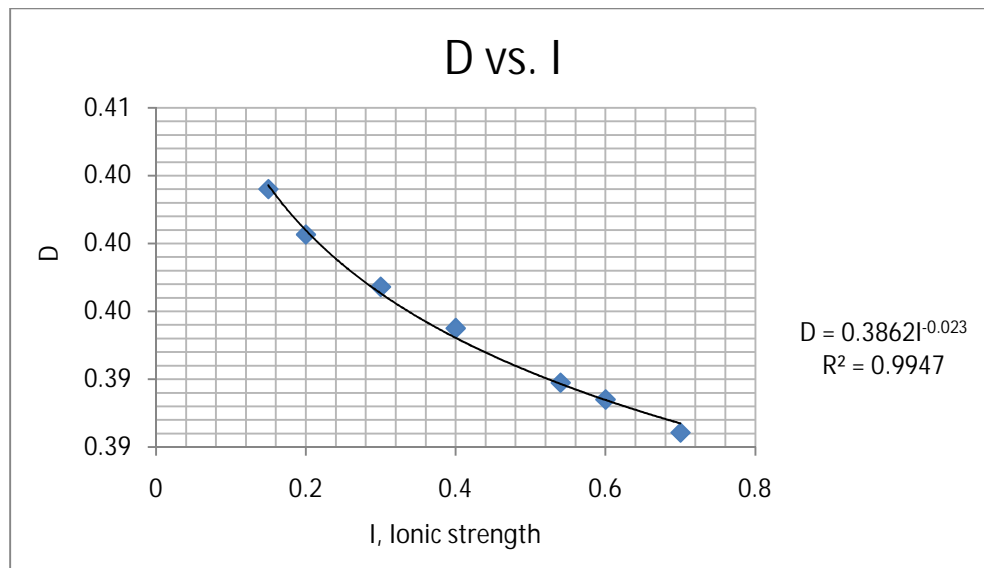


Figure 3.5 Empirical Constant (D) Versus Ionic Strength of Solution

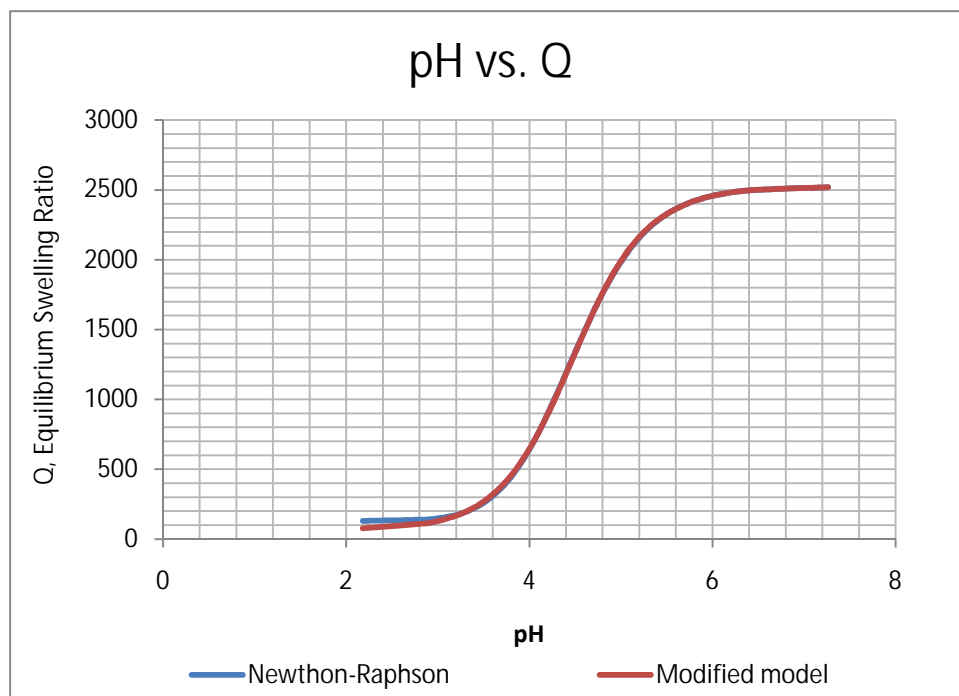


Figure 3.6 Comparison of Newton-Raphson and Modified Model

Chapter 4: Sensitivity Analysis of Thermally Active and pH-Sensitive Polymers

In this chapter, the UTGEL simulator, equipped with thermally active and pH-sensitive polymer models, was used to study the impact of polymer gels on conformance control and incremental oil recovery. This chapter is divided into two sections. The first section describes the sensitivity analysis of thermally active polymers. The second section describes the sensitivity analysis of pH-sensitive polymers.

4.1 SENSITIVITY ANALYSIS OF THERMALLY ACTIVE POLYMERS

A sensitivity analysis was conducted to determine the effects of treatment fluid concentration, treatment slug size, oil-to-water viscosity ratio, permeability contrast, and vertical to horizontal permeability ratio on incremental oil recovery through conformance control. All cases run with and without thermally active polymer to investigate the impact of treatment on oil recovery. Appendix A provides a sample UTGEL input file for a thermally active polymer.

4.1.1 Base Case Model

The base case model is a 3D model as shown in **Figure 4.1**. **Table 4.1** summarizes simulation data for the Bright Water® base case model. The injection rate is kept constant at 500 ft³/day. The high-permeability zone (thief zone) is located in the middle zone (layer 2). The thief zone permeability is 1500 mD and upper (layer 1) and lower zones (layer 3) have a constant permeability of 50 mD. Vertical-to-horizontal

permeability ratio (k_v / k_h) is 0.1. Porosity is 20% and constant throughout the model. Water is injected for 540 days (1 pore volume) and then is followed by 5% of the channel volume (CV) Bright Water® injection (7.5 days) using the same injection rate. The thermally active polymer is injected in 5000 ppm. The reservoir and injection temperatures are 200°F and 60°F, respectively. The thermally active polymer is activated at 150°F. The treatment is followed by 1 pore volume (PV) of water injection. **Figure 4.2** illustrates the temperature profile after 540 days of water injection and **Figure 4.3** illustrates the permeability reduction. As shown in **Figure 4.3**, the strongest permeability reduction is formed in the high permeability layer between the injection and production wells. **Figure 4.4** shows the incremental oil recovery and **Figure 4.5** shows incremental oil production resulted from thermally active polymer. Base case simulations indicate that thermally active polymer treatments divert flow into low permeability zones and increase incremental oil recovery.

4.1.2 Treatment Fluid Concentration

In this study, treatment concentrations of 5,000, 10,000, and 15,000 ppm were investigated to determine the effect on incremental oil recovery. **Figure 4.6** indicates that incremental oil recovery increases as treatment concentration is increased. A simple explanation of this behavior is that by increasing the treatment concentration, a high resistance bank can be formed in the high-permeability zones and divert the flow into unswept zones. However, 15,000 and 10,000 ppm treatments yield slightly more oil

recovery than a 5,000 ppm treatment. Therefore, economics may favor the use of small treatment concentrations.

4.1.3 Treatment Slug Size

In this study, 5%, 10%, and 15% of the channel volume (CV) slug sizes were investigated to determine the sensitivity of slug size on incremental oil recovery. Simulation results revealed that the treatment slug size depends on vertical-to-horizontal permeability ratio, gel dispersion (dilution), and mobility ratio, among others. **Figure 4.7** shows that injecting a bigger slug size is desirable for better treatment efficiency. Injecting a bigger slug size diverts flow into low-permeability zones and results in incremental oil. However, it is important to minimize the gel penetration into low-permeable zones; otherwise, it will reduce the ability of injected water to be diverted into previously unswept zones.

4.1.4 Vertical-to Horizontal Permeability Ratio

In this study, the vertical to horizontal permeability ratio (k_v / k_h) was investigated to determine its impact on the treatment's performance. **Figures 4.8** and **4.9** illustrate two cases in which all design parameters are kept the same except for the k_v / k_h . For low k_v / k_h values, the larger portion of thermally active polymer is placed in the high-permeable layers. As a result, the flow is diverted into unswept zones and significant incremental oil production is achieved from these zones. However, for high k_v / k_h

values, the thermally active polymer can cross-flow into low-permeable layers and reduce the permeability of the low-permeable zones. As a result, little conformance improvement is achieved and most of the oil is left in unswept zones. Therefore, simulation results indicate that low k_v/k_h is a desirable factor for better treatment efficiency as shown in **Figure 4.10**. It is worth mentioning that the vertical-to-horizontal permeability ratio depends on thief zone location, reservoir heterogeneity, mobility ratio, and flow pattern. Therefore, a detailed analysis is required to better understand the impact of k_v/k_h on incremental oil recovery.

4.1.5 Permeability Contrast

In this study, permeability contrasts of the thief zone and the rest of the reservoir were investigated to determine the impact on oil recovery. Simulation results reveal that permeability contrast appears to be one of the most important parameters that impacts treatment performance. **Figure 4.11** shows that high permeability contrast is a desirable factor for better treatment efficiency. It can be explained by the fact that the high-permeable layer takes the larger portion of the injected water and gel. As a result, the gel has more impact on reducing the permeability of the high-permeable layer.

4.1.6 Oil-to-Water Viscosity Ratio

Oil-to-water viscosity ratio was studied to determine its impact on incremental oil recovery. **Figure 4.12** shows the incremental oil recovery for different oil-to-water viscosity ratios. For lower viscosity ratio waterfloods, incremental oil recovery is lower

due to lower remaining oil saturation in the reservoir. In contrast, incremental oil recovery for higher viscosity ratios is lower because of viscous fingering. Since the water carrying thermally active polymer preferentially flows through viscous fingers, it diverts the flow into unswept zones upon activation. Therefore, a high oil-to-water viscosity ratio is a desirable factor for better treatment efficiency.

4.2 SENSITIVITY ANALYSIS OF pH-SENSITIVE POLYMERS

A sensitivity analysis was conducted to determine the effects of treatment fluid concentration, treatment slug size, oil-to-water viscosity ratio, permeability contrast, and vertical to horizontal permeability ratio on incremental oil recovery through conformance control. All cases run with and without pH-sensitive polymer to investigate the impact of treatment on oil recovery. Appendix B provides a sample UTGEL input file for a pH-sensitive polymer.

4.2.1 Base Case Model

The base case model is a 3D model as shown in **Figure 4.13**. **Table 4.2** summarizes simulation data for the pH-sensitive polymer base case model. The injection rate is kept constant at 500 ft³/day. The high-permeability zone (thief zone) is located in the middle zone (layer 2). The thief zone permeability is 1500 mD and upper (layer 1) and lower zones (layer 3) have a constant permeability of 50 mD. The vertical-to-horizontal permeability ratio (k_v / k_h) is 0.1. Porosity is 20% and constant throughout the model. Water is injected for 540 days (1 pore volume) and then followed by 5% of the

channel volume (CV) pH-sensitive polymer injection (7.5 days) using the same injection rate. The pH-sensitive polymer is injected in 0.5 weight%. The treatment is followed by 1 pore volume (PV) of water injection. **Figure 4.14** shows the incremental oil recovery and **Figure 4.15** shows incremental oil production resulting from pH-sensitive polymer treatment. Base case simulations indicate that pH-sensitive polymer treatments divert flow into low permeability zones and increase incremental oil recovery.

4.2.2 Treatment Fluid Concentration

In this study, treatment concentrations of 0.5, 1, and 1.5 weight% were investigated to determine the effect on incremental oil recovery. **Figure 4.16** indicates that incremental oil recovery increases as treatment concentration is increased. A simple explanation of this behavior is that by increasing the treatment concentration, a high resistance bank can be formed in the high-permeability zones and divert the flow into unswept zones.

4.2.3 Treatment Slug Size

In this study, 5%, 10%, and 15% of the channel volume (CV) slug sizes were investigated to determine the sensitivity of slug size on incremental oil recovery. Simulation results revealed that the treatment slug size depends on the vertical-to-horizontal permeability ratio, gel dispersion (dilution), and mobility ratio, among others. **Figure 4.17** shows that injecting a bigger slug size is desirable for better treatment efficiency. Injecting a bigger slug size diverts flow into low-permeability zones and

results in incremental oil. However, it is important to minimize the gel penetration into low-permeable zones; otherwise, it will reduce the ability of injected water to be diverted into previously unswept zones.

4.2.4 Vertical-to-Horizontal Permeability Ratio

In this study, the vertical to horizontal permeability ratio (k_v / k_h) was investigated to determine its impact on treatment performance. **Figure 4.18** illustrates the incremental oil recovery for different vertical to horizontal permeability ratios. Simulation results show that low k_v / k_h is a desirable factor for better treatment efficiency. The optimum k_v / k_h around 0.01 was observed during the simulation studies.

4.2.5 Permeability Contrast

In this study, permeability contrasts of the thief zone and the rest of the reservoir were investigated to determine the impact on oil recovery. Simulation results reveal that permeability contrast appears to be one of the most important parameters that impacts treatment performance. **Figure 4.19** shows that high permeability contrast is a desirable factor for better treatment efficiency. It can be explained by the fact that the high-permeable layer takes the larger portion of the injected water and gel. As a result, the gel has more impact on reducing the permeability of the high-permeable layer.

4.2.6 Oil-to-Water Viscosity Ratio

Oil-to-water viscosity ratio was studied to determine its impact on incremental oil recovery. **Figure 4.20** shows the incremental oil recovery for different oil-to-water viscosity ratios. Simulation results suggest that a high viscosity ratio is a desirable factor for better treatment efficiency. The optimum oil-to-water viscosity ratio approximately 8 was observed during the simulation studies.

4.3 SUMMARY AND CONCLUSIONS

Our sensitivity analysis results demonstrate that in-depth conformance control with thermally active polymer provide an efficient way of profile modification deep in the reservoir. Some of the important observations of this study include

- Bright Water® and pH-sensitive polymers are expandable materials which can create resistance to flow in high-permeable zones
- Bright Water® and pH-sensitive treatment result in diversion of water flow into unswept zones, low oil-water-ratio, and incremental oil recovery
- Polymer adsorption is a function of solution concentration, rock mineralogy, and slug size
- Permeability contrast appears to be one of the most important parameters that impacts treatment performance.

Table 4.1 Simulation Data for Base Case Bright Water® Treatment

Length, ft	300
Width, ft	300
Thickness, ft	15
Grid	15x15x3
Depth, ft	2000
Number of wells	2
Initial water saturation	0.3
Water viscosity, cP (at 25°F)	1.9
Oil viscosity, cP (at 25°F)	12
Bright Water® concentration, ppm	5000
Simulation time, PV	2
Permeability contrast	30
Reservoir temperature, °F	200
Activation temperature, °F	150
Porosity	0.2

Table 4.2 Simulation Data for Base Case pH-Sensitive Polymer Treatment

Length, ft	300
Width, ft	300
Thickness, ft	15
Grid	15x15x3
Depth, ft	2000
Number of wells	2
Initial water saturation	0.3
Water viscosity, cP	1
Oil viscosity, cP	4
Polymer concentration, weight%	0.5
Simulation time, PV	2
Permeability contrast	30
Porosity	0.2

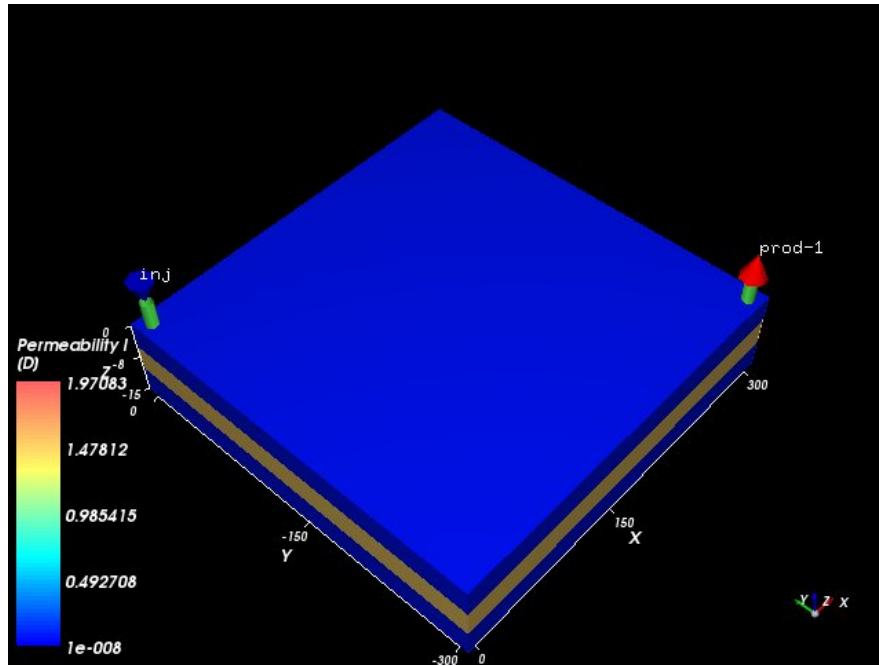


Figure 4.1 The Conceptual 3D Model with Three Layers. Permeability of the Thief Zone is 1500 mD and Other Layers are 50 mD.

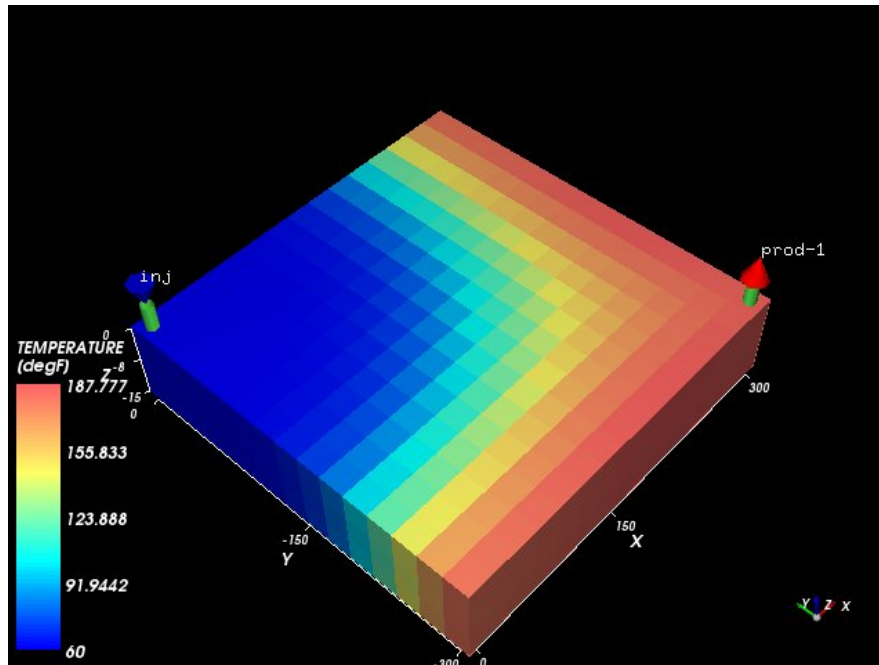


Figure 4.2 Temperature Profile after 540 Days (1 PV) of Water Injection

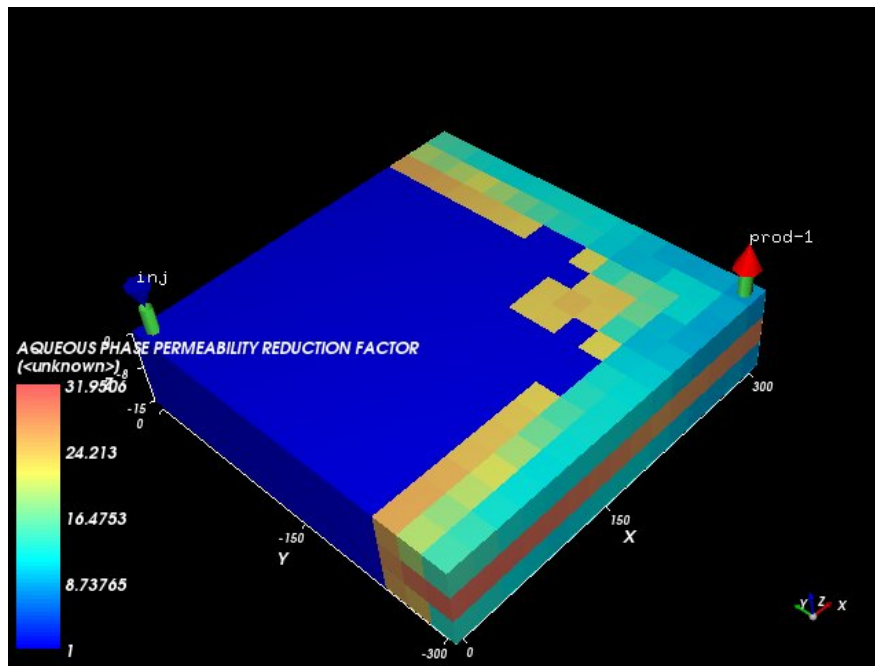


Figure 4.3 Permeability Reduction Factor in Thief Zone

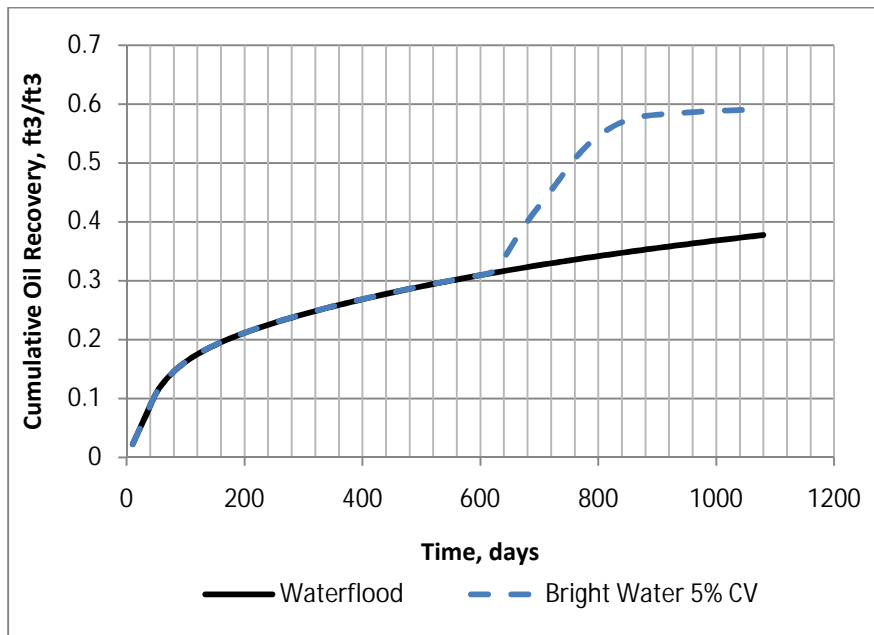


Figure 4.4 Cumulative Oil Recovery after Bright Water® Treatment

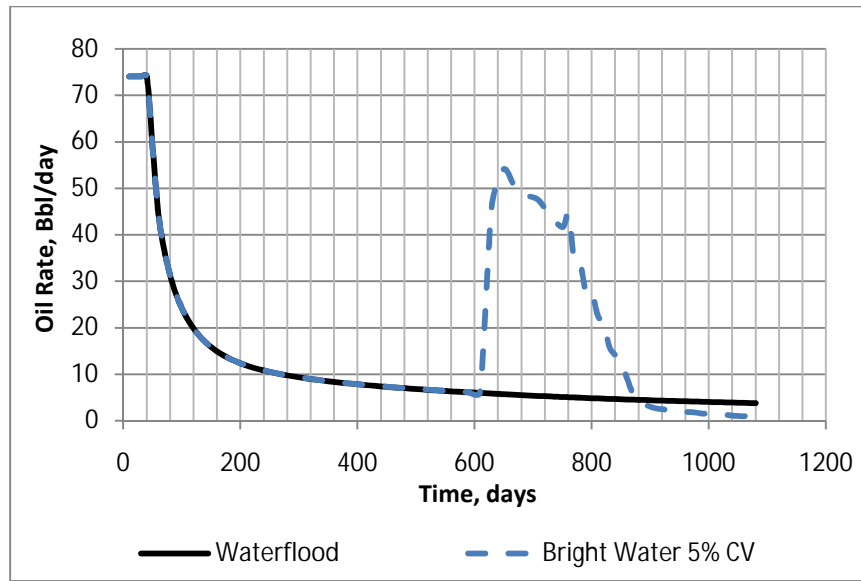


Figure 4.5 Incremental Oil Production Rate after Bright Water® Treatment

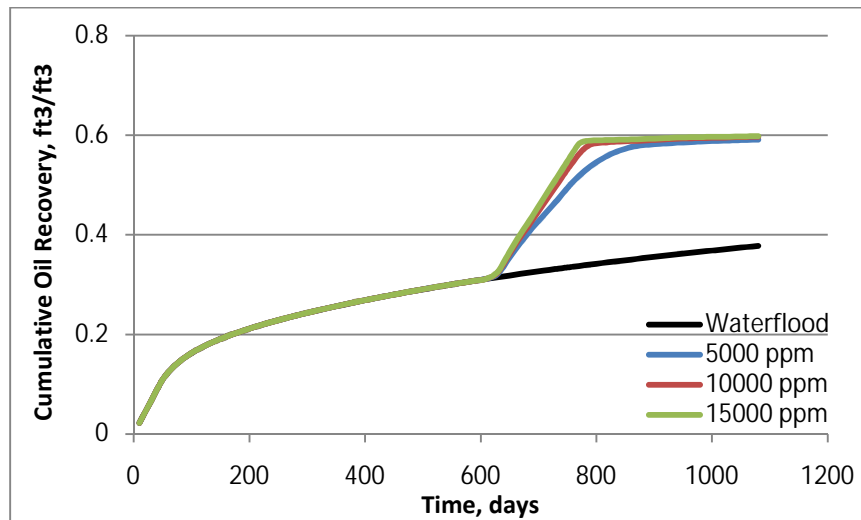


Figure 4.6 Comparison of Incremental Oil Recovery for Different Treatment Concentrations

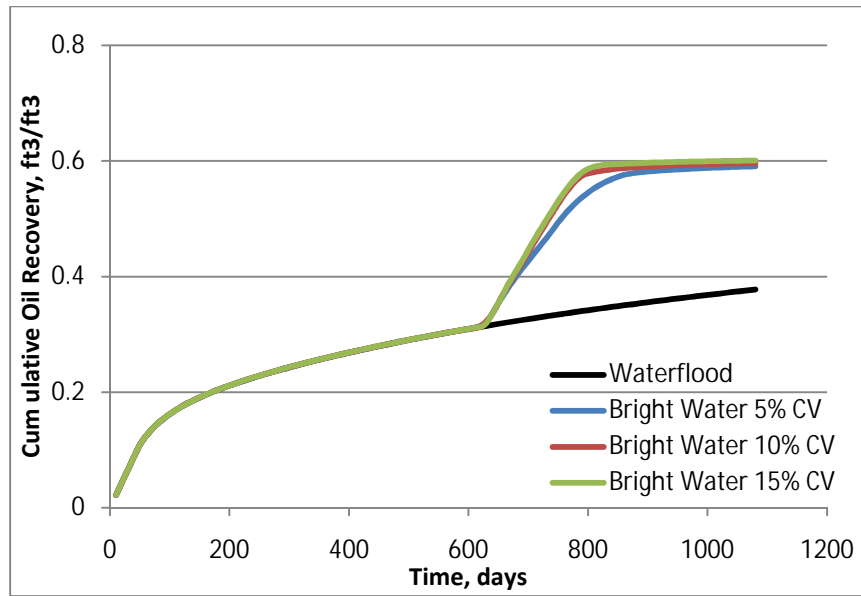


Figure 4.7 Comparison of Incremental Oil Recovery for Different Treatment Slug Sizes

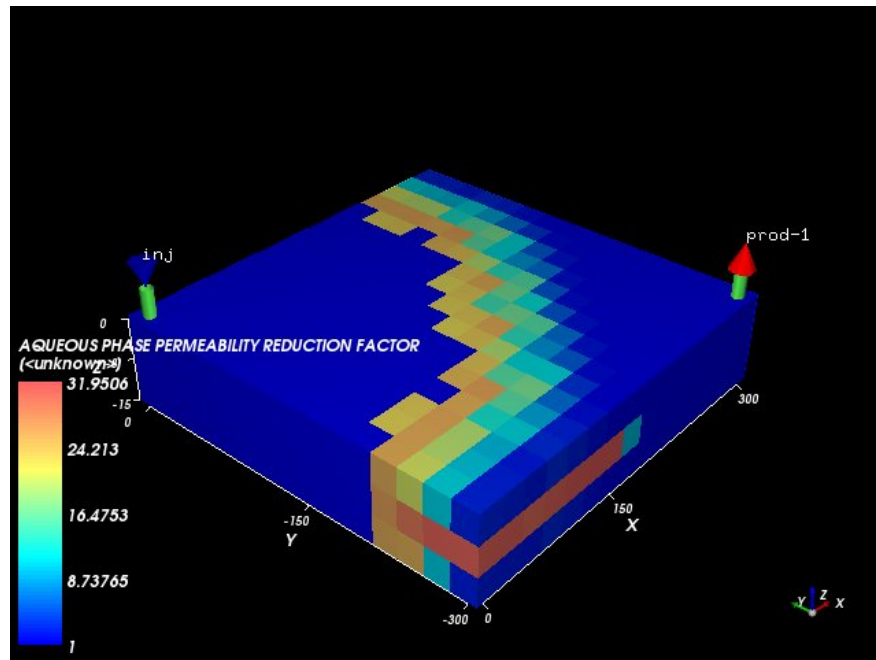


Figure 4.8 Permeability Reduction Profile for $k_v / k_h = 0.1$

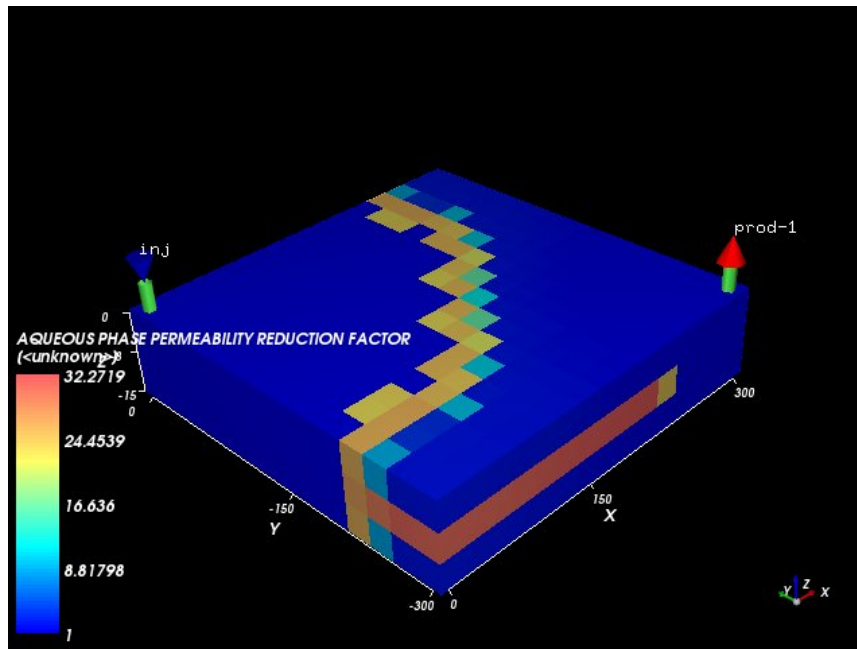


Figure 4.9 Permeability Reduction Profile for $k_v / k_h = 0.001$

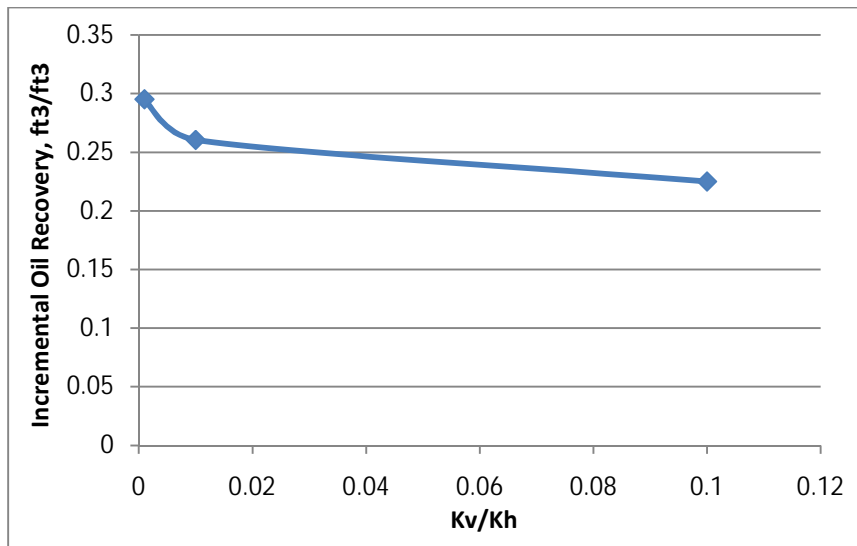


Figure 4.10 Impact of K_v / K_h on Incremental Oil Recovery

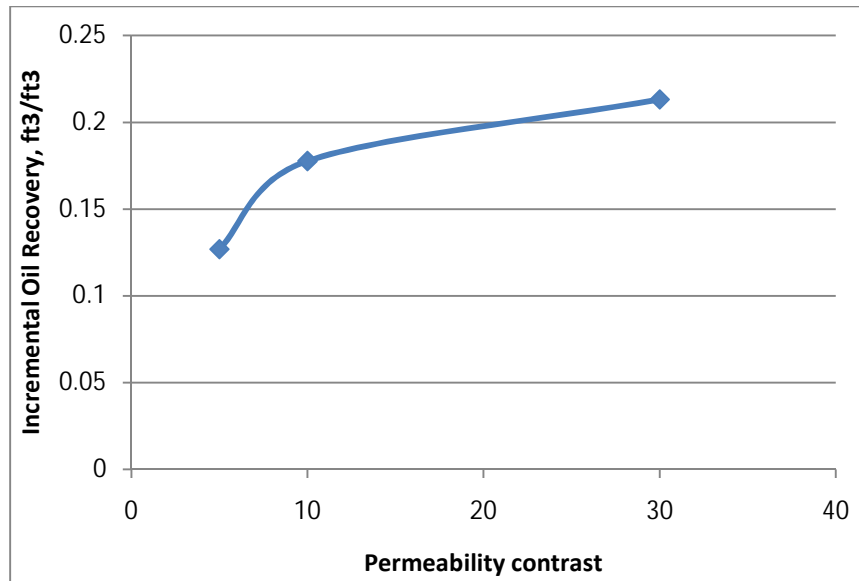


Figure 4.11 Impact of Permeability Contrast on Incremental Oil Recovery

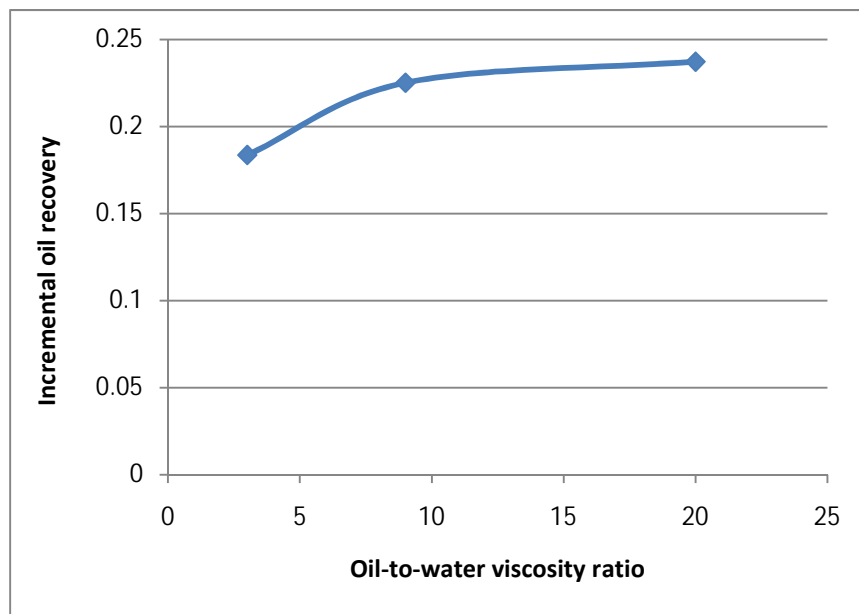


Figure 4.12 Impact of Oil-To-Water Viscosity Ratio on Incremental Oil Recovery

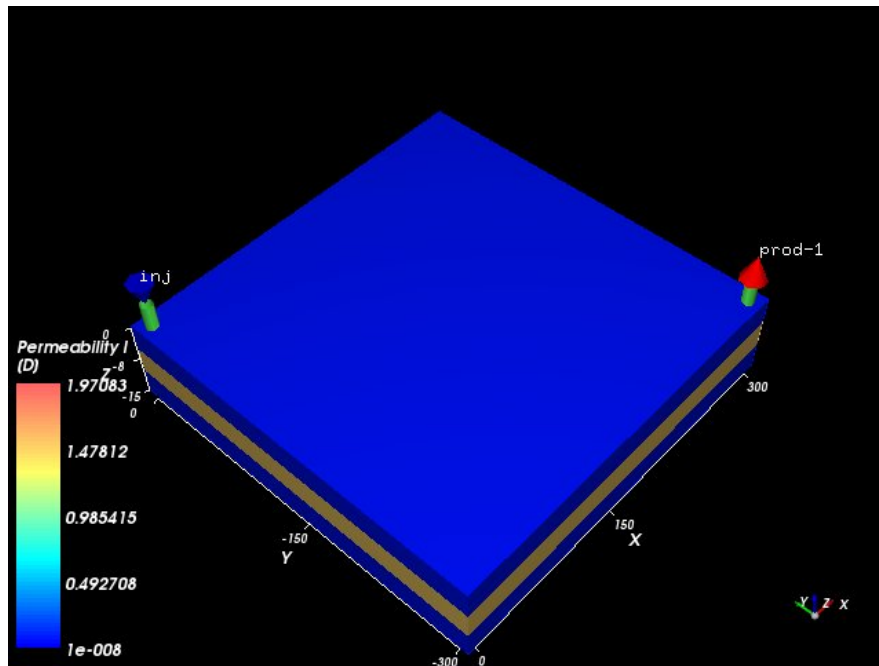


Figure 4.13 The Conceptual 3D Model with Three Layers. Permeability of the Thief Zone is 1500 mD and Other Layers are 50 mD.

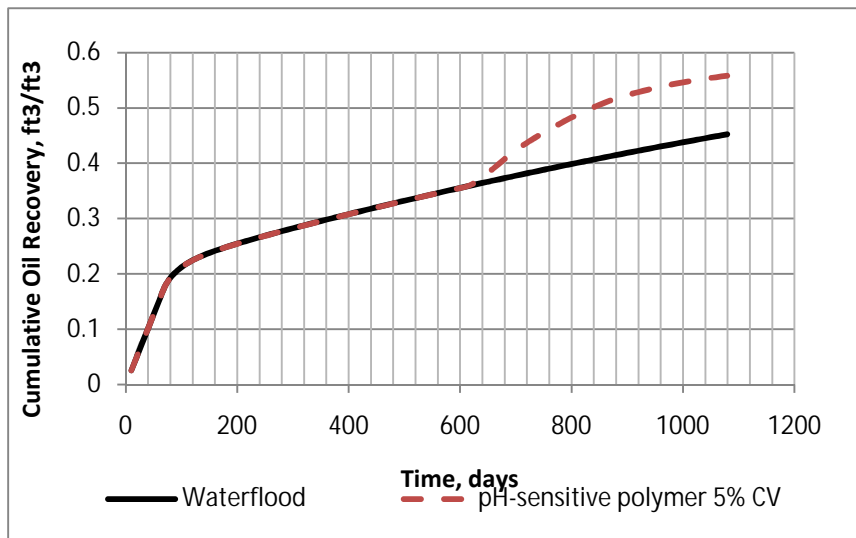


Figure 4.14 Cumulative Oil Recovery after pH-sensitive Polymer Treatment

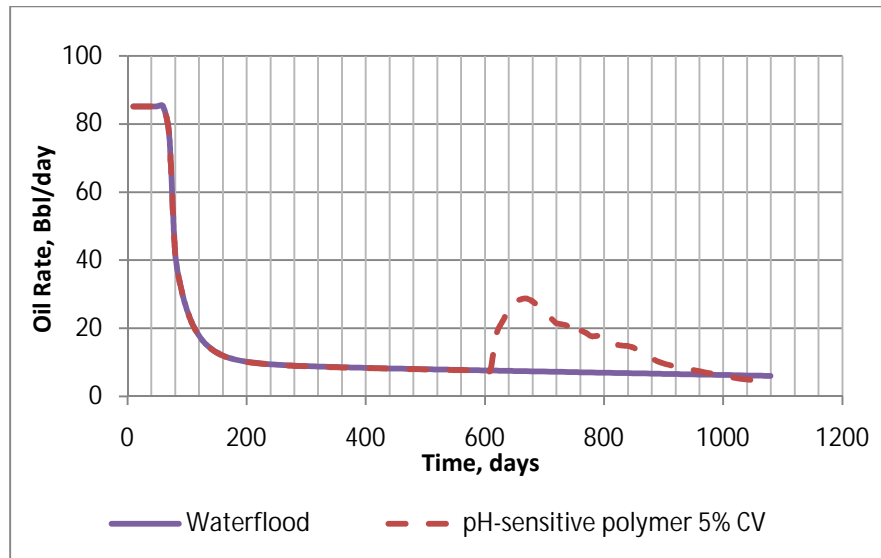


Figure 4.15 Incremental Oil Production Rate after pH-sensitive Polymer Treatment

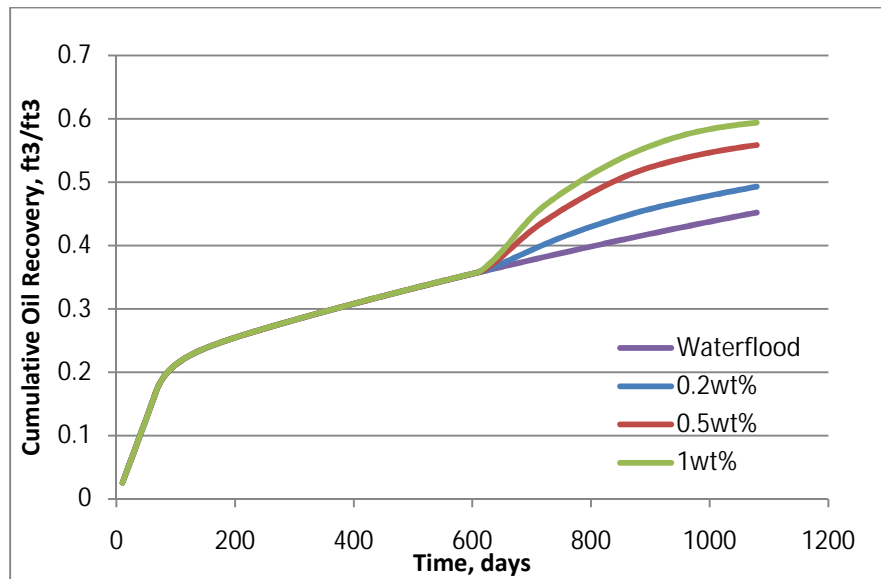


Figure 4.16 Comparison of Incremental Oil Recovery for Different Treatment Concentrations

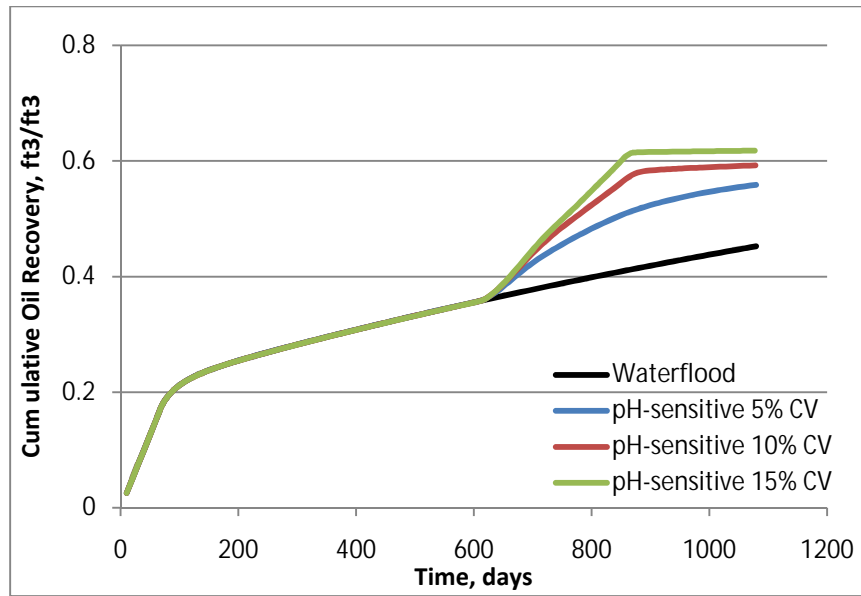


Figure 4.17 Comparison of Incremental Oil Recovery for Different Treatment Slug Sizes

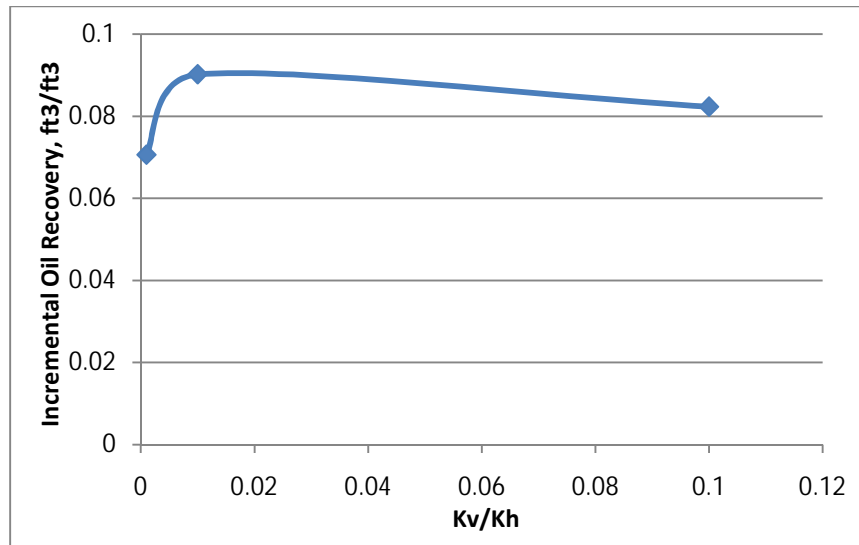


Figure 4.18 Impact of k_v / k_h on Incremental Oil Recovery

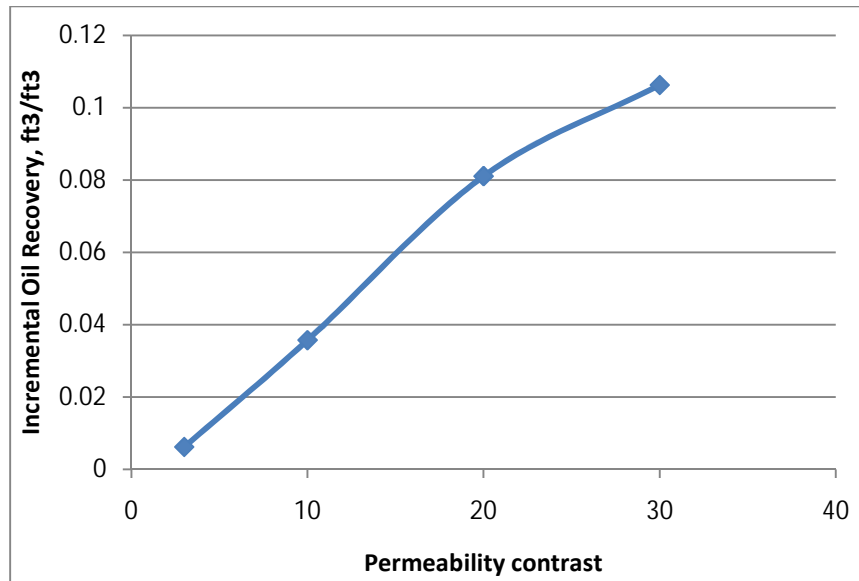


Figure 4.19 Impact of Permeability Contrast on Incremental Oil Recovery

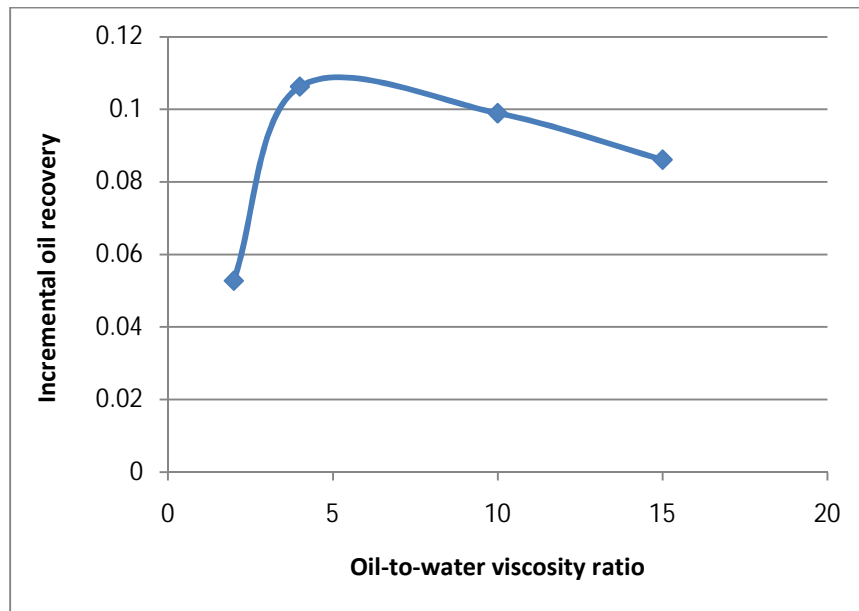


Figure 4.20 Impact of Oil-To-Water Viscosity Ratio on Incremental Oil Recovery

Chapter 5: Field Case Simulation of Thermally Active Polymers

5.1 INTRODUCTION

Simulation studies of three-dimensional thermally active polymer (Bright Water®) treatments for in-depth conformance control have been published by several authors. Garmeh *et al.* (2011) studied three-dimensional conceptual model using CMG simulator to evaluate benefits of Bright Water® in waterflooded reservoirs. They simulated thermally active polymers using an eight-layer reservoir model with a permeability contrast of 30:1 to investigate the treatment effect in more realistic three-dimensional simulations. Their results showed that the majority of the Bright Water® goes to the thief zone and; therefore, the most significant adsorption/retention and resistance factors occur in the high-permeable zones.

Izgec *et al.* (2012) investigated the effect of different parameters on the success of a conformance control treatment. They developed a methodology for accurate determination of the conformance slug size which is based on the temporal moment and residence time distribution analysis (RTDA) of interwell tests. Their studies showed that low k_v/k_h is desirable if the popping agent is placed near the producer while a low k_v/k_h is desirable for near injector placement. They concluded that activation, or placement location, is the most important variable in conformance improvement treatments with Bright Water® technology.

Most of thermally active polymer treatments reported in the literature have used only one or two wells. However, the number of simulated wells may have significant effect on conformance control agent injection and the treatment performance. In this chapter, Bright Water® treatment simulations were performed in a synthetic heterogeneous oil field case to divert the water flow into poorly swept zones.

5.2 SIMULATION STRATEGY

An area with length of 2100 ft and width of 2400 ft was simulated. The thickness of the simulated reservoir was 37 ft. There are seven production and ten injection wells in this area. The physical properties used for the simulation studies are given in **Table 5.1**. The injection rate of Producer 1 through Producer 6 was almost twice higher than Producer 7 through Producer 10 because of higher flow capacitance. The reservoir and injection temperatures are 180°F and 140°F, respectively. **Figure 5.1** shows the temperature profile before Bright Water® treatment. The thermally active polymer is activated at 150°F. **Figure 5.2** shows the permeability distribution used for this study. Appendix C provides a sample UTGEL input file for base case run.

5.2.1 Initial Water Saturation

The initial water saturation was obtained by simulating water injection starting at a residual saturation of 0.2 for all layers. The reservoir was waterflooded for 367 days (5 PV) until the average water saturation reached 0.72. The average water cut of production wells was around 0.98 after 367 days. **Figure 5.3** shows the water saturation profile after

367 days of water injection. As it is shown, all wells except Producer 1 and Producer 3 have reached high water saturation levels. Therefore, Producer 1 and Producer 3 were selected for treatment to divert the water flow into unswept zones. Poor sweep efficiency was caused by high permeability contrast (12:1) between thief zone and matrix.

5.2.2 Thermally Active Polymer Treatments

Bright Water® was injected for 14.5 days (0.2 PV) at $24036.5 \text{ ft}^3 / D$ for Injector 1 through Injector 6 and $14036.5 \text{ ft}^3 / D$ for Injector 7 through Injector 10. Treatment concentration was varied from 1000 to 3000 ppm to allow enough permeability reduction factor in thief zones. **Figure 5.4** shows that injection well bottomhole pressure increased after Bright Water® activation compared to water injection. The bottomhole pressure should be measured periodically to prevent from fracturing the reservoir. The water injection resumed after the treatment. The injection rate was kept constant to allow enough time for Bright Water® to form resistance to flow deep in the reservoir.

5.3 SIMULATION RESULTS

Figure 5.5 shows that aqueous phase permeability reduction was developed by gel activation close to the Producers 1 and 7. The maximum permeability reduction factor was around 170 and this value was enough to modify water flow profile in these simulation studies.

Figure 5.6 and **Figure 5.7** show that Bright Water® treatment resulted in an increase in the oil cut for Producer 1 and Producer 3 as well. **Figure 5.8** also shows that

Bright Water® treatment resulted in incremental oil recovery compared to waterflood. Our results suggest that in-depth profile modification caused additional oil to be swept toward the producing wells.

The resistance factor created by polymer viscosity and adsorption in the thief zones is believed to be the main factor that diverts chase water to displace unswept oil zones. **Figure 5.9** compares water-oil-ratio response for case with and without gel treatment at producer 1. As it is shown, water-oil-ratio of Producer 1 significantly drops from 60 to about 1. Producer 3 also positively responded to the treatment and showed decrease in water-oil-ratio from 50 to about 1 as shown in **Figure 5.10**.

Our results showed that permeability reduction is a function of slug size, polymer concentration, and adsorption level. Simulation studies also indicate that it is more desirable to place the Bright Water® bank deep in the reservoir, close to producer.

5.4 SUMMARY AND CONCLUSIONS

Our simulation studies demonstrate that in-depth conformance control with thermally active polymer provide an efficient way of profile modification deep in the reservoir. Some of the important observations of this study include:

- Bright Water® is an expandable material that can create resistance to flow in high-permeable zones
- Bright Water® treatment results in diversion of water flow into unswept zones, low oil-water-ratio, and increase in the oil cut

- Polymer adsorption is a function of solution concentration, rock mineralogy, and slug size
- It is more desirable to place the Bright Water® deep in the reservoir and close to producer.

Table 5.1 Simulation Data for Field Case

Length, ft	2100
Width, ft	2400
Thickness, ft	37
Grid	11x12x19
Depth, ft	1965.77
Number of wells	17
Initial water saturation	0.2
Water viscosity, cP	1.5
Oil viscosity, cP	3.4
Bright Water® concentration, ppm	1000-3000
Simulation time, PV	10
Permeability contrast	12
Reservoir temperature, °F	180
Activation temperature, °F	140

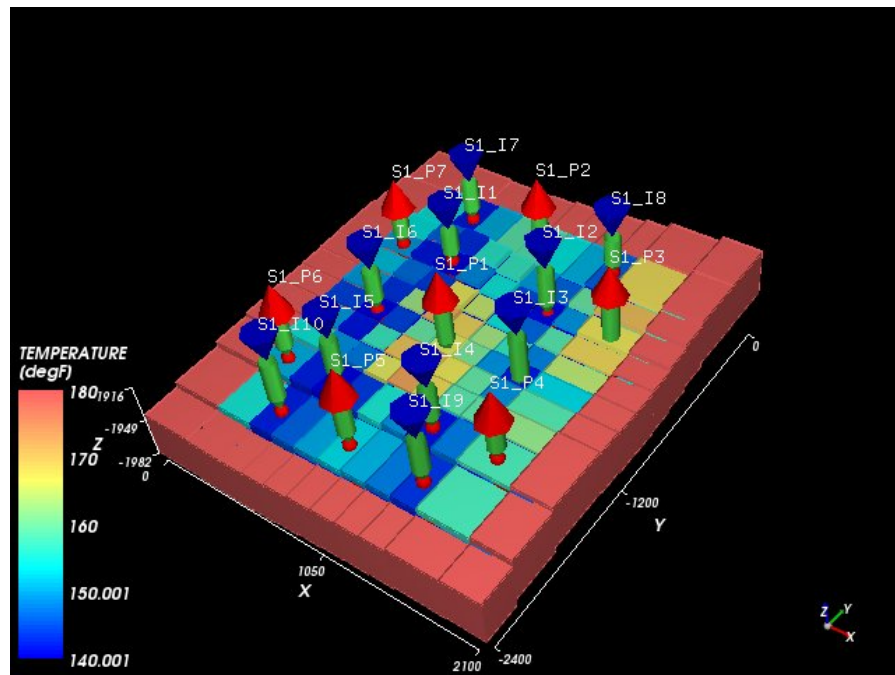


Figure 5.1 Temperature Profile before Bright Water® Treatment

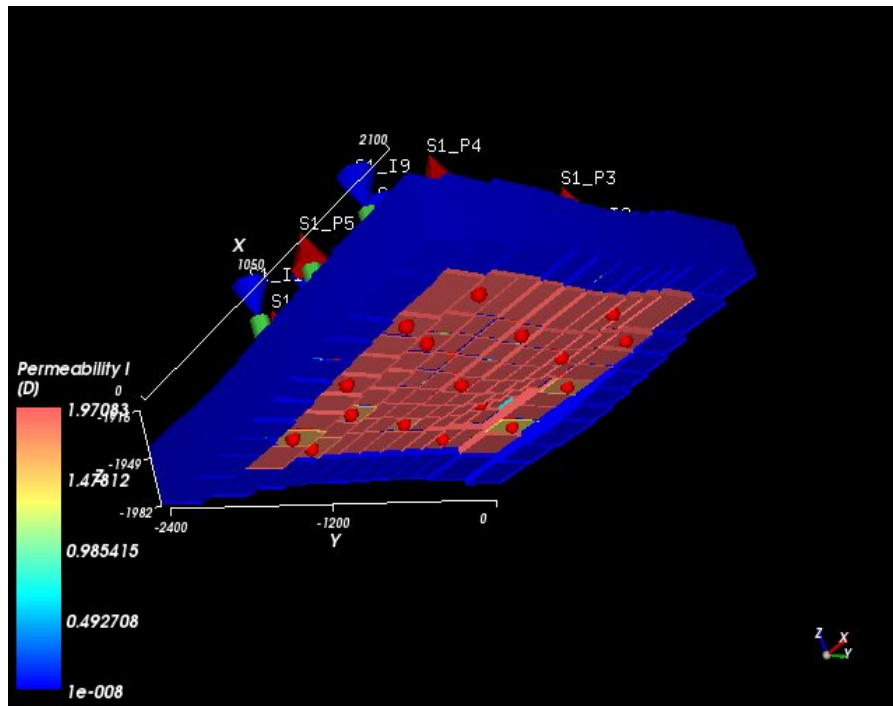


Figure 5.2 Permeability Distribution in the Field

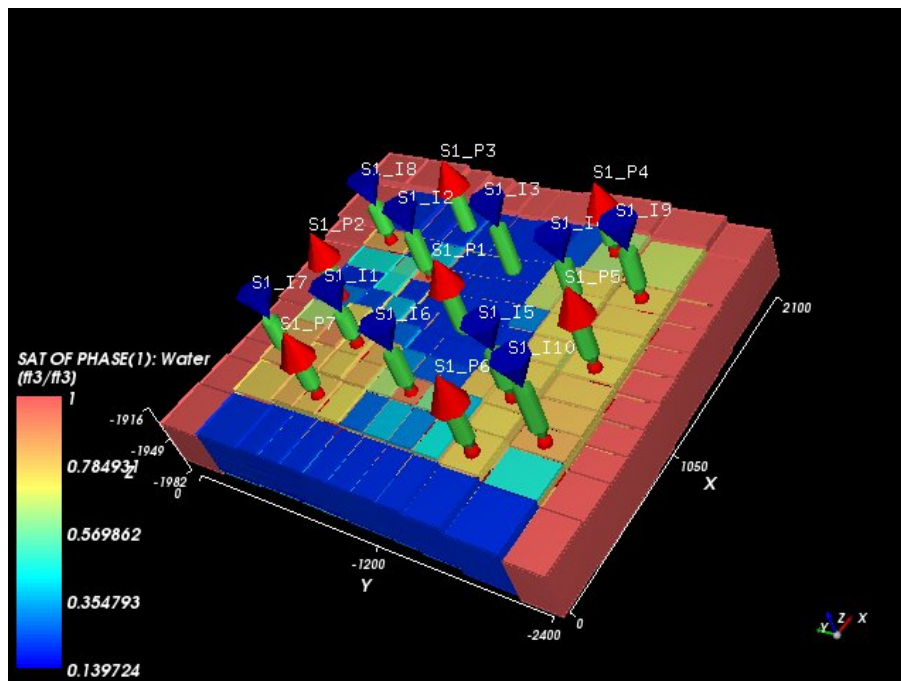


Figure 5.3 Water Saturation Profile after 367 days (5 PV)

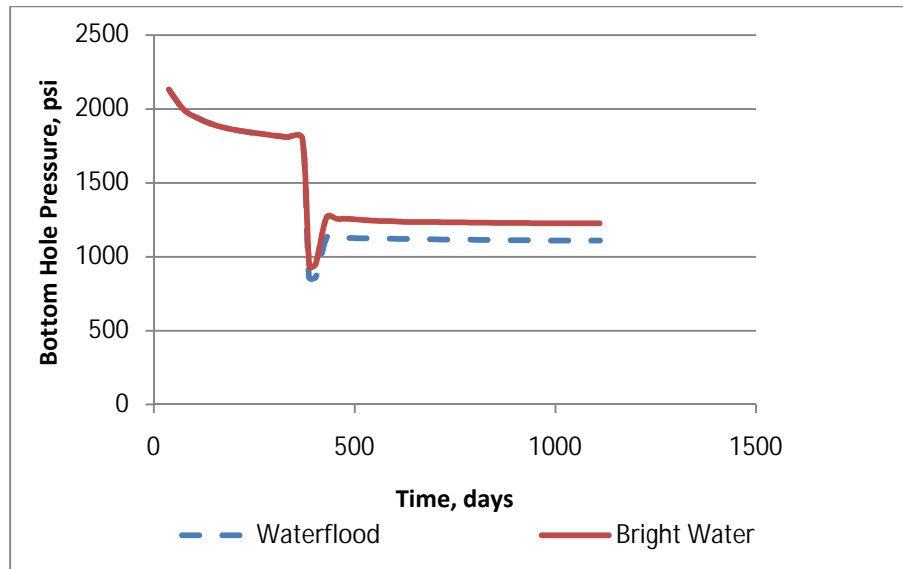


Figure 5.4 Comparison of Bottomhole Pressure for Waterflood and Bright Water® Treatment

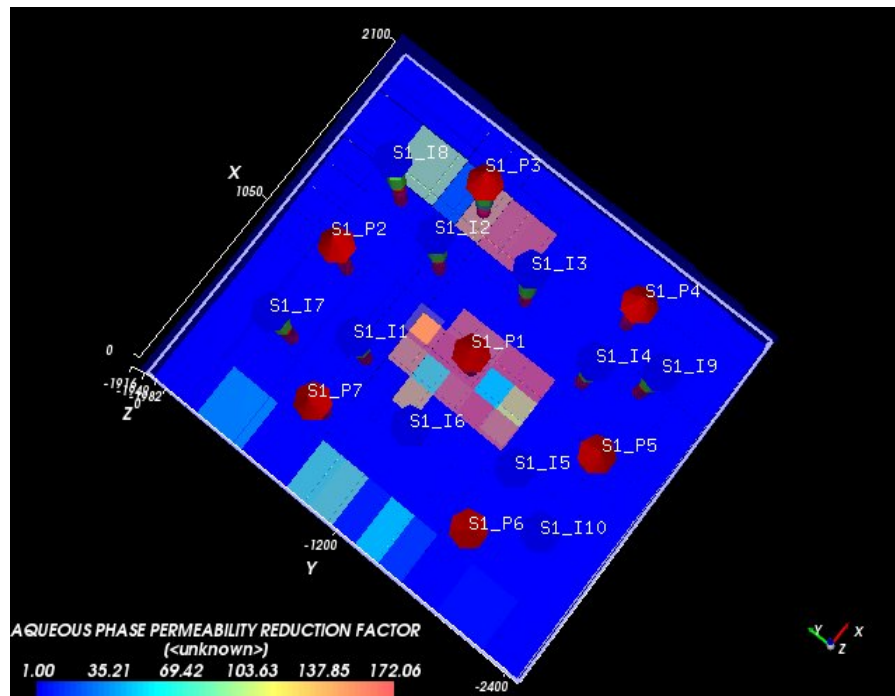


Figure 5.5 Permeability Reduction Profile

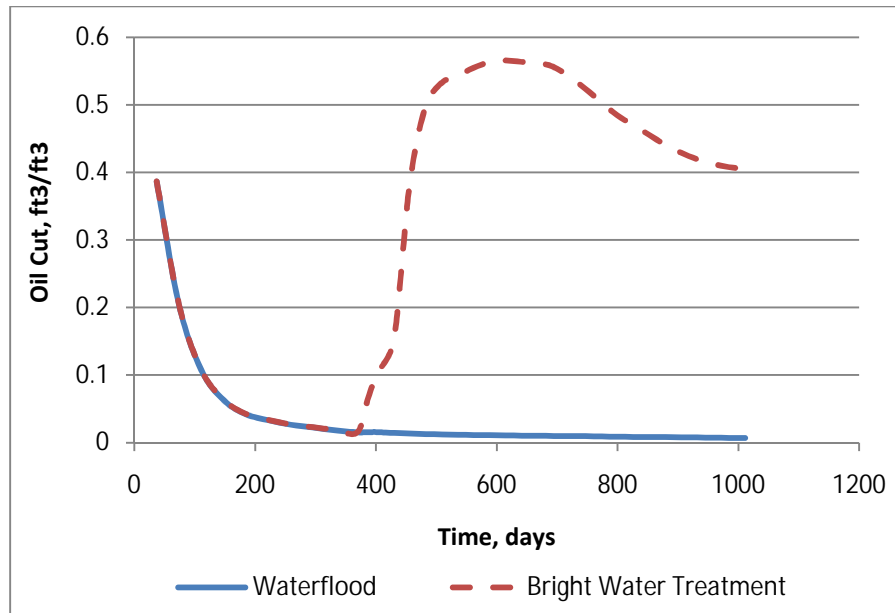


Figure 5.6 Comparison of Oil Cut for Waterflood and Bright Water® Treatment at Producer 1.

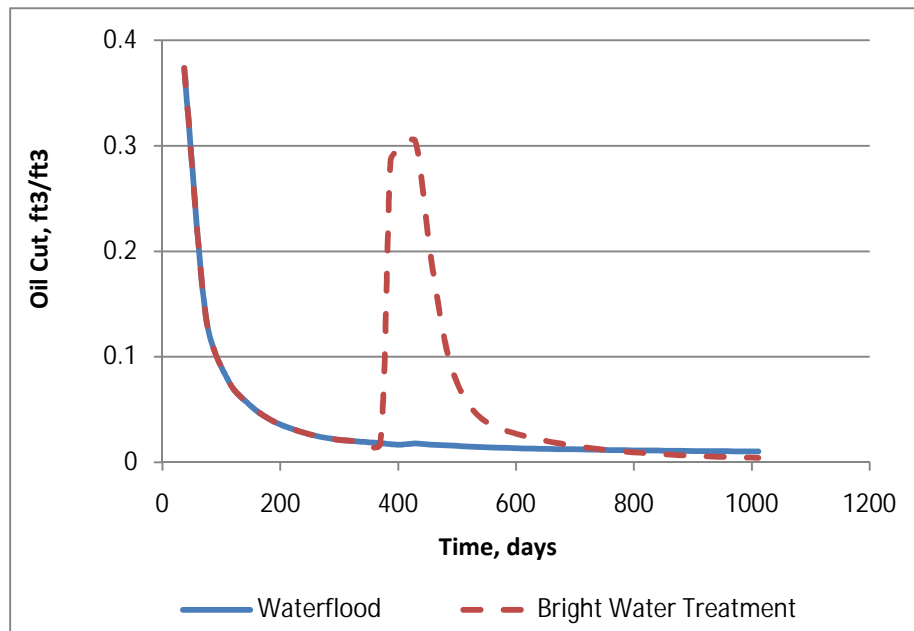


Figure 5.7 Comparison of Oil Cut for Waterflood and Bright Water® Treatment at Producer 3

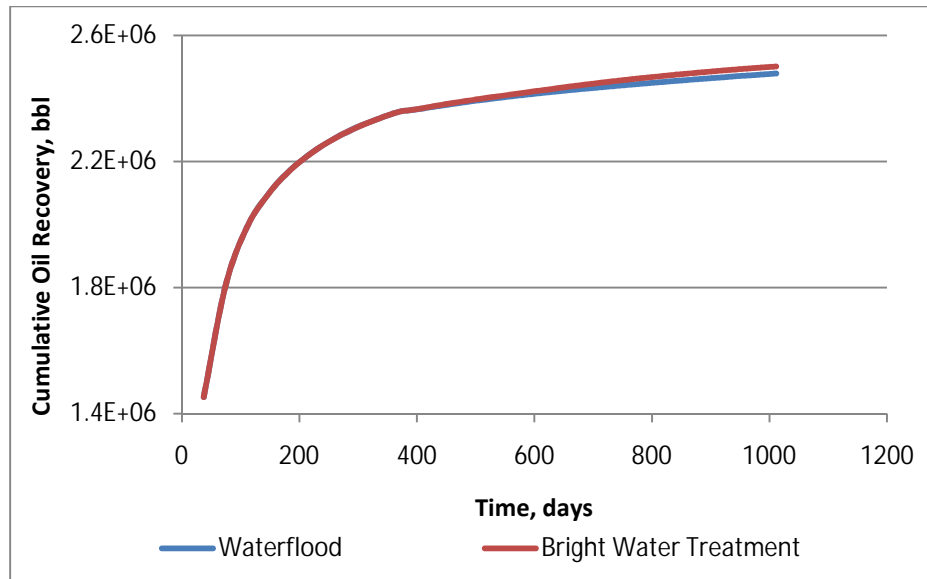


Figure 5.8 Comparison of Cumulative Oil Recovery for Waterflood and Bright Water Treatment

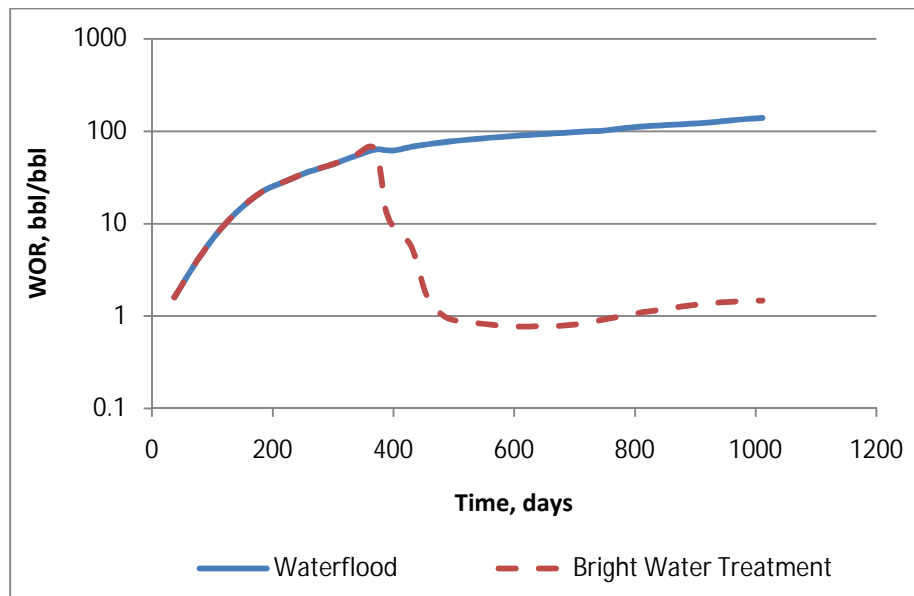


Figure 5.9 Comparison of Water-Oil-Ratio for Waterflood and Bright Water® Treatment at Producer 1

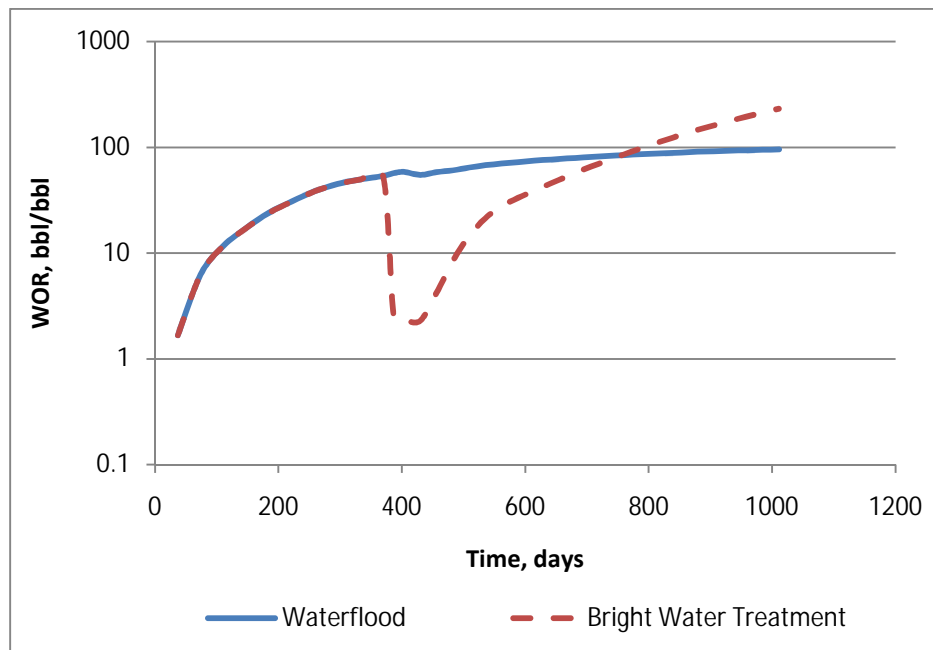


Figure 5.10 Comparison of Water-Oil-Ratio for Waterflood and Bright Water® Treatment at Producer 3

Chapter 6: Summary, Conclusions, and Recommendations

6.1 SUMMARY

Chemical treatments involving injection of preformed or in-situ formed gels are widely used in relatively high-permeability zones to improve sweep efficiency. One of the main advantages of gel treatments is fast response and relatively low cost compared with other conformance control methods.

In this study, the modeling of thermally active and pH-sensitive polymers was described to accurately predict treatment designs. The modified model was also described to calculate the equilibrium swelling ratio in terms of pH and ionic strength of solution.

UTGEL simulator was used in this study to evaluate the effectiveness of thermally active and pH-sensitive polymer gel treatments through synthetic and more realistic field case simulations. Treatment design parameters such as polymer concentration, vertical-to-horizontal permeability ratio, slug size, oil-to-water viscosity ratio, and permeability contrast were studied to better understand their impact on treatment performance.

6.2 CONCLUSIONS

- The modified model was developed to calculate equilibrium swelling ratio in terms of pH and ionic strength of solution.
- The modeling of pH-sensitive and thermally active polymer was successfully implemented in UTGEL.

- Permeability contrast appears to be one of the most parameters that impact treatment performance.
- Thermally Active and pH-sensitive polymer treatment results in diversion of water flow into unswept zones, low oil-water-ratio, and increase in the oil cut
- Polymer adsorption is a function of solution concentration, rock mineralogy, and slug size.
- It is more desirable to place the thermally active polymer deep in the reservoir and close to producer.

6.3 RECOMMENDATIONS

- Develop a geochemical modeling procedure to accurately predict acid-mineral reactions during preflush and propagation of pH-sensitive polymers through the reservoir.
- Investigate the use of second crosslinker in order to increase the gel resistance to wash out.
- Modeling and development of gel treatments using gas or water alternating with gas is recommended.

Appendix A

```

CC*****
CC
CC BRIEF DESCRIPTION OF DATA SET
CC
CC*****
CC THERMALLY ACTIVE POLYMER TREATMENT 15X15X3
CC
CC LENGTH (FT): 1640.5      PROCESS: GEL TREATMENT
CC THICKNESS (FT): VARIABLE    INJ. RATE (FT3/DAY): VARIABLE
CC WIDTH (FT): 1640.5      AD41=8.66,CRK=0.20,BRK=100,SOR=0.2
CC POROSITY: 0.30      COORDINATES: CARTESIAN
CC GRID BLOCKS: 15x15x3      PERMEABILITY: 3D STOCHASTIC PERM.
CC DATE: 10/27/2009      USED MDM METHOD TO GENERATE K FIELD
CC LDX=LDY=1.0,LDZ=0.33,VDP=0.3,SEED=1100,RW=4.3(INJ)
CC
CC*****
CC
CC*****
CC
CC RESERVOIR DESCRIPTION
CC
CC*****
CC
CC Run number
*---- RUNNO
3DBWG1
CC
CC Title and run description
*---- title(i)
3DBWG1

CC
CC SIMULATION FLAGS
*---- IMODE IMES IDISPC IREACT ICOORD ITREAC ITC IENG KGOPT
      1      2      3      0      1      0      0      1      7
CC
CC no. of gridblocks,flag specifies constant or variable grid size,unit
*---- NX  NY  NZ  IDXYZ  IUNIT
      15  15  3   0      0
CC
CC constant grid block size in x,y,and z
*---- dx1      dy1      dz1
      20      20.      5.0
CC
CC total no. of components,no. of tracers,no. of gel components
*----n  ntw  ng
      7   0   1
CC
CC Name of the components

```

```

*----spname(i) for i=1 to n
Water
Oil
CL
Polymer
Chloride
Calcium
BWG
CC
CC flag indicating if the component is included in calculations or not
*----icf(kc) for kc=1,n
  1 1 0 0 1 1 1
CC
CC*****
CC
CC  OUTPUT OPTIONS
CC
CC*****
CC
CC
CC FLAG TO WRITE TO UNIT 3,FLAG FOR PV OR DAYS TO PRINT OR TO STOP THE
RUN
*---- ICUMTM ISTOP
      0      0
CC
CC FLAG INDICATING IF THE PROFILE OF KCTH COMPONENT SHOULD BE WRITTEN
*---- IPRFLG(KC),KC=1,N
  1 1 0 0 1 1 1
CC
CC FLAG FOR PRES.,SAT.,TOTAL CONC.,TRACER CONC.,CAP.,GEL, ALKALINE
PROFILES
*---- IPPRES IPSAT IPCTOT IPGEL IPTEMP
      1      1      1      1      1
CC
CC FLAG FOR WRITING SEVERAL PROPERTIES TO UNIT 4 (Prof)
*---- ICKL IVIS IPER ICSE
      0      1      1      0
CC
CC FLAG for variables to PROF output file
*---- IADS IVEL IRKF IPHSE
      1      0      1      0
CC
CC*****
CC
CC  RESERVOIR PROPERTIES
CC
CC*****
CC
CC
CC MAX. SIMULATION TIME (DAYS)
*---- TMAX
      1080.0
CC

```

```

CC ROCK COMPRESSIBILITY (1/PSI), STAND. PRESSURE(PSIA)
*---- COMPR          PSTAND
      0              1000
CC
CC FLAGS INDICATING CONSTANT OR VARIABLE POROSITY, X,Y,AND Z
PERMEABILITY
*---- IPOR1 IPERMX IPERMY IPERMZ IMOD ITRNZ INTG
      0        2        3        3        0        0        0
CC
CC VARIABLE POROSITY OVER RESERVOIR
*---- POR(I),FOR I=1 TO NX*NY*NZ
      0.2
CC
CC VARIABLE PERMEABILITY OVER RESERVOIR
*---- PERMX(I),FOR I=1 TO NX*NY*NZ
      225*50.0 225*1500.0 225*50.0
CC
CC Y DIRECTION PERMEABILITY IS DEPENDENT ON X DIRECTION PERMEABILITY
*---- CONSTANT PERMEABILITY MULTIPLIER FOR Y DIRECTION PERMEABILITY
      1
CC
CC VARIABLE PERMEABILITY OVER RESERVOIR
*---- PERMZ(I),FOR I=1 TO NX*NY*NZ
      0.1
CC
CC FLAG FOR CONSTANT OR VARIABLE DEPTH, PRESSURE, WATER
SATURATION,INITIAL AQUEOUS PHASE COMPOSITIONS
*----IDEPTH IPRESS ISWI
      0        0        0
CC
CC CONSTANT DEPTH (FT)
*---- D111
      2000
CC
CC CONSTANT PRESSURE (PSIA)
*---- PRESS1
      100
CC
CC CONSTANT INITIAL WATER SATURATION
*---- SWI
      0.3
CC
CC BRINE SALINITY AND DIVALENT CATION CONCENTRATION (MEQ/ML)
*---- C50    C60
      0.00831 0.00551
CC
CC*****
CC
CC PHYSICAL PROPERTY DATA
CC
CC*****
CC
CC

```

```

CC THE CSE SLOPE PARAMETER FOR CALCIUM AND ALCOHOL 1 AND ALCOHOL 2
*---- beta6
      0.8
CC
CC LOG10 OF OIL/WATER INTERFACIAL TENSION
*---- xiftw
      1.3
CC
CC FLAG FOR RELATIVE PERMEABILITY AND CAPILLARY PRESSURE MODEL
*---- iperm  IRTYPE
      0      0
CC
CC FLAG FOR CONSTANT OR VARIABLE REL. PERM. PARAMETERS
*---- isrw  iprw  iew
      0      0      0
CC
CC CONSTANT RES. SATURATION OF PHASES 1,2,AND 3 AT LOW CAPILLARY NO.
*---- slrwc  s2rwc
      0.2      0.2
CC
cc CONSTANT ENDPOINT REL. PERM. OF PHASES 1,2,AND 3 AT LOW CAPILLARY NO.
*---- p1rwc  p2rwc
      0.2      1
CC
CC CONSTANT REL. PERM. EXPONENT OF PHASES 1,2,AND 3 AT LOW CAPILLARY
NO.
*---- e1wc  e2wc
      1.5      2
CC
CC WATER AND OIL VISCOSITY , RESERVOIR TEMPERATURE
*---- VIS1  VIS2  TSTAND
      1.9      12      25
cc
cc oil viscosity parameters
*--- bv1  bv2
      2000  1500
CC
CC COMPOSITIONAL PHASE VISCOSITY PARAMETERS
*---- ALPHAV1  ALPHAV2  ALPHAV3  ALPHAV4  ALPHAV5
           4           5           0           0.9           0.7
CC
CC PARAMETERS TO CALCULATE POLYMER VISCOSITY AT ZERO SHEAR RATE
*---- AP1  AP2  AP3
      0      0      0
CC
CC PARAMETER TO COMPUTE CSEP,MIN. CSEP, AND SLOPE OF LOG VIS. VS. LOG
CSEP
*---- BETAP  CSE1  SSLOPE
      20      0.01  -0.53
CC
CC PARAMETER FOR SHEAR RATE DEPENDENCE OF POLYMER VISCOSITY
*---- GAMMAC  GAMHF  POWN  IPMOD  ISHEAR  RWEFF  gamhf2
      4          280      2.2      0      0      0.25      0

```

```

CC
CC CC FLAG FOR POLYMER PARTITIONING, PERM. REDUCTION PARAMETERS
*---- IPOLYM  EPHI3  EPHI4  BRK  CRK  RKCUT
      1      1.      1.      100  0.2    10
CC
CC SPECIFIC WEIGHT FOR COMPONENTS 1,2,3,7,8 ,Coefficient of oil and GRAVITY FLAG
*---- DEN1  DEN2  IDEN
      62.428  55.568    2
CC
CC FLAG FOR CHOICE OF UNITS ( 0:BOTTOMHOLE CONDITION , 1: STOCK TANK)
*----- ISTB
      0
CC
CC COMPRESSIBILITY FOR VOL. OCCUPYING COMPONENTS 1,2,3,7,AND 8
*---- COMPC(1)  COMPC(2)
      0          0
CC
CC CONSTANT OR VARIABLE PC PARAM., WATER-WET OR OIL-WET PC CURVE
FLAG
*---- ICPC  IEPC  IOW
      0      0      0
CC
CC CAPILLARY PRESSURE PARAMETER, CPC0
*---- CPC0
      0
CC
CC CAPILLARY PRESSURE PARAMETER, EPC0
*---- EPC0
      2
CC
CC MOLECULAR DIFFUSION COEF. KCTH COMPONENT IN PHASE 1
*---- D(KC,1),KC=1,N
      0 0  0  0  0  0  0  0  0  0  0  0  0
CC
CC MOLECULAR DIFFUSION COEF. KCTH COMPONENT IN PHASE 2
*---- D(KC,2),KC=1,N
      0 0  0  0  0  0  0  0  0  0  0  0
CC
CC LONGITUDINAL AND TRANSVERSE DISPERSIVITY OF PHASE 1
*---- ALPHAL(1)  ALPHAT(1)
      1          0
CC
CC LONGITUDINAL AND TRANSVERSE DISPERSIVITY OF PHASE 2
*---- ALPHAL(2)  ALPHAT(2)
      1          0
CC
CC SURFACTANT AND POLYMER ADSORPTION PARAMETERS
*---- AD41  AD42  B4D  IADK  FADS  REFK
      8.66    0    100    0    0    0
CC
CC PARAMETERS FOR CATION EXCHANGE OF CLAY AND SURFACTANT
*---- QV  XKC
      0    0

```



```

CC
CC
*---- IRKFOLD
      2
CC
CC
*---- APOLADM ABWGADM CRKPOL CRKBWG CLIMBWG
      1000      0.3      1      1.12      0.0
CC
CC
*---- AG1      AG2      AG3
      .053      .000023      0
CC
CC
*---- ALPHBWP ALPHBWG
      0      0
CC
CC
*---- ADBWGLIM,CBWGT
      0.3      100
CC
CC
*---- ADBWG0 ADBWGS ADBWGT ADBWGK ADBWG
      8.66      0      10      -0.01      10.
CC
CC
*---- TEMTRBWG CCRLRBWG CPOLRBWG CBWGRBWG
      150.0      0.0      0.0      0.0
CC
CC
*---- BWB0 BWKC0
      0.055      0.055
CC
CC
*---- BWRKCP0,BWRKCC0
      7e-5      3.8e-4
CC
CC
*---- initial res. temp (F)
      200.
CC
CC silica - rock heat cap. - 35 btu/ft3-F,
*---- dens  crtc  cvspr  cvsp(1)  cvsp(2)
      165      48      0.2      0.8      0.51
CC
CC
*---- ihlos
      0
CC
CC*****
CC
CC  WELL DATA
CC

```

```

CC*****
CC
CC
NO. CC TOTAL NUMBER OF WELLS, WELL RADIUS FLAG, FLAG FOR TIME OR COURANT
*---- NWELL IRO ITIME NWREL
      2      1      1      2
CC
SKIN CC WELL ID,LOCATIONS,AND FLAG FOR SPECIFYING WELL TYPE, WELL RADIUS,
*---- IDW IW JW IFLAG RW SWELL IDIR IFIRST ILAST IPRF
      1      1      1      1      0.2864      0      3      1      3      0
CC
CC WELL NAME
*---- WELNAM
inj
CC
CC ICHEK , MAX. AND MIN. ALLOWABLE BOTTOMHOLE PRESSURE AND RATE
*---- ICHEK PWFMIN PWFMAX QTMIN QTMAX
      0      0      30000      0      9000
CC
SKIN CC WELL ID,LOCATIONS,AND FLAG FOR SPECIFYING WELL TYPE, WELL RADIUS,
*---- IDW IW JW IFLAG RW SWELL IDIR IFIRST ILAST IPRF
      2      15      15      2      0.2864      0      3      1      3      0
CC
CC WELL NAME
*---- WELNAM
prod-1
CC
CC ICHEK , MAX. AND MIN. ALLOWABLE BOTTOMHOLE PRESSURE AND RATE
*---- ICHEK PWFMIN PWFMAX QTMIN QTMAX
      0      0      30000      0      50000
CC
CC ID,INJ. RATE AND INJ. COMP. FOR RATE CONS. WELLS FOR EACH PHASE (L=1,3)
*---- ID QI(M,L) C(M,KC,L)
      1 500.0 1 0 0 0 0.00831 0.00551 0
      1 0 0 0 0 0 0 0 0
cc
cc
*---- id tinj
      1 60
CC
3) CC ID, BOTTOM HOLE PRESSURE FOR PRESSURE CONSTRAINT WELL (IFLAG=2 OR
*---- ID PWF
      2 100
CC
CC CUM. INJ. TIME , AND INTERVALS (PV OR DAY) FOR WRITING TO OUTPUT FILES
*---- TINJ CUMPR1 CUMHI1 WRHPV WRPRF RSTC
      540 10. 10. 10. 10. 100000
CC
CC THE INI. TIME STEP,CONC. TOLERANCE,MAX.,MIN. time steps

```

```

*---- DT   DELC   DTMAX      DTMIN
      0.001  0.01   0.4       0.04
CC
CC IRO, ITIME, NEW FLAGS FOR ALL THE WELLS ( WATER INJ.)
*---- IRO ITIME IFLAG
      2  1   1  2
CC
CC NUMBER OF WELLS CHANGES IN LOCATION OR SKIN OR PWF
*----NWEL1
      1
CC
CC WELL ID,LOCATIONS,AND FLAG FOR SPECIFYING WELL TYPE, WELL RADIUS,
SKIN
*---- IDW   IW   JW      RW   SWELL IDIR IFIRST ILAST IPRF
      1     1   1       0.2864  0     3     1     3     1
CC
CC kwell
*---- perf of each layer
      0  1  0
CC
CC WELL NAME
*---- WELNAM
inj
CC
CC ICHEK , MAX. AND MIN. ALLOWABLE BOTTOMHOLE PRESSURE AND RATE
*---- ICHEK   PWFMIN   PWFMAX   QTMIN   QTMAX
      0       0       30000   0       9000
CC
CC NUMBER OF WELLS WITH RATE CHANGES, ID
*----NWEL1 ID
      1     1
CC
CC ID,INJ. RATE AND INJ. COMP. FOR RATE CONS. WELLS FOR EACH PHASE (L=1,3)
*---- ID   QI(M,L)   C(M,KC,L)
      1   500.0  1  0  0  0  0.00831  0.00551  5000
      1    0    0  0  0  0  0       0       0
cc
cc
*---- id tinj
      1  60
CC
CC CUM. INJ. TIME , AND INTERVALS (PV OR DAY) FOR WRITING TO OUTPUT FILES
*---- TIN1   CUMPR1   CUMHI1   WRHPV   WRPRF   RSTC
      549     1.       1.       1       1.       100000
CC
CC THE INI. TIME STEP,CONC. TOLERANCE,MAX.,MIN. time steps
*---- DT   DELC   DTMAX      DTMIN
      0.001  0.01   0.4       0.04
CC
CC IRO, ITIME, NEW FLAGS FOR ALL THE WELLS ( WATER INJ.)
*---- IRO ITIME IFLAG
      2  1   1  2
CC

```

```

CC NUMBER OF WELLS CHANGES IN LOCATION OR SKIN OR PWF
*----NWEL1
  1
CC
SKIN CC WELL ID,LOCATION,AND FLAG FOR SPECIFYING WELL TYPE, WELL RADIUS,
*---- IDW  IW  JW   RW  SWELL IDIR IFIRST ILAST IPRF
      1    1   1    0.2864  0    3    1    3    0
CC
CC WELL NAME
*---- WELNAM
    inj
CC
CC ICHEK , MAX. AND MIN. ALLOWABLE BOTTOMHOLE PRESSURE AND RATE
*---- ICHEK  PWFMIN  PWFMAX  QTMIN  QTMAX
      0        0      30000    0      9000
CC
CC NUMBER OF WELLS WITH RATE CHANGES, ID
*----NWEL1 ID
  1    1
CC
CC ID,INJ. RATE AND INJ. COMP. FOR RATE CONS. WELLS FOR EACH PHASE (L=1,3)
*---- ID  QI(M,L)  C(M,KC,L)
      1  500.0  1  0  0  0  0.00831  0.00551  0
      1   0    0  0  0  0  0        0        0
cc
cc
*---- id tinj
  1  60
CC
CC CUM. INJ. TIME , AND INTERVALS (PV OR DAY) FOR WRITING TO OUTPUT FILES
*---- TINJ  CUMPR1  CUMHI1  WRHPV  WRPRF  RSTC
      740    20     20     20     20    100000
CC
CC THE INI. TIME STEP,CONC. TOLERANCE,MAX.,MIN. time steps
*---- DT  DELC  DTMAX  DTMIN
      0.001  0.01   0.4    0.04
CC
CC IRO, ITIME, NEW FLAGS FOR ALL THE WELLS ( WATER INJ.)
*---- IRO ITIME IFLAG
      2  1  1  2
CC
CC NUMBER OF WELLS CHANGES IN LOCATION OR SKIN OR PWF
*----NWEL1
  0
CC
CC NUMBER OF WELLS WITH RATE CHANGES, ID
*----NWEL1 ID
  1    1
CC
CC ID,INJ. RATE AND INJ. COMP. FOR RATE CONS. WELLS FOR EACH PHASE (L=1,3)
*---- ID  QI(M,L)  C(M,KC,L)
      1  500.0  1  0  0  0  0.00831  0.00551  0

```

```

      1  0  0  0  0  0  0  0  0  0
cc
cc
*--- id tinj
      1  60
CC
CC CUM. INJ. TIME , AND INTERVALS (PV OR DAY) FOR WRITING TO OUTPUT FILES
*---- TINJ   CUMPR1   CUMHI1   WRHPV   WRPRF   RSTC
      1080   10.      10       10      10      100000
CC
CC THE INI. TIME STEP, CONC. TOLERANCE, MAX., MIN. time steps
*---- DT    DELC    DTMAX      DTMIN
      0.001  0.01    0.4       0.04

```

Appendix B

```

CC*****
CC
CC BRIEF DESCRIPTION OF DATA SET :
CC
CC*****
CC
CC
CC
CC LENGTH (FT) :          PROCESS :
CC THICKNESS (FT) :      INJ. RATE (FT3/DAY) :
CC WIDTH (FT) :
CC POROSITY :            COORDINATES : CARTESIAN
CC GRID BLOCKS :        PERMEABILITY :
CC
CC
CC*****
CC
CC*****
CC
CC RESERVOIR DESCRIPTION
CC
CC*****
CC
CC Run number
*---- RUNNO
3D Ph-sensitive gel
CC
CC Title and run description
*---- title(i)

CC
CC SIMULATION FLAGS
*---- IMODE IMES IDISPC ICWM ICAP IREACT IBIO ICOORD ITREAC ITC IGAS IENG
      1      2      3      0      0      1      0      1      0      0      0      0
CC
CC no. of gridblocks,flag specifies constant or variable grid size,unit
*---- NX  NY  NZ  IDXYZ  IUNIT
      15  15   3   0      0
CC
C GRID SIZE OF BLOCK IN X DIRECTION
*---- DX(I), FOR I=1 TO NX
      20.0 20.0 5.0
CC
CC total no. of components,no. of tracers,no. of gel components
*----n  no  ntw  nta  ngc  ng  noth
      14  0   0   0   0   6   0
CC
CC Name of the components

```

```

*----spname(i) for i=1 to n
Water
Oil
none
none
calcium
none
none
none
none
none
none
none
H+
Polymer
CC
CC flag indicating if the component is included in calculations or not
*----icf(kc) for kc=1,n
1 1 0 0 1 0 0 0 0 0 0 0 0
CC
CC*****
CC
CC
CC OUTPUT OPTIONS
CC
CC
CC*****
CC
CC
CC FLAG TO WRITE TO UNIT 3,FLAG FOR PV OR DAYS TO PRINT OR TO STOP THE
RUN
*---- ICUMTM ISTOP IOUTGMS
0 0 2
CC
CC FLAG INDICATING IF THE PROFILE OF KCTH COMPONENT SHOULD BE WRITTEN
*---- IPRFLG(KC),KC=1,N
1 1 0 0 1 0 0 0 0 0 0 0 0
CC
CC FLAG FOR PRES.,SAT.,TOTAL CONC.,TRACER CONC.,CAP.,GEL, ALKALINE
PROFILES
*---- IPPRES IPSAT IPCTOT IPBIO IPCAP IPGEL IPALK IPTEMP IPOBS
0 1 1 0 0 1 0 1 0
CC
CC FLAG FOR WRITING SEVERAL PROPERTIES TO UNIT 4 (Prof)
*---- ICKL IVIS IPER ICNM ICSE IHYSTP IFOAMP INONEQ
0 1 0 0 0 0 0 0
CC
CC FLAG for variables to PROF output file
*---- IADS IVEL IRKF IPHSE
0 0 1 0
CC
CC*****
CC
CC RESERVOIR PROPERTIES
CC

```

```

CC*****
CC
CC
CC MAX. SIMULATION TIME (DAYS)
*---- TMAX
      1080.0
CC
CC ROCK COMPRESSIBILITY (1/PSI), STAND. PRESSURE(Psia)
*---- COMPR          PSTAND
      0              1000.0
CC
CC FLAGS INDICATING CONSTANT OR VARIABLE POROSITY, X,Y,AND Z
PERMEABILITY
*---- IPOR1 IPERMX IPERMY IPERMZ IMOD ITRNZ INTG
      0  2  3  3  0  0  0
CC
CC VARIABLE POROSITY OVER RESERVOIR
*---- POR(I),FOR I=1 TO NX*NY*NZ
      0.2
CC
CC VARIABLE X-PERMEABILITY (MILIDARCY) FOR BLOCK I = 1,NX*NY*NZ
*----PERMX(I) I=1,NX*NY*NZ
      225*50 225*150 225*50
CC
CC VARIABLE Y-PERMEABILITY (MILIDARCY) FOR BLOCK J = 1,NX*NY*NZ
*----FACTY
      1.0
CC
CC VARIABLE Z-PERMEABILITY (MILIDARCY) FOR BLOCK K = 1,NX*NY*NZ
*----FACTZ
      0.1
CC
CC FLAG FOR CONSTANT OR VARIABLE DEPTH, PRESSURE, WATER
SATURATION,INITIAL AQUEOUS PHASE cOMPOSITIONS
*----IDEPTH IPRESS ISWI ICWI
      0  0  0  -1
CC
CC DEPTH OF TOP GRID BLOCK (1,1,1) AND THE RESERVOIR DIP ANGLES ARE
SPECIFIED
*---- D111
      0
CC
CC INITIAL PRESSURE FOR A POINT AT A SPECIFIED DEPTH IS SPECIFIED
*---- PINIT
      14.7
CC
CC CONSTANT INITIAL WATER SATURATION
*---- SWI
      0.3
CC
CC BRINE SALINITY AND DIVALENT CATION CONCENTRATION (MEQ/ML)
*---- C50    C60
      0.3    0

```



```

CC
CC*****
CC
CC PHYSICAL PROPERTY DATA
CC
CC*****
CC
CC
CC OIL CONC. AT PLAIT POINT FOR TYPE II(+)AND TYPE II(-), CMC
*---- c2plc c2prc epsme ihand
      0      1    0.0001  0
CC
CC flag indicating type of phase behavior parameters
*---- ifghbn
      0
CC SLOPE AND INTERCEPT OF BINODAL CURVE AT ZERO, OPT., AND 2XOPT
SALINITY
CC FOR ALCOHOL 1
*---- hbns70 hbnc70 hbns71 hbnc71 hbns72 hbnc72
      0.001  0.03  0.191  0.026  0.363  0.028
CC SLOPE AND INTERCEPT OF BINODAL CURVE AT ZERO, OPT., AND 2XOPT
SALINITY
CC FOR ALCOHOL 2
*---- hbns80 hbnc80 hbns81 hbnc81 hbns82 hbnc82
      0      0      0      0      0      0
CC
CC LOWER AND UPPER EFFECTIVE SALINITY FOR ALCOHOL 1 AND ALCOHOL 2
*---- csel7 cseu7 csel8 cseu8
      .65   .9    0.    0.
CC
CC THE CSE SLOPE PARAMETER FOR CALCIUM AND ALCOHOL 1 AND ALCOHOL 2
*---- beta6 beta7 beta8
      0      0      0
CC
CC FLAG FOR ALCOHOL PART. MODEL AND PARTITION COEFFICIENTS
*---- ialc opsk7o opsk7s opsk8o opsk8s
      0      0      0      0      0
CC
CC NO. OF ITERATIONS, AND TOLERANCE
*---- nalmax epsalc
      20    0.0001
CC
CC ALCOHOL 1 PARTITIONING PARAMETERS IF IALC=1
*---- akwc7 akws7 akm7 ak7 pt7
      4.671  1.79  48   35.31  0.222
CC
CC ALCOHOL 2 PARTITIONING PARAMETERS IF IALC=1
*---- akwc8 akws8 akm8 ak8 pt8
      0      0      0      0      0
CC
CC ift model flag
*---- ift
      0

```

```

CC
CC INTERFACIAL TENSION PARAMETERS
*---- g11  g12  g13  g21  g22  g23
      13  -14.8  0.007  13  -14.5  0.01
CC
CC LOG10 OF OIL/WATER INTERFACIAL TENSION
*---- xiftw
      1.477
CC
CC ORGANIC MASS TRANSFER FLAG
*---- imass icor
      0      0
cc
cc
*---- iwalt iwalf
      0      0
CC
CC CAPILLARY DESATURATION PARAMETERS FOR PHASE 1, 2, AND 3
*---- itrap  t11      t22      t33
      0      1865.    28665.46  364.2
CC
CC FLAG FOR RELATIVE PERMEABILITY AND CAPILLARY PRESSURE MODEL
*---- iperm  IRTYPE
      0      0
CC
CC FLAG FOR CONSTANT OR VARIABLE REL. PERM. PARAMETERS
*---- isrw  iprw  iew
      0      0      0
CC
CC CONSTANT RES. SATURATION OF PHASES 1,2,AND 3 AT LOW CAPILLARY NO.
*---- slrwc  s2rwc  s3rwc
      0.147  0.25   0.147
CC
CC CONSTANT ENDPOINT REL. PERM. OF PHASES 1,2,AND 3 AT LOW CAPILLARY
NO.
*---- plrwc  p2rwc  p3rwc
      .13771  0.9148  .13771
CC
CC CONSTANT REL. PERM. EXPONENT OF PHASES 1,2,AND 3 AT LOW CAPILLARY
NO.
*---- elwc  e2wc  e3wc
      2.1817  1.40475  2.1817
CC
CC WATER AND OIL VISCOSITY , RESERVOIR TEMPERATURE
*---- VIS1  VIS2  TSTAND
      1      4.0    0.0
CC
CC COMPOSITIONAL PHASE VISCOSITY PARAMETERS
*---- ALPHAV1  ALPHAV2  ALPHAV3  ALPHAV4  ALPHAV5
      0.0      0.0      0.0      0.000865  4.153
CC
CC PARAMETERS TO CALCULATE POLYMER VISCOSITY AT ZERO SHEAR RATE
*---- AP1  AP2  AP3

```

```

0.05 0.02 0
CC
CC PARAMETER TO COMPUTE CSEP,MIN. CSEP, AND SLOPE OF LOG VIS. VS. LOG
CSEP
*---- BETAP CSE1 SSLOPE
10 0.01 0.169
CC
CC PARAMETER FOR SHEAR RATE DEPENDENCE OF POLYMER VISCOSITY
*---- GAMMAC GAMHF POWN IPMOD ishear rweff
4 0.0 1.8 0 0 0.25 0
CC
CC CC FLAG FOR POLYMER PARTITIONING, PERM. REDUCTION PARAMETERS
*---- IPOLYM EPHI3 EPHI4 BRK CRK RKCUT
1 1. 1 0. 0.0 10
CC
CC SPECIFIC WEIGHT FOR COMPONENTS 1,2,3,7,8 ,Coefficient of oil and GRAVITY FLAG
*---- DEN1 DEN2 DEN23 DEN3 DEN7 DEN8 IDEN
0.433 0.3897 0.3897 0.42 0.346 0 2
CC
CC FLAG FOR CHOICE OF UNITS ( 0:BOTTOMHOLE CONDITION , 1: STOCK TANK)
*----- ISTB
0
CC
CC COMPRESSIBILITY FOR VOL. OCCUPYING COMPONENTS 1,2,3,7,AND 8
*---- COMPC(1) COMPC(2) COMPC(3) COMPC(7) COMPC(8)
0 0 0 0 0
CC
CC CONSTANT OR VARIABLE PC PARAM., WATER-WET OR OIL-WET PC CURVE
FLAG
*---- ICPC IEPC IOW
0 0 0
CC
CC CAPILLARY PRESSURE PARAMETER, CPC0
*---- CPC0
0
CC
CC CAPILLARY PRESSURE PARAMETER, EPC0
*---- EPC0
2
CC
CC MOLECULAR DIFFUSION COEF. KCTH COMPONENT IN PHASE 1
*---- D(KC,1),KC=1,N
0 0 0 0 0 0 0 0 0 0 0 0 0 0 0
CC
CC MOLECULAR DIFFUSION COEF. KCTH COMPONENT IN PHASE 2
*---- D(KC,2),KC=1,N
0 0 0 0 0 0 0 0 0 0 0 0 0 0 0
CC
CC MOLECULAR DIFFUSION COEF. KCTH COMPONENT IN PHASE 3
*---- D(KC,3),KC=1,N
0 0 0 0 0 0 0 0 0 0 0 0 0 0 0
CC
CC LONGITUDINAL AND TRANSVERSE DISPERSIVITY OF PHASE 1

```

```

*---- ALPHAL(1)  ALPHAT(1)
      2          0.4
CC
CC LONGITUDINAL AND TRANSVERSE DISPERSIVITY OF PHASE 2
*---- ALPHAL(2)  ALPHAT(2)
      2          0.4
CC
CC LONGITUDINAL AND TRANSVERSE DISPERSIVITY OF PHASE 3
*---- ALPHAL(3)  ALPHAT(3)
      0          0
CC
CC flag to specify organic adsorption calculation
*---- iadso
      0
CC
CC SURFACTANT AND POLYMER ADSORPTION PARAMETERS
*---- AD31  AD32  B3D  AD41  AD42  B4D  IADK  IADS1  FADS  REFK
      0      0  1000  7.875  0    500    0    0      0    0
CC
CC PARAMETERS FOR CATION EXCHANGE OF CLAY AND SURFACTANT
*---- QV    XKC    XKS    EQW
      0      0      0      1
CC
CC PARAMETERS FOR GELATION KINETICS
*---- KGOPT
      5
CC
CC
* --- AQ1,AQN1,AQ2,AQN2,AQ3,AQN3,AQ4,AQN4
184.49 -0.592 182.06 -0.637 4.5024 -0.0049 0.3862 -0.023
CC
CC
* --- AVISQ,BVISQ,AKEMP,AETAINF,AE1,AE2,AE3,AE4,AE5
      0.11    1.19    0.4      0.0    -0.03  0.04 .0 1.00e-7 1.0
CC
CC*****
CC
CC WELL DATA
CC
CC*****
CC
CC
CC FLAG FOR SPECIFIED BOUNDARY AND ZONE IS MODELED
*---- IBOUND  IZONE
      0          0
CC
CC TOTAL NUMBER OF WELLS, WELL RADIUS FLAG, FLAG FOR TIME OR COURANT
NO.
*----NWELL  IRO  ITIME  NWREL
      2      2    1      2
CC
CC WELL ID,LOCATIONS,AND FLAG FOR SPECIFYING WELL TYPE, WELL RADIUS,
SKIN

```

```

*----IDW IW JW IFLAG RW SWELL IDIR IFIRST ILAST IPRF
      1  1  1  1  .5  0.  3  1  3  0
CC
CC WELL NAME
*---- WELNAM
INJECTOR
CC
CC ICHEK MAX. AND MIN. ALLOWABLE BOTTOMHOLE PRESSURE AND RATE
*----ICHEK PWFMIN PWFMAX QTMIN QTMAX
      0  0.0  5801.6  0.0  5615.
CC
SKIN CC WELL ID, LOCATION, AND FLAG FOR SPECIFYING WELL TYPE, WELL RADIUS,
*----IDW IW JW IFLAG RW SWELL IDIR IFIRST ILAST IPRF
      2 15 15  2  .5  0.  3  1  3  0
CC
CC WELL NAME
*---- WELNAM
PRODUCER
CC
CC MAX. AND MIN. ALLOWABLE BOTTOMHOLE PRESSURE AND RATE
*----ICHEK PWFMIN PWFMAX QTMIN QTMAX
      0  0.0  5000.  0.0  50000.
CC
CC ID,INJ. RATE AND INJ. COMP. FOR RATE CONS. WELLS FOR EACH PHASE (L=1,3)
*----ID QI(M,L) C(M,KC,L)
      1 500.0 1.0 0.0 0.0 0.0 0.3 0.0 0.0 0.0 0.0 0.0 0.0 0.0 0.0
      1  0.0 0.0 0.0 0.0 0.0 0.0 0.0 0.0 0.0 0.0 0.0 0.0 0.0 0.0
      1  0.0 0.0 0.0 0.0 0.0 0.0 0.0 0.0 0.0 0.0 0.0 0.0 0.0 0.0
CC
3) CC ID, BOTTOM HOLE PRESSURE FOR PRESSURE CONSTRAINT WELL (IFLAG=2 OR
*----ID PWF
      2 14.7
CC
CC CUM. INJ. TIME , AND INTERVALS (PV OR DAY) FOR WRITING TO OUTPUT FILES
*----TINJ CUMPR1 CUMHI1 WRHPV WRPRF RSTC
      540 10 10 10 10 10
CC
CC FOR IMES=2 ,THE INI. TIME STEP,CONC. TOLERANCE,MAX.,MIN. COURANT NO.
*----DT DCLIM CNMAX CNMIN
      0.001 0.01 0.4 0.04
cc
cc FLAG FOR INDICATING BOUNDARY CHANGE
** ----IBMOD
      0
CC34567890-----2-----3-----4-----5-----6-----7-----8
CC IRO, ITIME, NEW FLAGS FOR ALL THE WELLS (SURF/POLYMER
*---- IRO ITIME IFLAG
      2 1 1 2
CC
CC NUMBER OF WELLS CHANGES IN LOCATION OR SKIN OR PWF
*----NWEL1

```

```

0
CC
CC NUMBER OF WELLS WITH RATE CHANGES, ID
*----NWEL1 ID
      1      1
CC
CC ID,INJ. RATE AND INJ. COMP. FOR RATE CONS. WELLS FOR EACH PHASE (L=1,3)
*----ID QI(M,L) C(M,KC,L)
      1 500 1. 0.0 0.0 0.0 0.3 0. 0. 0. 0. 0. 0. 0. 0.1E-3 0.5
      1 0. 0. 0. 0. 0. 0. 0. 0. 0. 0. 0. 0. 0. 0. 0.
      1 0. 0. 0. 0. 0. 0. 0. 0. 0. 0. 0. 0. 0. 0. 0.
CC
CC CUM. INJ. TIME , AND INTERVALS (PV) FOR WRITING TO OUTPUT FILES
*----TINJ CUMPR1 CUMHI1(PROFIL) WRHPV(HIST) WRPRF(PLOT) RSTC
      549      10      10      10      10      10
CC
CC FOR IMES=2 ,THE INI. TIME STEP,CONC. TOLERANCE,MAX.,MIN. Courant No.
*----DT DCLIM CNMAX CNMIN
      0.001      0.01      0.4      0.04
cc
cc FLAG FOR INDICATING BOUNDARY CHANGE
** ----IBMOD
      0
CC34567890-----2-----3-----4-----5-----6-----7-----8
CC IRO, ITIME, NEW FLAGS FOR ALL THE WELLS (SURF/POLYMER
*---- IRO ITIME IFLAG
      2 1      1 2
CC
CC NUMBER OF WELLS CHANGES IN LOCATION OR SKIN OR PWF
*----NWEL1
      0
CC
CC NUMBER OF WELLS WITH RATE CHANGES, ID
*----NWEL1 ID
      1      1
CC
CC ID,INJ. RATE AND INJ. COMP. FOR RATE CONS. WELLS FOR EACH PHASE (L=1,3)
*----ID QI(M,L) C(M,KC,L)
      1 500.0 1.0 0. 0. 0. 0.3 0. 0. 0. 0. 0. 0. 0. 0. 0.
      1 0. 0. 0. 0. 0. 0. 0. 0. 0. 0. 0. 0. 0. 0. 0.
      1 0. 0. 0. 0. 0. 0. 0. 0. 0. 0. 0. 0. 0. 0. 0.
CC
CC CUM. INJ. TIME , AND INTERVALS (PV) FOR WRITING TO OUTPUT FILES
*----TINJ CUMPR1 CUMHI1(PROFIL) WRHPV(HIST) WRPRF(PLOT) RSTC
      1080      10      10      10      10      10
CC
CC FOR IMES=2 ,THE INI. TIME STEP,CONC. TOLERANCE,MAX.,MIN. Courant No.
*----DT DCLIM CNMAX CNMIN
      0.001      0.01      0.4      0.04

```

Appendix C

```

CC*****
cC
CC BRIEF DESCRIPTION OF DATA SET :
CC
CC*****
CC
CC
CC
CC LENGTH (FT) :          PROCESS :
CC THICKNESS (FT) :      INJ. RATE (FT3/DAY) :
CC WIDTH (FT) :
CC POROSITY :            COORDINATES : CARTESIAN
CC GRID BLOCKS :        PERMEABILITY :
CC
CC
CC*****
CC
CC*****
CC
CC RESERVOIR DESCRIPTION
CC
CC*****
CC
CC Run number
*----RUNNO (title)-Type the Grid Number below
UTMIN2
CC
CC
*----HEADER (need 3 lines)
s-1119
Alcohol Included-DW' paper
SP flood (09/15/09)
CC
CC SIMULATION FLAGS
*---- IMODE IMES IDISPC IREACT ICOORD ITREAC ITC ieng KGOPT
      1      2      3      0      1      0      0      1      7
CC
CC NUMBER OF GRID BLOCKS AND FLAG SPECIFIES CONSTANT OR VARIABLE
GRID SIZE
*----NX NY NZ IDXYZ IUNIT
      11  12  19   2   0
CC Grid Properties Given By Chevron
CC CONSTANT GRID BLOCK SIZE IN X, Y, AND Z (in ft)
*----DX
300    225    150    150    150
150    150    150    150    300
225
CC Grid Properties Given By Chevron
CC CONSTANT GRID BLOCK SIZE IN X, Y, AND Z (in ft)

```

```

*----DY
300    300    150    150.00006    149.99994
150    150    150    150    225
300    225
CC
CC Grid Properties Given By Chevron
*----DZ (this is mean from NET from ecl2gocad) total thickness is about 68 ft
2 2 2 2 2 2 2 2 2 2 2 2 2 2 2 1
CC
CC TOTAL NO. OF COMPONENTS, NO. OF TRACERS, NO. OF GEL COMPONENTS
*----N NTw ng
      7    0    1
CC
CC All species must be present even for standard waterflood.
*---- species name (total 7)
Water
Oil
CL
Polymer
Chloride
Calcium
BWG
CC
CC FLAG INDICATING IF THE COMPONENT IS INCLUDED IN CALCULATIONS OR
NOT
*----ICF(KC) FOR KC=1,N
      1 1 0 0 1 0 1
CC
CC*****
CC
CC OUTPUT OPTIONS
CC
CC*****
CC
CC ICOPSM=0==>ECHO TO UNIT 5; ICUMTM=0==>TIME PRINTING;istop=1==>PV SPEC
CC FLAG TO ECHO THE INPUT, FLAG TO WRITE TO UNIT 5, FLAG FOR PV OR DAYS
*----ICUMTM ISTOP
      1      1
CC
CC FLAG INDICATING IF THE PROFILE OF KCTH COMPONENT SHOULD BE WRITTEN
*----IPRFLG(KC),KC=1,N
      1 1 0 0 1 0 1
CC
CC FLAG FOR PRES,SAT.,TOTAL CONC.,TRACER CONC.,CAP.,GEL, ALKALINE
PROFILES
*----IPPRES IPSAT IPCTOT IPGEL IPTEMP
      1      1      1      1      1
CC ICKL is phase conc. (K is component and L is phase)
CC FLAG FOR WRITING SEVERAL PROPERTIES TO UNIT 6 (PROFIL)
*----ICKL IVIS IPER ICSE
      1      1      1      1
CC
CC FLAG FOR WRITING SEVERAL PROPERTIES TO UNIT 6 (PROFIL)

```



```

*----IADS IVEL IRKF IPHSE
      1      0      1      0
CC
CC*****
CC
CC  RESERVOIR PROPERTIES
CC
CC*****
CC
CC
CC MAX. SIMULATION TIME
*---- TMAX
      10
CC
CC ROCK COMPRESSIBILITY (1/PSI), STAND. PRESSURE(PSIA)
*----COMPR PSTAND
      0.00000 14.7
CC Porosity Values For Each Grid Input Given Through Include Files
CC FLAGS INDICATING CONSTANT OR VARIABLE POROSITY, X,Y,AND Z
PERMEABILITY
*----IPOR1 IPERMX IPERMY IPERMZ IMOD ITRANZ INTG
      4      4      4      4      1      0      0
CC Depth To The Top Layer Input Given Through Include Files
CC FLAG FOR CONSTANT OR VARIABLE DEPTH, PRESSURE, WATER SATURATION
*----DEPTH IPRESS ISWI
      4      1      0
CC
CC 4/10/2009- Chevron
*----IPRESS DEPTH
      550. 1965.77185
CC 4/10/2009- Chevron
CC WATER SATURATION
*----ISWI
      0.2
CC
CC FLAG FOR RESERVOIR PROPERTY MODIFICATION
*----IMPOR IMKX IMKY IMKZ IMSW
      0      1      1      1      0
CC
CC NUMBER OF REGIONS WITH MODIFIED X PERMEABILITY
*----NMOD1
      17
CC
CC FIRST AND LAST INDEX IN X,Y,Z DIRECTION,MODIFIED METHOD,CONSTANT
VALUE.
*---- IMIN IMAX JMIN JMAX KMIN KMAX IFACT FACTX
      4 4      4      4      19      19      2      0.3826
      8 8      4      4      19      19      2      0.6546
      9 9      7      7      19      19      2      0.3729
      8 8      10     10     19      19      2      0.3708
      4 4      10     10     19      19      2      0.3561
      3 3      7      7      19      19      2      0.3739
      3 3      2      2      19      19      2      0.3117

```

9	9	2	2	19	19	2	0.734
9	9	11	11	19	19	2	0.5459
3	3	11	11	19	19	2	0.637
6	6	7	7	19	19	2	0.5878
6	6	2	2	19	19	2	0.2139
10	10	4	4	19	19	2	0.6652
10	10	10	10	19	19	2	0.3931
6	6	11	11	19	19	2	0.4183
2	2	10	10	19	19	2	0.5491
2	2	4	4	19	19	2	0.6232

CC

CC NUMBER OF REGIONS WITH MODIFIED Y PERMEABILITY

*---- NMOD2

17

CC

CC FIRST AND LAST INDEX IN X,Y,Z DIRECTION,MODIFIED METHOD,CONSTANT

VALUE.

*----	IMIN	IMAX	JMIN	JMAX	KMIN	KMAX	IFACT	FACTX
4	4	4	4	19	19	2	0.3826	
	8	8	4	4	19	19	2	0.6546
	9	9	7	7	19	19	2	0.3729
	8	8	10	10	19	19	2	0.3708
	4	4	10	10	19	19	2	0.3561
	3	3	7	7	19	19	2	0.3739
	3	3	2	2	19	19	2	0.3117
	9	9	2	2	19	19	2	0.734
	9	9	11	11	19	19	2	0.5459
	3	3	11	11	19	19	2	0.637
	6	6	7	7	19	19	2	0.5878
	6	6	2	2	19	19	2	0.2139
	10	10	4	4	19	19	2	0.6652
	10	10	10	10	19	19	2	0.3931
	6	6	11	11	19	19	2	0.4183
	2	2	10	10	19	19	2	0.5491
	2	2	4	4	19	19	2	0.6232

CC

CC NUMBER OF REGIONS WITH MODIFIED Z PERMEABILITY

*---- NMOD3

17

CC

CC FIRST AND LAST INDEX IN X,Y,Z DIRECTION,MODIFIED METHOD,CONSTANT

VALUE.

*----	IMIN	IMAX	JMIN	JMAX	KMIN	KMAX	IFACT	FACTX
4	4	4	4	19	19	2	0.3826	
	8	8	4	4	19	19	2	0.6546
	9	9	7	7	19	19	2	0.3729
	8	8	10	10	19	19	2	0.3708
	4	4	10	10	19	19	2	0.3561
	3	3	7	7	19	19	2	0.3739
	3	3	2	2	19	19	2	0.3117
	9	9	2	2	19	19	2	0.734
	9	9	11	11	19	19	2	0.5459
	3	3	11	11	19	19	2	0.637

6	6	7	7	19	19	2	0.5878
6	6	2	2	19	19	2	0.2139
10	10	4	4	19	19	2	0.6652
10	10	10	10	19	19	2	0.3931
6	6	11	11	19	19	2	0.4183
2	2	10	10	19	19	2	0.5491
2	2	4	4	19	19	2	0.6232

CC formation water (3000 ppm NaCl)

CC CONSTANT CHLORIDE AND CALCIUM CONCENTRATIONS (MEQ/ML)

*----C50 C60
0.0513 0.0

CC

CC*****

CC utchem requires 2 alochols

CC PHYSICAL PROPERTY DATA

CC

CC*****

CC

CC DW'S INPUT FILE FOR CORE FLOOD C (SPE 113965)

CC THE CSE SLOPE PARAMETER FOR CALCIUM AND ALCOHOL 1 AND ALCOHOL 2

*----BETA6
0.0

CC

CC LOG10 OF OIL/WATER INTERFACIAL TENSION

*----XIFTW
1.48

CC

CC relative perm. flag (0:imbibition corey,1:first drainage corey)

*----iperm IRTYPE
0 0

CC RESIDUAL SATURATION FOR EACH PHASE INPUT GIVEN THROUGH INCLUDE

FILES

CC FLAG FOR CONSTANT OR VARIABLE REL. PERM. PARAMETERS

*----ISRW IPRW IEW
4 0 0

CC

CC CONSTANT ENDPOINT REL. PERM. OF PHASES 1,2,AND 3 AT LOW CAPILLARY

NO.

*----P1RW P2RWZ
.30 0.7

CC CHEVRON - 04/10/2009

CC VARIABLE REL. PERM. EXPONENT OF PHASES 1,2,AND 3 AT LOW CAPILLARY

NO.

*----E1W E2W
2 2

CC SPE 113965

CC WATER AND OIL VISCOSITY at reference temperature, RESERVOIR TEMPERATURE

(leave zero)

*----VIS1 VIS2 TEMPV
1.5 3.4 30.

CC

CC oil viscosity parameters

*---- bv1 bv2

```

0 0
CC
CC
*----ALPHA1 ALPHA2 ALPHA3 ALPHA4 ALPHA5
      .1      2.5    0.1      0.1    0.1
CC
CC PARAMETERS TO CALCULATE POLYMER VISCOSITY AT ZERO SHEAR RATE
*----AP1  AP2  AP3
      0    0    0
CC
CC PARAMETER TO COMPUTE CSEP,MIN. CSEP, AND SLOPE OF LOG VIS. VS. LOG
CSEP
*----BETAP CSE1  SSLOPE
      20    0.01  -0.53
CC
CC PARAMETER FOR SHEAR RATE DEPENDENCE OF POLYMER VISCOSITY (50%
shear ~ 10 cP)
*----GAMMAC GAMHF POWN  IPMOD ISHEAR  RWEFF GAMHF2
      4      280    2.2    0      0      0.4    0
CC
CC FLAG FOR POLYMER (4) PARTITIONING, PERM. REDUCTION PARAMETERS
*----IPOLYM EPHI3 EPHI4  BRK  CRK  rkcut
      1      1.    1    100    0.2  10
CC
CC SPECIFIC WEIGHT FOR COMPONENTS 1,2,3,7,AND 8 , AND GRAVITY FLAG
*----DEN1  DEN2  IDEN
      62.428  55.568  2
CC
CC FLAG FOR CHOICE OF UNITS ( 0:BOTTOMHOLE CONDITION , 1: STOCK TANK)
*----ISTB
      1
CC
CC FVF FOR PHASE 1,2
*----(FVF(L),L=1,NPHAS)
      1  1.083
CC
CC COMPRESSIBILITY FOR VOL. OCCUPYING COMPONENTS 1,2,3,7,AND 8
*----COMPC(1) COMPC(2)
      0.00000  0.0000
CC
CC CONSTANT OR VARIABLE PC PARAM., WATER-WET OR OIL-WET PC CURVE
FLAG
*----ICPC  IEPC  IOW
      0    0    0
CC
CC CAPILLARY PRESSURE PARAMETERS, CPC
*----CPC
      0.
CC
CC CAPILLARY PRESSURE PARAMETERS, EPC
*----EPC
      2.
CC

```

```

CC MOLECULAR DIFFUSIVITY OF KCTH COMPONENT IN PHASE 1 (D(KC),KC=1,N)
*----D(1) D(2) D(3) D(4) D(5) D(6) D(7) D(8) D(9) D(10) D(11)
      0.  0.  0.  0.  0.  0.  0
CC
CC MOLECULAR DIFFUSIVITY OF KCTH COMPONENT IN PHASE 2 (D(KC),KC=1,N)
*----D(1) D(2) D(3) D(4) D(5) D(6) D(7) D(8) D(9) D(10) D(11)
      0.  0.  0.  0.  0.  0.  0
CC
CC LONGITUDINAL AND TRANSVERSE DISPERSIVITY (ft) OF PHASE 1
*----ALPHAL(1)  ALPHAT(1)
           4          0.4
CC
CC LONGITUDINAL AND TRANSVERSE DISPERSIVITY OF PHASE 2
*----ALPHAL(2)  ALPHAT(2)
           4          0.4
CC
CC SURFACTANT AND POLYMER ADSORPTION PARAMETERS
*---- AD41  AD42  B4D   iadk   fads   refk(mD)
      8.66   0.   100.   0     0.     0
CC
CC PARAMETERS FOR CATION EXCHANGE OF CLAY AND SURFACTANT MW (needed
for cation exch)
*----QV   XKC
      0.    0.
CC
CC
*---- IRKFOLD
      2
CC
CC
*---- APOLADM ABWGADM CRKPOL CRKBWG CLIMBWG
      1000        0.3      1      1.8      0.0
CC
CC
*---- AG1    AG2    AG3
      .005   .00260   0
CC
CC
*---- ALPHBWP ALPHBWG
           0          0
CC
CC
*---- ADBWGLIM,CBWGT
           0.3      100.0
CC
CC
*---- ADBWG0 ADBWGS ADBWGT ADBWGK ADBWG
      8.66   0    10   -0.01  10.
CC
CC
*---- TEMTRBWG CCRLRBWG CPOLRBWG CBWGRBWG
      150.0        0.0      0.0      0.0
CC

```



```

CC
CC
*----kprf
    0 0 1 1 0 0 1 1 1 1 1 1 1 1 1 1 1 1
CC
CC WELL NAME
*---- WELNAM
S1_I2
CC
CC MAX. AND MIN. ALLOWABLE BOTTOMHOLE PRESSURE AND RATE
*----ICHEK  PWFMIN  PWFMAX  QTMIN  QTMAX
        0      300.0   1300.0      0.0   84219
CC
SKIN CC WELL ID,LOCATION,AND FLAG FOR SPECIFYING WELL TYPE, WELL RADIUS,
*----IDW IW  JW  IFLAG  RW  SWELL IDIR IFIRST  ILAST  IPRF
        3   9   7    1    0.4    0    3    1    19    1
cc
cc
*----kprf
    0 0 0 0 0 0 0 1 1 1 1 1 1 1 1 1 1 1
CC
CC WELL NAME
*---- WELNAM
S1_I3
CC
CC MAX. AND MIN. ALLOWABLE BOTTOMHOLE PRESSURE AND RATE
*----ICHEK  PWFMIN  PWFMAX  QTMIN  QTMAX
        0      300.0   1300.0      0.0   84219
CC
SKIN CC WELL ID,LOCATION,AND FLAG FOR SPECIFYING WELL TYPE, WELL RADIUS,
*----IDW IW  JW  IFLAG  RW  SWELL IDIR IFIRST  ILAST  IPRF
        4   8  10    1    0.4    0    3    1    19    1
cc
cc
*----kprf
    1 1 0 1 0 0 0 1 1 1 1 1 1 1 1 1 1 1
CC
CC WELL NAME
*---- WELNAM
S1_I4
CC
CC MAX. AND MIN. ALLOWABLE BOTTOMHOLE PRESSURE AND RATE
*----ICHEK  PWFMIN  PWFMAX  QTMIN  QTMAX
        0      300.0   1300.0      0.0   84219
CC
CC WELL ID,LOCATION,AND FLAG FOR SPECIFYING WELL TYPE, WELL RADIUS
*----IDW IW  JW  IFLAG  RW  SWELL IDIR IFIRST  ILAST  IPRF
        5   4  10    1    0.4    0    3    1    19    1
cc
cc
*----kprf

```

```

      11110111111111111111
CC
CC WELL NAME
*---- WELNAM
S1_I5
CC
CC MAX. AND MIN. ALLOWABLE BOTTOMHOLE PRESSURE AND RATE
*----ICHEK  PWFMIN  PWFMAX  QTMIN  QTMAX
      0      300.0  1300.0      0.0   84219
CC
SKIN CC WELL ID,LOCATIONS,AND FLAG FOR SPECIFYING WELL TYPE, WELL RADIUS,
*----IDW IW  JW  IFLAG  RW  SWELL IDIR IFIRST  ILAST  IPRF
      6   3  7    1    0.4    0    3    1    19    1
cc
cc
*----kprf
      01111111111111111111
CC
CC WELL NAME
*---- WELNAM
S1_I6
CC
CC MAX. AND MIN. ALLOWABLE BOTTOMHOLE PRESSURE AND RATE
*----ICHEK  PWFMIN  PWFMAX  QTMIN  QTMAX
      0      300.0  1300.0      0.0   84219
CC
SKIN CC WELL ID,LOCATIONS,AND FLAG FOR SPECIFYING WELL TYPE, WELL RADIUS,
*----IDW IW  JW  IFLAG  RW  SWELL IDIR IFIRST  ILAST  IPRF
      7   3  2    1    0.4    0    3    1    19    1
CC
CC
*----kprf
      11111111111111111111
CC
CC WELL NAME
*---- WELNAM
S1_I7
CC
CC MAX. AND MIN. ALLOWABLE BOTTOMHOLE PRESSURE AND RATE
*----ICHEK  PWFMIN  PWFMAX  QTMIN  QTMAX
      0      300.0  1300.0      0.0   84219
CC
SKIN CC WELL ID,LOCATIONS,AND FLAG FOR SPECIFYING WELL TYPE, WELL RADIUS,
*----IDW IW  JW  IFLAG  RW  SWELL IDIR IFIRST  ILAST  IPRF
      8   9  2    1    0.4    0    3    1    19    1
cc
cc
*----kprf
      11010011111111111111
CC

```



```

CC WELL NAME
*---- WELNAM
S1_I8
CC
CC MAX. AND MIN. ALLOWABLE BOTTOMHOLE PRESSURE AND RATE
*----ICHEK  PWFMIN  PWFMAX  QTMIN  QTMAX
          0    300.0    1300.0    0.0    84219
CC
SKIN CC WELL ID,LOCATION,AND FLAG FOR SPECIFYING WELL TYPE, WELL RADIUS,
*----IDW IW  JW  IFLAG  RW  SWELL IDIR IFIRST  ILAST  IPRF
          9   9  11      1  0.4    0      3   1      19    1
cc
cc
*----kprf
    11111111111111111111
CC
CC WELL NAME
*---- WELNAM
S1_I9
CC
CC MAX. AND MIN. ALLOWABLE BOTTOMHOLE PRESSURE AND RATE
*----ICHEK  PWFMIN  PWFMAX  QTMIN  QTMAX
          0    300.0    1300.0    0.0    84219
CC
SKIN CC WELL ID,LOCATION,AND FLAG FOR SPECIFYING WELL TYPE, WELL RADIUS,
*----IDW IW  JW  IFLAG  RW  SWELL IDIR IFIRST  ILAST  IPRF
          10   3  11      1  0.4    0      3   1      19    1
cc
cc
*----kprf
    11110111111111111111
CC
CC WELL NAME
*---- WELNAM
S1_I10
CC
CC MAX. AND MIN. ALLOWABLE BOTTOMHOLE PRESSURE AND RATE
*----ICHEK  PWFMIN  PWFMAX  QTMIN  QTMAX
          0    300.0    1300.0    0.    84219
CC
SKIN CC WELL ID,LOCATION,AND FLAG FOR SPECIFYING WELL TYPE, WELL RADIUS,
*----IDW IW  JW  IFLAG  RW  SWELL IDIR IFIRST  ILAST  IPRF
          11   6   7      2  0.4    0   3      1   19    1
cc
cc
*----kprf
    00000111111111111111
CC
CC WELL NAME
*---- WELNAM

```

```

S1_P1
CC DW, max 10000 bbls/d
CC MAX. AND MIN. ALLOWABLE BOTTOMHOLE PRESSURE AND RATE
*----ICHEK PWFMIN PWFMAX QTMIN QTMAX
      0    300.0    1300.    0.0 -56146.0
CC
SKIN CC WELL ID,LOCATION,AND FLAG FOR SPECIFYING WELL TYPE, WELL RADIUS,
*----IDW IW JW IFLAG RW SWELL IDIR IFIRST ILAST IPRF
      12  6  2    2  0.4    0    3    1    9    1
cc
cc
*----kprf
      1 1 1 1 1 0 1 1 1 1 1 1 1 1 1 1 1 1 1 1 1 1
CC
CC WELL NAME
*---- WELNAM
S1_P2
CC
CC MAX. AND MIN. ALLOWABLE BOTTOMHOLE PRESSURE AND RATE
*----ICHEK PWFMIN PWFMAX QTMIN QTMAX
      0    300.0    1400.    0.0 -28073
CC
SKIN CC WELL ID,LOCATION,AND FLAG FOR SPECIFYING WELL TYPE, WELL RADIUS,
*----IDW IW JW IFLAG RW SWELL IDIR IFIRST ILAST IPRF
      13 10  4  2    0.4    0    3    1    19    1
cc
cc
*----kprf
      0 0 0 0 0 0 0 0 0 0 0 0 0 0 0 0 1 1 1 1
CC
CC WELL NAME
*---- WELNAM
S1_P3
CC
CC MAX. AND MIN. ALLOWABLE BOTTOMHOLE PRESSURE AND RATE
*----ICHEK PWFMIN PWFMAX QTMIN QTMAX
      0    300.    0  1400.    0.0 -28073
CC
SKIN CC WELL ID,LOCATION,AND FLAG FOR SPECIFYING WELL TYPE, WELL RADIUS,
*----IDW IW JW IFLAG RW SWELL IDIR IFIRST ILAST IPRF
      14 10 10    2  0.4    0    3    1    19    1
cc
cc
*----kprf
      1 1 1 1 0 0 1 1 1 1 1 1 1 1 1 1 1 1 1 1
CC
CC WELL NAME
*---- WELNAM
S1_P4
CC

```

```

CC MAX. AND MIN. ALLOWABLE BOTTOMHOLE PRESSURE AND RATE
*----ICHEK  PWFMIN  PWFMAX  QTMIN  QTMAX
          0    300.0    1400.    0.0  -28073
CC
SKIN CC WELL ID,LOCATION,AND FLAG FOR SPECIFYING WELL TYPE, WELL RADIUS,
*----IDW IW  JW  IFLAG  RW  SWELL IDIR IFIRST  ILAST  IPRF
          15  6  11  2    0.4    0  3    1    19    1
cc
cc
*----kprf
      1 1 1 1 0 1 1 1 1 1 1 1 1 1 1 1 1 1 1 1 1 1
CC
CC WELL NAME
*---- WELNAM
S1_P5
CC
CC MAX. AND MIN. ALLOWABLE BOTTOMHOLE PRESSURE AND RATE
*----ICHEK  PWFMIN  PWFMAX  QTMIN  QTMAX
          0    300.0    1400.    0.0  -28073
CC
SKIN CC WELL ID,LOCATION,AND FLAG FOR SPECIFYING WELL TYPE, WELL RADIUS,
*----IDW IW  JW  IFLAG  RW  SWELL IDIR IFIRST  ILAST  IPRF
          16  2  10  2    0.4    0  3    1    19    1
cc
cc
*----kprf
      1 1 1 0 1 1 1 1 1 1 1 1 1 1 1 1 1 1 1 1 1 1
CC
CC WELL NAME
*---- WELNAM
S1_P6
CC
CC MAX. AND MIN. ALLOWABLE BOTTOMHOLE PRESSURE AND RATE
*----ICHEK  PWFMIN  PWFMAX  QTMIN  QTMAX
          0    300.0    1400.    0.0  -28073
CC
SKIN CC WELL ID,LOCATION,AND FLAG FOR SPECIFYING WELL TYPE, WELL RADIUS,
*----IDW IW  JW  IFLAG  RW  SWELL IDIR IFIRST  ILAST  IPRF
          17  2  4  2    0.4    0  3    1    19    1
cc
cc
*----kprf
      1 1 1 1 1 1 1 1 1 1 1 1 1 1 1 1 1 1 1 1 1 1
CC
CC WELL NAME
*---- WELNAM
S1_P7
CC
CC MAX. AND MIN. ALLOWABLE BOTTOMHOLE PRESSURE AND RATE
*----ICHEK  PWFMIN  PWFMAX  QTMIN  QTMAX

```

```

0    300.0    1400.    0.0    -28073
CC
CC Pressure constrained producer
*----WELL ID PWF
  1 44916.8    1.    0.    0    0    0.05130    0.    0
  1 0.          0.    0.    0.    0.    0.          0.    0
cc
cc
*--- id tinj
  1 140
CC
CC Pressure constrained producer
*----WELL ID PWF
  2 44916.8    1.    0.    0    0    0.05130    0.    0
  2 0.          0.    0.    0.    0.    0.          0.    0
cc
cc
*--- id tinj
  2 140
CC
CC Pressure constrained producer
*----WELL ID PWF
  3 44916.8    1.    0.    0    0    0.05130    0.    0
  3 0.          0.    0.    0.    0.    0.          0.    0
cc
cc
*--- id tinj
  3 140
CC
CC id,INJ. RATE AND INJ. COMP. FOR RATE CONS. WELLS FOR EACH PHASE(L=1,3)
*----id QI(M,L) C(M,KC,L) (need to keep 2nd and 3rd lines for oil and ME)
  4 44916.8    1.    0.    0    0    0.0513    0.    0
  4 0.          0.    0.    0.    0.    0.          0.    0
cc
cc
*--- id tinj
  4 140
CC
CC id,INJ. RATE AND INJ. COMP. FOR RATE CONS. WELLS FOR EACH PHASE(L=1,3)
*----id QI(M,L) C(M,KC,L) (need to keep 2nd and 3rd lines for oil and ME)
  5 44916.8    1.    0.    0    0    0.0513    0.    0
  5 0.          0.    0.    0.    0.    0.          0.    0
cc
cc
*--- id tinj
  5 140
CC
CC id,INJ. RATE AND INJ. COMP. FOR RATE CONS. WELLS FOR EACH PHASE(L=1,3)
*----id QI(M,L) C(M,KC,L) (need to keep 2nd and 3rd lines for oil and ME)
  6 44916.8    1.    0.    0    0    0.0513    0.    0
  6 0.          0.    0.    0.    0.    0.          0.    0
cc
cc

```

```

*--- id tinj
    6 140
CC
CC id,INJ. RATE AND INJ. COMP. FOR RATE CONS. WELLS FOR EACH PHASE(L=1,3)
*----id QI(M,L) C(M,KC,L) (need to keep 2nd and 3rd lines for oil and ME)
    7 22458.4 1. 0. 0 0 0.05130 0. 0
    7 0. 0. 0. 0. 0. 0. 0. 0
cc
cc
*--- id tinj
    7 140
CC
CC id,INJ. RATE AND INJ. COMP. FOR RATE CONS. WELLS FOR EACH PHASE(L=1,3)
*----id QI(M,L) C(M,KC,L) (need to keep 2nd and 3rd lines for oil and ME)
    8 22458.4 1. 0. 0 0 0.0513 0. 0
    8 0. 0. 0. 0. 0. 0. 0. 0
cc
cc
*--- id tinj
    8 140
CC
CC id,INJ. RATE AND INJ. COMP. FOR RATE CONS. WELLS FOR EACH PHASE(L=1,3)
*----id QI(M,L) C(M,KC,L) (need to keep 2nd and 3rd lines for oil and ME)
    9 22458.4 1. 0. 0 0 0.0513 0. 0
    9 0. 0. 0. 0. 0. 0. 0. 0
cc
cc
*--- id tinj
    9 140
CC
CC id,INJ. RATE AND INJ. COMP. FOR RATE CONS. WELLS FOR EACH PHASE(L=1,3)
*----id QI(M,L) C(M,KC,L) (need to keep 2nd and 3rd lines for oil and ME)
    10 22458.4 1. 0. 0 0 0.0513 0. 0
    10 0. 0. 0. 0. 0. 0. 0. 0
cc
cc
*--- id tinj
    10 140
CC
CC Pressure constrained producer
*----WELL ID PWF
    11 300.0
CC
CC Pressure constrained producer
*----WELL ID PWF
    12 300.0
CC
CC Pressure constrained producer
*----WELL ID PWF
    13 300.0
CC
CC Pressure constrained producer
*----WELL ID PWF

```

```

14      300.0
CC
CC Pressure constrained producer
*----WELL ID PWF
      15      300.0
CC
CC Pressure constrained producer
*----WELL ID PWF
      16      300.0
CC
CC Pressure constrained producer
*----WELL ID PWF
      17      300.0
CC
CC CUM. INJ. TIME , AND INTERVALS (PV OR DAY) FOR WRITING TO OUTPUT FILES
(3.7.8)
*----TINJ CUMPR1 CUMHI2 WRHPV(HIST) WRPRF(PLOT) RSTC
      5      0.5      0.5      0.5      0.5      0.5
CC
CC FOR IMES=2 ,THE INI. TIME STEP,CONC. TOLERANCE,MAX.,MIN. time steps
*----DT DCLIM CNMAX CNMIN
      0.00001 0.01 0.4 0.04
CC
CC IRO, ITIME, NEW FLAGS FOR ALL THE WELLS ( WATER INJ.)
*----IRO ITIME IFLAG
      2 1 10*1 7*2
CC
CC NUMBER OF WELLS CHANGES IN LOCATION OR SKIN OR PWF
*----NWEL1
      0
CC
CC NUMBER OF WELLS WITH RATE CHANGES, ID
*----NWEL2 ID
      10 1 2 3 4 5 6 7 8 9 10
CC
CC Pressure constrained producer
*----WELL ID PWF
      1 14036.5 1. 0. 0 0 0.0513 0. 3000
      1 0. 0. 0. 0. 0. 0. 0. 0
cc
cc
*--- id tinj
      1 140
CC
CC Pressure constrained producer
*----WELL ID PWF
      2 14036.5 1. 0. 0 0 0.0513 0. 3000
      2 0. 0. 0. 0. 0. 0. 0. 0
cc
cc
*--- id tinj
      2 140
CC

```

```

CC Pressure constrained producer
*----WELL ID PWF
  3 14036.5 1. 0. 0 0 0.05130 0. 3000
  3 0. 0. 0. 0. 0. 0. 0. 0
cc
cc
*--- id tinj
  3 140
CC
CC id,INJ. RATE AND INJ. COMP. FOR RATE CONS. WELLS FOR EACH PHASE(L=1,3)
*----id QI(M,L) C(M,KC,L) (need to keep 2nd and 3rd lines for oil and ME)
  4 24036.5 1. 0. 0 0 0.0513 0. 3000
  4 0. 0. 0. 0. 0. 0. 0. 0
cc
cc
*--- id tinj
  4 140
CC
CC id,INJ. RATE AND INJ. COMP. FOR RATE CONS. WELLS FOR EACH PHASE(L=1,3)
*----id QI(M,L) C(M,KC,L) (need to keep 2nd and 3rd lines for oil and ME)
  5 24036.5 1. 0. 0 0 0.05130 0. 3000
  5 0. 0. 0. 0. 0. 0. 0. 0
cc
cc
*--- id tinj
  5 140
CC
CC id,INJ. RATE AND INJ. COMP. FOR RATE CONS. WELLS FOR EACH PHASE(L=1,3)
*----id QI(M,L) C(M,KC,L) (need to keep 2nd and 3rd lines for oil and ME)
  6 24036.5 1. 0. 0 0 0.05130 0. 3000
  6 0. 0. 0. 0. 0. 0. 0. 0
cc
cc
*--- id tinj
  6 140
CC
CC id,INJ. RATE AND INJ. COMP. FOR RATE CONS. WELLS FOR EACH PHASE(L=1,3)
*----id QI(M,L) C(M,KC,L) (need to keep 2nd and 3rd lines for oil and ME)
  7 12036.5 1. 0. 0 0 0.05130 0. 3000
  7 0. 0. 0. 0. 0. 0. 0. 0
cc
cc
*--- id tinj
  7 140
CC
CC id,INJ. RATE AND INJ. COMP. FOR RATE CONS. WELLS FOR EACH PHASE(L=1,3)
*----id QI(M,L) C(M,KC,L) (need to keep 2nd and 3rd lines for oil and ME)
  8 12036.5 1. 0. 0 0 0.05130 0. 3000
  8 0. 0. 0. 0. 0. 0. 0. 0
cc
cc
*--- id tinj
  8 140

```

```

CC
CC id,INJ. RATE AND INJ. COMP. FOR RATE CONS. WELLS FOR EACH PHASE(L=1,3)
*----id QI(M,L) C(M,KC,L) (need to keep 2nd and 3rd lines for oil and ME)
  9 12036.5 1. 0. 0 0 0.05130 0. 3000
  9 0. 0. 0. 0. 0. 0. 0
cc
cc
*--- id tinj
  9 140
CC
CC id,INJ. RATE AND INJ. COMP. FOR RATE CONS. WELLS FOR EACH PHASE(L=1,3)
*----id QI(M,L) C(M,KC,L) (need to keep 2nd and 3rd lines for oil and ME)
 10 12036.5 1. 0. 0 0 0.05130 0. 3000
 10 0. 0. 0. 0. 0. 0. 0
cc
cc
*--- id tinj
 10 140
CC
CC CUM. INJ. TIME , AND INTERVALS (PV OR DAY) FOR WRITING TO OUTPUT FILES
*---- TINJ CUMPR1 CUMHI1 WRHPV WRPRF RSTC
      5.2 0.1 0.1 0.1 0.1 0.1
CC
CC FOR IMES=2 ,THE INI. TIME STEP,CONC. TOLERANCE,MAX.,MIN. time steps
*----DT DCLIM CNMAX CNMIN
0.00001 0.01 0.4 0.04
CC
CC IRO, ITIME, NEW FLAGS FOR ALL THE WELLS ( WATER INJ.)
*---- IRO ITIME IFLAG
  2 1 10*1 7*2
CC
CC NUMBER OF WELLS CHANGES IN LOCATION OR SKIN OR PWF
*----NWEL1
  0
CC
CC NUMBER OF WELLS WITH RATE CHANGES, ID
*----NWEL2 ID
 10 1 2 3 4 5 6 7 8 9 10
CC
CC Pressure constrained producer
*----WELL ID PWF
  1 24916.8 1. 0. 0 0 0.0513 0. 0
  1 0. 0. 0. 0. 0. 0. 0
cc
cc
*--- id tinj
  1 140
CC
CC Pressure constrained producer
*----WELL ID PWF
  2 24916.8 1. 0. 0 0 0.0513 0. 0
  2 0. 0. 0. 0. 0. 0. 0
cc

```



```

cc
*--- id tinj
  2 140
CC
CC Pressure constrained producer
*----WELL ID PWF
  3 24916.8 1. 0. 0 0 0.0513 0. 0
  3 0. 0. 0. 0. 0. 0. 0. 0
cc
cc
*--- id tinj
  3 140
CC
CC id,INJ. RATE AND INJ. COMP. FOR RATE CONS. WELLS FOR EACH PHASE(L=1,3)
*----id QI(M,L) C(M,KC,L) (need to keep 2nd and 3rd lines for oil and ME)
  4 24916.8 1. 0. 0 0 0.0513 0. 0
  4 0. 0. 0. 0. 0. 0. 0. 0
cc
cc
*--- id tinj
  4 140
CC
CC id,INJ. RATE AND INJ. COMP. FOR RATE CONS. WELLS FOR EACH PHASE(L=1,3)
*----id QI(M,L) C(M,KC,L) (need to keep 2nd and 3rd lines for oil and ME)
  5 24916.8 1. 0. 0 0 0.0513 0. 0
  5 0. 0. 0. 0. 0 0. 0. 0
cc
cc
*--- id tinj
  5 140
CC
CC id,INJ. RATE AND INJ. COMP. FOR RATE CONS. WELLS FOR EACH PHASE(L=1,3)
*----id QI(M,L) C(M,KC,L) (need to keep 2nd and 3rd lines for oil and ME)
  6 24916.8 1. 0. 0 0 0.0513 0. 0
  6 0. 0. 0. 0. 0. 0. 0. 0
cc
cc
*--- id tinj
  6 140
CC
CC id,INJ. RATE AND INJ. COMP. FOR RATE CONS. WELLS FOR EACH PHASE(L=1,3)
*----id QI(M,L) C(M,KC,L) (need to keep 2nd and 3rd lines for oil and ME)
  7 12916.8 1. 0. 0 0 0.0513 0. 0
  7 0. 0. 0. 0. 0. 0. 0. 0
cc
cc
*--- id tinj
  7 140
CC
CC id,INJ. RATE AND INJ. COMP. FOR RATE CONS. WELLS FOR EACH PHASE(L=1,3)
*----id QI(M,L) C(M,KC,L) (need to keep 2nd and 3rd lines for oil and ME)
  8 12916.8 1. 0. 0 0 0.0513 0. 0
  8 0. 0. 0. 0. 0 0. 0. 0

```

```

cc
cc
*--- id tinj
      8 140
CC
CC id,INJ. RATE AND INJ. COMP. FOR RATE CONS. WELLS FOR EACH PHASE(L=1,3)
*----id QI(M,L) C(M,KC,L) (need to keep 2nd and 3rd lines for oil and ME)
      9 12916.8 1. 0. 0 0 0.0513 0. 0
      9 0.      0. 0. 0. 0. 0.      0. 0
cc
cc
*--- id tinj
      9 140
CC
CC id,INJ. RATE AND INJ. COMP. FOR RATE CONS. WELLS FOR EACH PHASE(L=1,3)
*----id QI(M,L) C(M,KC,L) (need to keep 2nd and 3rd lines for oil and ME)
      10 12916.8 1. 0. 0 0 0.0513 0. 0
      10 0.      0. 0. 0. 0. 0.      0. 0
cc
cc
*--- id tinj
      10 140
CC
C CUM. INJ. TIME , AND INTERVALS (PV OR DAY) FOR WRITING TO OUTPUT FILES
*---- TINJ  CUMPR1  CUMHI1  WRHPV  WRPRF  RSTC
      10      0.2      0.2      0.2      0.2      0.2
CC
CC FOR IMES=2 ,THE INI. TIME STEP,CONC. TOLERANCE,MAX.,MIN. time steps
*----DT      DCLIM  CNMAX  CNMIN
      0.00001      0.01  0.4  0.04

```

Nomenclature

English Symbols

A_p	Coefficient for polymer viscosity equation
A_G	Coefficient for gel viscosity equation
A	Empirical constant to fit “ pH vs. Q ” curve
B	Empirical constant to fit “ pH vs. Q ” curve
b_k	Input parameter
b_G	Input parameter
b_{rk}	Input parameter which depends on the gel type
C	Empirical constant to fit “ pH vs. Q ” curve
C_{CL}	Crosslinker concentration
C_{CL_0}	Crosslinker reaction rate multiplier
C_p	Polymer concentration
C_{p_0}	Polymer reaction rate multiplier
C_{rk}	Input parameter which depends on the gel type
C_{SEP}^s	Factor that allows for dependence of polymer viscosity on salinity and hardness
C_{SEP}	Effective salinity for polymer
C_{11}	Water concentration in the aqueous phase
C_{51}	Anion concentration in the aqueous phase
C_{61}	Calcium concentration in the aqueous phase
C_{TG}	Gel threshold concentration for cubic term
$C_{G,1}^*$	Concentration of component in water after adsorption
\hat{C}_{max}	Maximum adsorption
c_j	Concentration of j -ion in solution inside of the polymer network
c_j^*	Concentration of j -ion in solution outside of the polymer network.
D	Empirical constant to fit “ pH vs. Q ” curve
E	Empirical constant to fit “ pH vs. Q ” curve
E_G	Temperature dependence parameters of gel
E_p	Temperature dependence parameters of polymer
$[H^+]$	Concentration of hydrogen ion.
I	Ionic strength of solvent

K_a	Dissociation constant of ionizable groups on polymer
\bar{k}	Average permeability
k_x	Absolute permeability in the x direction
k_y	Absolute permeability in the y direction
k_z	Absolute permeability in the z direction
l	Phase l
$\overline{M_c}$	Average polymer molecular weight between crosslinks
$\overline{M_n}$	Average molecular weight of polymer before crosslinking
n	Polymer specific constants
P_α	Empirical coefficient
Q	Equilibrium swelling ratio
$R_{K,BWG\max}$	Gel maximum resistance factor at the maximum gel \hat{C}_{\max} adsorption
$R_{K,\max}$	Maximum resistance factor at the maximum adsorption \hat{C}_{\max}
$R_{K,P\max}$	Polymer maximum resistance factor at the maximum polymer \hat{C}_{\max} adsorption
$R_{RF,\max}$	Maximum residual resistance factor
r_{BWG}	Reaction rate coefficient of BWG
r_{CL}	Reaction rate coefficient of crosslinker
r_P	Reaction rate coefficient of polymer
$[RCOO^-]$	Concentration of dissociated polymer chains
$[RCOOH]$	Concentration of undissociated polymer chains
S_k	Input parameter
S_l	Saturation of phase l
S_p	slope of $\left(\frac{\mu_p^0 - \mu_w}{\mu_w}\right)$ vs. C_{SEP} on a log-log plot
T_{ref}	Reference temperature
u_l	Darcy flux of phase l
u_{xl}	Darcy flux in x direction
u_{yl}	Darcy flux in y direction
u_{zl}	Darcy flux in z direction
V_1	Molar volume of solvent

Greek Symbols

α	Empirical constant
β_p	Input parameter to the model measured in the laboratory
β_k	Temperature coefficient
γ	Shear rate
$\dot{\gamma}$	Shear rate
$\dot{\gamma}_{1/2}$	Shear rate at which viscosity is the average of μ^0 and μ_w
$\dot{\gamma}_{eq}$	Equivalent shear rate
$\dot{\gamma}_c$	$3.97C \text{ sec}^{-1}$
$ \eta $	Intrinsic viscosity
η	Polymer solution viscosity at a specific shear rate
η_o	Limiting Newtonian viscosity at the low shear limit
η_∞	Limiting Newtonian viscosity at the high shear limit
k_{rl}	Relative permeability of phase l
λ	Polymer specific constants
$\mu_{k,ref}$	Viscosity at a reference temperature T_{ref}
μ_w	Water viscosity
μ_1	Chemical potential of the swelling agent
χ_1	Polymer-solvent interaction parameter
ϕ	Porosity
$\nu_{2,s}$	Polymer volume fraction in the swollen network
$\bar{\nu}$	Specific molar volume of dry polymer
$\nu_{2,r}$	Polymer volume fraction in the relaxed state
$\nu_{2,s}$	Polymer volume fraction

REFERENCES

- Akanni , O.O. 2010. Analysis of In-Depth Profile Modification Reservoir Sweep Improvement and Comparison with Polymer Flooding for Improved Oil Recovery, MS thesis, New Mexico Institute of Mining and Technology, Socorro, New Mexico, U.S., 2010.
- Al-Anazi, H. and Sharma, M.M. 2002. Use of a pH Sensitive Polymer for Conformance Control. Paper SPE 73782 presented at the International Symposium and Exhibition on Formation Damage Control held in Louisiana, 20-21 February 2002.
- Bai, B., Liu, Y., Coste, J-P., and Li, L. 2007. Preformed Particle Gel for Conformance Control: Transport Mechanism through Porous Media. SPE Res. Eval. & Eng. 10(2). SPE-89468-PA, 2007.
- Bai, B. *et al.* 2012. Preformed Particle Gel for Conformance Control. Final Report, U.S. Department of Energy, DOE Contract N0.: 07123-2, U.S. DOE, Washington, DC, March 2012.
- Bird, R.B., Armstrong, R.C, and Hassager, O. 1977. Dynamics of Polymeric Liquids. Vol. 1: Fluid Mechanics, John Wiley & Sons, 1977.
- Brannon-Peppas, L., and Peppas, N.A. 1988. Structural Analysis of Charged Polymeric Networks. Polymer Bull., 20, 1988.
- Brannon-Peppas, L. 1990. Preparation and Characterization of Crosslinked Hydrophilic Networks in Absorbent Polymer Technology. Studies in Polymer Sci., 8, Brannon-Peppas, L., and Harland., eds, 1990.
- Brannon-Peppas, L., and Peppas, N.A. 1990. The Equilibrium Swelling Behavior of Porous and Non-Porous Hydrogels. Absorbent Polymer Technology, Studies in Polymer Sci., 8, Brannon-Peppas, L., and Harland , R.S., eds, 1990.
- Brannon-Peppas, L., and Peppas, N.A. 1991. Equilibrium Swelling Behavior of pH-Sensitive Hydrogels. Chem Eng. Sci., 46(3), 1991.
- Bray, J.C., and Merril, E.W. 1973. Poly(vinyl Alcohol) Hydrogels. Formation by Electron Beam Irradiation of Aqueous Solutions and Subsequent Crystallization. J. Appl. Polym. Sci., 17, 1973.
- Budtova, T.V., Budtov V. P., Navard, P., and Frenkel, S.Y. 1994. Rheological Properties of Highly Swollen Hydrogel Suspensions. J. Appl. Polym. Sci., 52, 1994.
- Canella, W. J., Huh, C., and Seright, R. S. 1988. Prediction of Xanthan Rheology in Porous Media. SPE 18089 presented at 63rd Annual Tech. Conf. SPE, Houston, TX, October, 1988.
- Chang, H.L., Sui, X., Xiao, L., Guo, Z., Yao, X., Chen, G., Song, K., and Mack, J. C. Successful Field Pilot of In-Depth Colloidal Dispersion Gel (CDG) Technology in Daqing Oil Field. Paper SPE 89460 presented at the 2004 SPE/DOE Fourteenth Symposium on Oil Recovery held in Tulsa, Oklahoma, U.S.A., 17-21 April 2004.
- Chauveteau, G., Tabary, R., Renard, M., and Omari, A. 1999. Controlling In-Situ Gelation of Polyacrylamides by Zirconium for Water Shutoff. Paper SPE 50752 presented at the SPE International Symposium on Oilfield Chemistry, Houston, 16-19 February, 1999.

Cheung, S. 2007. A Swelling Polymer for In-Depth Profile Modification: Update on Field Applications. Presented at the SPE Applied Technology Workshop of Chemical Methods of Reducing Water Production, San Antonio, U.S.A., 4-6 March, 2007.

Coste, J.-P., Liu, Y., Bai, B., Li, Y., Shen, P., Wang, Z., and Zhu, G. 2000. In-Depth Fluid Diversion by Pre-Gelled Particles. Laboratory Study and Pilot Testing. Paper SPE 59362 presented at the SPE/DOE improved Oil Recovery Symposium, Tulsa, 3-5 April, 2000.

Delshad, M., Varavei, J., and Sepehrnoori, K. The University of Texas at Austin Gel Simulator (UTGEL), 2011.

Fielding Jr., R.C., Gibsons, D.H., and Legrand F.P. 1994. In-Depth Drive Fluid Dispersion Using an Evolution of Colloidal Dispersion Gels and New Bulk Gels: An Operational Case History of North Rainbow ranch Unit. Paper SPE/DOE 27773 presented at the SPE/DOE Ninth Symposium on Improved Oil Recovery held in Tulsa, Oklahoma, U.S.A., 17-20 April 1994.

Flory, P.J. 1953. Principles of Polymer Chemistry, Ithaca, New York. Cornell University Press.

Frampton, H., Morgan, J.C., Cheung, K.T., and Williams, D. 2004. Development of a Novel Waterflood Conformance Control System. Paper SPE 89391 presented at the 2004 SPE/DOE Fourteenth Symposium on Improved Oil Recovery held in Tulsa, Oklahoma, U.S.A., 17-21 April.

Garmeh, R., Izadi, M., Salehi, M., Romero, J.L., Thomas, C.P., Manrique, E.J. 2011. Thermally Active Polymer to Improve Sweep Efficiency of Waterfloods: Simulation and Pilot Design Approaches. Paper SPE 144234 presented at the SPE Enhanced Oil Recovery Conference held in Kuala Lumpur, Malaysia, 19-21 July, 2011.

Ghaddab, F., Kaddour, K., Tesconi, M., Brancolini, A., Carniani, C., Galli, G. 2010. El Borma – Brightwater: A Tertiary Method for Enhancing Oil Recovery for a Mature Field. Paper SPE 136140 presented at the SPE Production and Operations Conference and Exhibition held in Tunis, Tunisia, 8-10 June, 2010.

Huh, C., Choi, S.K., Sharma, M.M. A Rheological Model for pH-Sensitive Ionic Polymer Solutions for Optimal Mobility Control Applications. Paper SPE 96914 presented at 2005 SPE Annual Technical Conference and Exhibition, Dallas, TX, October 9-12, 2005.

Izgec, O., Shook, G.M. 2012. Design Considerations of Waterflood Conformance Control with Temperature-triggered Low Viscosity Sub-Micron Polymer. Paper SPE 153898 presented at SPE Western Regional Meeting held in Bakersfield, California, U.S.A., 19-23 March, 2012.

Lalehrokh, F. and Bryant, S.L. 2009. Application of pH-Triggered Polymers for Deep Conformance Control in Fractured Reservoirs. Paper SPE 124773 presented at the 2009 SPE Annual Technical Conference and Exhibition held in New Orleans, Louisiana, U.S.A., 4-7 October 2009.

Lalehrokh, F. 2010. Application of pH-Triggered Polymers to Increase Sweep Efficiency in Fractured Reservoirs. PhD dissertation.

Lane, R.H. and Seright, R.S. 2000. Gel Water Shutoff in Fractured or Faulted Horizontal Wells. Paper SPE 65527 presented at the SPE/PS-CIM International Conference on Horizontal Well Technology, Calgary, Canada, 6-8 November, 2000.

Lange, E.A., and Huh, C. 1994. A Polymer Thermal Decomposition Model and its Application in Chemical EOR Process Simulation. Paper SPE/DOE 27822 presented at SPE/DOE Improved Oil Recovery Symp., Tulsa, OK, U.S.A., April 17-20 1994.

Larkin, R., and Creel, P. 2002. Methodologies and Solutions to Remediate Inter-Well Communication Problems on the SACROC CO₂ EOR Project – A Case Study. Paper SPE 113305 presented at the SPE/DOE Symposium on Improved Oil Recovery, Tulsa, 19-23 April 2008.

Lee, R., R.Seright, M.Hightower, A.Sattler, M.Cather, B.McPherson, L.Wrotenbery, D. Martin, and M.Whitworth, 2002. Strategies for Produced Water Handling in New Mexico. Presented at the 2002 Ground Water Protection Council Produced Water Conference, Colorado Springs, CO, October 16-17, 2002.

Liang, J-T., Lee, R.L., and Seright R.S. 1993. Gel Placement in Production Wells. SPE Prod & Fac 8(4); Trans., AIME, 295. SPE-20211-PA.

Lin, E. 1981. A Study of Micellar/Polymer Flooding Using a Compositional Simulator, PhD dissertation, The University of Texas at Austin.

Liu J. 1993. High-Resolution Methods for Enhanced Oil Recovery Simulation, PhD dissertation, The University of Texas at Austin.

Lugo, N. Offshore Field Experience with Brightwater®. In: The Force ART Work Shop Water based EOR Diversion Techniques; 2010 January 20; Stavanger, Norway. Available at: http://www.force.org/PDW-Seminars/EOR%20Diversion_Jan_2009/Presentations/Nancy%20Lugo,%20Chevron%2020.1.2010.ppt

Mack, J.C. and Smith, J.E. 1994. In-Depth Colloidal Dispersion Gels Improve Oil Recovery Efficiency. Paper SPE/DOE 27780 presented at the SPE/DOE Ninth Symposium on Improved Oil Recovery held in Tulsa, Oklahoma, U.S.A., 17-20 April 1994.

Meter, D.M. and R.B.Bird. 1994. Tube Flow of Non-Newtonian Polymer Solutions, Part I and II-Laminar Flow and Rheological Models. AICHE J., November 1964.

Mustoni, J.L., Norman, C.A., Denyer, P. 2010. Deep Conformance Control by a Novel Thermally Active Particle System to Improve Sweep Efficiency in Mature Waterfloods of the San Jorge Basin. Paper SPE 129732 presented at the SPE/DOE Symposium on Improved Oil Recovery held in Tulsa, Oklahoma, 24-28 April 2010.

Needham, R.B., Threlkeld, C.B., and Gall, J.W. 1974. Control of Water Mobility Using Polymers and Multivalent Cations. Paper SPE 4747 prepared for the Improved Oil Recovery Symposium of the SPE of AIME, held in Tulsa, Oklahoma, April 22-24 1974.

O'Brien, W.J., Stratton, J.J. Jr., and Lane, R.H. 1999. Mechanistic Reservoir Modeling Improves Fissure Treatment Gel Design in Horizontal Injectors, Idd El Shargi North Dome Field, Qatar. Paper SPE 56743 presented at the SPE Annual Technical Conference and Exhibition, Houston, 3-6 October 1999.

Ohms, D., Graff, C.J., Frampton, H., Morgan, J.C., Cheung, S., Yancey, K., and Chang, K.T. 2009. Incremental Oil Success from Waterflood Sweep Improvement in Alaska. Paper SPE 121761 presented at the 2009 SPE International Symposium on Oilfield Chemistry held in 20-22 April 2009 in The Woodlands, Texas, U.S.A.

Pritchett, J., Frampton, H., Brinkman, J., Morgan, J., Chang, K.T., Goodgame, J. 2003. Field Application of a New In-Depth Waterflood Conformance Improvement Tool. Paper SPE 84897 presented at the SPE International Improved Oil Recovery Conference in Asia Pacific held in Kuala Lumpur, Malaysia, 20-21 October 2003.

Ranganathan, R., Lewis, R., McCool, C.S., Green, D.W., Willhite, G.P. Experimental Study of the Gelation Behavior of a Polyacrylamide/Aluminum Citrate Colloidal-Dispersion Gel System. SPE J. 1998.

Root, P.J. and Skiba, F.F. 1965. Crossflow Effects during an Idealized Displacement Process in a Stratified Reservoir. SPE 958, 1965.

Rousseau, D., Chauveteau, G., Renard, M., Tabray, R., Zaitoun, A., Mallo, P., Braun, O., and Omari, A. 2005. Rheology and Transport in Porous Media of New Water Shutoff/Conformance Control Microgels. Paper SPE 93254 in proceedings of the SPE International Symposium on Oilfield Chemistry held in Houston, Texas, February 2-4 2005.

Rousennac, B. and Toschi, C. 2010. Brightwater Trial in Salema Field (Campos Basin, Brazil). Paper SPE 131299 presented at the SPE EUROPEC/EAGE Annual Conference and Exhibition held in Barcelona, Spain, 14-17 June 2010.

Seright, R.S. and Liang, J. 1994. A Survey of Field Applications of Gel Treatments for Water Shutoff. Paper SPE 26991 presented at the III Latin American/Caribbean Petroleum Engineering Conference held in Buenos Aires, Argentina, 27-29 April 1994.

Seright R.S. and Lee R.L. 1999. Gel Treatments for Reducing Channeling in Naturally Fractured Reservoirs. SPE Prod & Fac 14(4). SPE-59095-PA.

Seright R.S., Lane, R.H., and Sydansk, R.D. 2003. A Strategy for Attacking Excess Water Production. SPE Prod & Fac 18(3). SPE-84966-PA.

Seright R.S., Zhang G., Akanni, O.O., Wang, D. 2011. A Comparison of Polymer Flooding with In-Depth Profile Modification. Paper CSUG/SPE 146087 was presented at the Canadian Unconventional Resources Conference held in Calgary, Alberta, Canada, 15-17 November 2011.

Shi, J., Varavei, A., Huh, C., Delshad, M., Sepehrnoori, K., and Li, X. 2011. Transport Model Implementation and Simulation of Microgel Processes for Conformance and Mobility Control Purposes. Energy Fuels, 2011, 25(11).

Smith, J.E. 1995. 1995. Performance of 18 Polymers in Aluminum Citrate Colloidal Dispersion Gels. Paper SPE 28989 was presented at the SPE International symposium on Oilfield Chemistry held in San Antonio, TX, U.S.A., 14-17 February 1995.

Sorbie, K.S. 1991. Polymer-Improved Oil Recovery. Blackie, Glasgow and London.

Spildo, K., Skauge, A. Aara, M.G., and Tweheyo, M.T. 2009. A New Polymer Application for North Sea Reservoirs. SPE Res. Eval. Eng. 2009, 12(3), 427-432.

Sydansk, R.D., Xiong, Y., Al-Dhafeeri, A., Schrader, R.J., and Seright, R.S. 2005. More than 12 Years' Experience with a Successful Conformance-Control Polymer-Gels Technology. SPE Prod. Fac. 2005, 20(3), 240-249.

Sydansk, R.D. and Deright, R.S. 2007. When and Where Relative Permeability Modification Water-Shutoff Treatments Can be Successfully Applied. SPE Prod & Oper 22(2). SPE-99371-PA.

Sydansk, R.D. and Romero-Zeron. 2011. Reservoir Conformance Improvement. Society of Petroleum Engineers, Richardson, Texas, U.S.A.

Woods, P., Schramco, K., Turner, D., Dalrymple, D., and Vinson, E. 1986. In-Situ Polymerization Controls CO₂/Water Channeling at Lick Creek. Paper SPE 14958 presented at the SPE Enhanced Oil Recovery Symposium, Tulsa, 20-23 April 1986.

Wreath, D., Pope, G.A., and Sepehrnoori, K. 1990. Dependence of Polymer Apparent Viscosity on the Permeable Media and Flow Conditions. In Situ 14(3), 263-284.

Yanez, P.A.P., Mustoni, J.L., Relling, M.F., and Chang, K. 2007. New Attempt in Improving Sweep Efficiency at the Mature Koluel Kaike and Piedra Clavada Waterflooding Projects of the S. Jorge Basin in Argentina. Paper SPE 107923 was presented at the 2007 SPE Latin American and Caribbean Petroleum Engineering Conference held in Buenos Aires, Argentina, 15-18 April 2007.

Zhang, H. and Bai, B. 2010. Preformed Particle Gel Transport through Open Fractures and its Effect on Water Flow. Paper SPE 129908 in proceedings of the SPE Improved Oil Recovery Symposium held in Tulsa, OK, April 24-28, 2010.